

Biochemical and molecular investigation of the HOP/STI1 protein family in plants

Dissertation

zur Erlangung des akademischen Grades
Doctor rerum naturalium (Dr. rer. nat.)

vorgelegt der

Naturwissenschaftlichen Fakultät I
Biowissenschaften

der Martin-Luther-Universität Halle-Wittenberg

von

Frau Christiane Hedtmann

geb. am: 28.01.1983 in Osterburg

Gutachter

1. Prof. Dr. Klaus Humbeck
2. PD Dr. Hans-Peter Mock
3. Prof. Dr. Hans-Jörg Jacobsen

Halle (Saale), den 27.06.2012

1.	Abstract.....	1
2.	Introduction	2
2.1.	Detection and functional characterisation of a HOP/STI1 protein in tobacco.....	2
2.2.	The role of HOP/STI1 proteins in mammalia and yeast.....	3
2.3.	Plant-encoded HOP/STI1 proteins	6
2.4.	The HOP/STI1 isoforms in Arabidopsis (STIAT)	7
2.5.	HOP/STI1 proteins participate in plant stress response network	9
2.6.	Hsp70 and Hsp90 protein families in Arabidopsis – the potential interaction partners of STIAT isoforms.....	12
2.7.	Aims of the work	14
3.	Material and Methods	16
3.1.	Plant material and plant growth.....	16
3.2.	Antibodies	16
3.2.1.	Preparation of STINT specific antibody	16
3.2.2.	Other antibodies.....	17
3.3.	Preparation of total proteins extracts, determination of protein concentration, SDS-PAGE and immunodetection.....	18
3.3.1.	Preparation of total proteins extracts and determination of protein content	18
3.3.2.	SDS-PAGE and immunodetection	18
3.3.3.	Two-dimensional protein gel electrophoresis and immunodetection.....	19
3.4.	Transcriptional analysis using Geneinvestigator.....	20
3.5.	Identification and characterisation of STIAT T-DNA insertion mutants	20
3.6.	Methods for subcellular localisation of proteins	21
3.6.1.	<i>In silico</i> analysis tools.....	21
3.6.2.	Fractionation of all nuclei	21
3.6.3.	Enrichment of leaf plasma membrane proteins	22
3.7.	Size exclusion chromatography of the putative STINT complex	22
3.8.	Blue native PAGE and native immunodetection of the STINT complex.....	23
3.9.	Protein identification methods.....	23
3.9.1.	Peptide mass fingerprinting by MALDI-TOF MS	23
3.9.2.	<i>De novo</i> sequencing of peptides by nanoLC-ESI-Q-TOF MS/MS	24
3.10.	Immunoprecipitation of STIAT isoforms	25
3.11.	Expression and purification of proteins in <i>E. coli</i>	25
3.12.	<i>In vitro</i> interaction studies of STIAT isoforms with its putative interaction partners....	26
3.13.	Tandem affinity purifications of STINT and STI1.....	27
3.13.1.	Tandem affinity purification of heterologous STINT in Arabidopsis	27
3.13.2.	Tandem affinity purification of STI1 in yeast.....	27
3.14.	Enrichment of phosphorylated peptides.....	28
3.14.1.	Immobilized metal ion affinity chromatography	28
3.14.2.	Phos-tag agarose	30
3.15.	Preparative IEF of STIAT isoforms	31
3.16.	Ion exchange chromatography of STIAT isoforms.....	31
4.	Results	33

4.1.	Characterisation of STIAT isoform expression.....	33
4.1.1.	Identification and analysis of <i>stiat1-1</i> and <i>stiat2-1</i> T-DNA insertion lines.....	33
4.1.2.	Morphological characterisation of <i>stiat1-1</i> and <i>stiat2-1</i> during abiotic stresses.....	34
4.1.3.	STIAT isoform expression in <i>stiat1-1</i> and <i>stiat2-1</i> during abiotic stresses.....	37
4.1.4.	Identification of STIAT isoforms under control and heat conditions.....	40
4.1.5.	Gene and protein of STIAT3 isoform is induced after heat stress and present over the time of elevated temperature	45
4.1.6.	Organ-dependent expression of STIAT isoforms in Columbia-0	46
4.2.	Intracellular distribution of STIAT isoforms	48
4.2.1.	Prediction of STIAT isoform localisation using <i>in silico</i> tools.....	48
4.2.2.	STIAT1 and STIAT2 are localised in cytosol and nucleus.....	51
4.2.3.	STIAT1 and STIAT2 can partially associate with membranes.....	52
4.3.	<i>In silico</i> analysis of regulatory elements of STIAT isoforms	53
4.4.	Isolation and characterisation of STIAT/STINT interaction partners	57
4.4.1.	<i>In silico</i> prediction of STIAT isoform interaction partners.....	57
4.4.2.	Co-localisation of STIAT1 and STIAT2 isoforms with specific members of the Hsp90 and Hsp70 families in cytosol and nucleus	60
4.4.3.	Size exclusion chromatography revealed participation of STINT in high molecular weight fraction and occurrence as a dimer in tobacco.....	61
4.4.4.	Blue native PAGE confirmed the occurrence of the STINT protein as a dimer	62
4.4.5.	Immunoprecipitation of STIAT interaction partners in Arabidopsis	65
4.4.6.	Heterologous expression of STIAT isoforms and their potential interaction partners in <i>E. coli</i>	67
4.4.7.	<i>In vitro</i> interaction studies of STIAT2 with Hsp70-5 revealed plenty of background and unspecific binding of the Hsp	69
4.4.8.	Tandem affinity purification of heterologous STINT protein in Arabidopsis revealed Hsp90 and Hsp70 as interacting proteins.....	73
4.4.9.	Tandem affinity purification of STI1 protein in yeast revealed Hsp90 and Hsp70 as interacting proteins	74
4.5.	Are the STIAT isoforms modified by phosphorylation?	77
4.5.1.	Analysis of 2-D protein pattern of recombinant STIAT1 and STIAT2.....	77
4.5.2.	Method development for enrichment of phosphopeptides from casein using immobilized metal ion affinity chromatography and Phos-tag agarose	80
4.5.3.	Enrichment of phosphopeptides from STIAT2 using Phos-tag agarose.....	82
4.5.4.	Enrichment of STIAT isoforms from Arabidopsis leaf extract using preparative isoelectric focussing.....	84
4.5.5.	Enrichment of STIAT isoforms from Arabidopsis leaf extract using ion exchange chromatography	85
5.	Discussion.....	87
5.1.	Summary and outline	87
5.2.	Characterisation of STIAT isoform expression during plant development	88
5.2.1.	STIAT1 and STIAT2 share redundant function.....	88
5.2.2.	STIAT3 is differentially expressed, indicating specific functions during abiotic stress responses and in developmental processes	89
5.3.	Intracellular distribution of STIAT isoforms	91
5.3.1.	STIAT1 and STIAT2 are localised in cytosol and nucleus.....	91
5.3.2.	STIAT1 and STIAT2 are partially associated to membranes	92
5.4.	<i>In silico</i> analysis of regulatory elements of STIAT isoforms	94

5.5.	Isolation and characterisation of STINT/ STIAT interaction partners	96
5.5.1.	Co-expression of putative STIAT interaction partners in Arabidopsis	97
5.5.2.	STINT participates in protein complexes and is present as a native dimer	97
5.5.3.	Identification of STIAT interaction partners in Arabidopsis	98
5.5.4.	Heterologous STINT interacts with cytosolic Hsp90 and Hsp70 members in Arabidopsis.....	100
5.5.5.	Comparison of the interaction partners of STINT in Arabidopsis and STI1 in yeast	101
5.6.	Are the STIAT isoforms modified by phosphorylation?	103
5.6.1.	Phosphorylated peptides in recombinant STIAT1 and STIAT2	103
5.6.2.	Ion exchange chromatography separates phosphorylated STIAT isoforms	104
5.7.	Summary: What are the possible functions of STIAT isoforms?.....	105
6.	References	107
7.	Abbreviations.....	118
8.	Acknowledgements	120
9.	Curriculum vitae.....	121
10.	Affirmation.....	124
11.	Appendix	125

1. Abstract

Human HOP (Heat shock protein 70/90 organising protein) and yeast STI1 (Stress-inducible protein 1) are best characterized Hsp70/Hsp90 co-chaperones in their organisms. The model plant *Arabidopsis thaliana* encodes three members of the HOP/STI1 family, but knowledge of their biological function is limited. In this thesis, investigation of Arabidopsis HOP/STI1 proteins (STIAT) and a homologous protein in tobacco (STINT) was performed to identify roles during control and stress defence mechanisms.

STIAT1 and STIAT2 share redundant function as mutant lines for the two isoforms show normal growth response after cold and heat stress treatment. Expression analysis using immunoblottings revealed co-expression of both isoforms in leaves under control, cold and heat conditions with higher abundance after stress application. The third isoform STIAT3 was exclusively expressed in leaves after heat treatment. In stems and flowers of Arabidopsis all three STIAT isoforms were present under control conditions in different amounts, while they were not detectable in roots.

Immunodetection of subcellular fractions showed co-localisation of STIAT1 and STIAT2 isoforms in cytosol and nucleus of leaves with lower abundance in the latter compartment. A partial association of these two isoforms to membranes was also detected.

The *in silico* analysis of the putative STIAT promoter sequences supported the regulation by diverse abiotic stress factors, phytohormones and light.

The characterisation of putative interaction partners of STIAT1 and STIAT2 revealed co-localisation with Hsp90 and Hsp70 isoforms in cytosol and nucleus. Immunoprecipitation led to the purification of the STIAT isoforms, whereas TAP purification identified the cytosolic isoforms of the Hsp's as interacting proteins with the homologous tobacco STINT in Arabidopsis. Additional components of the protein complex are still unknown. The application of TAP was verified in yeast resulting in co-purification of Hsp's with STI1. The native dimeric state of STINT was obtained during the investigations of the STINT complex in tobacco.

The analysis of recombinant STIAT1 and STIAT2 by 2-D PAGE resulted in a chain of four to five spots. One phosphorylation site in each isoform was identified so far. For the analysis of STIAT isoform modification *in planta*, enrichment approaches are essential. Ion exchange chromatography separated phosphorylated and dephosphorylated STIAT isoforms, which can be enhanced by the addition of phosphatase inhibitor during protein extraction.

2. Introduction

2.1. Detection and functional characterisation of a HOP/STI1 protein in tobacco

Trichomes are known to be specialized leaf structures functioning in stress defence (Wagner 1991, Wang *et al.* 2002). A recent study compared the proteome pattern of leaf trichomes with residual leaf tissue aiming at characterizing the protein complement of trichomes in tobacco (Amme *et al.* 2005). Many stress-associated proteins as well as enzymes of the antioxidative stress defence system such as cytosolic Cu/Zn superoxide dismutase, glutathione peroxidase, and pathogenesis-related proteins were more abundant in trichomes relative to leaves. One protein was identified as a stress-related protein based on a homology to a sequence from *Arabidopsis thaliana* (*A. thaliana*). In analogy to the stress-inducible protein of *Arabidopsis* (gi:15221564), this novel tobacco protein was referred to as STINT (stress-induced protein in *Nicotiana tabacum*).

The STINT protein sequence contains three tetratricopeptid repeat (TPR) domains, two aspartate-proline (DP) repeats and one nuclear localization signal (NLS) which was in accordance with previously described HOP (heat shock protein 70/90 organising protein) heterologues in human (Honore *et al.* 1992) and yeast (Nicolet and Craig 1989). The functional characterisation of STINT in tobacco was initiated by cloning the protein and producing polyclonal antibody to study its expression. Immunodetection with antiserum against STINT showed the expression of STINT in various tissues and an induction after heat and cold stress in leaf (Figure 1). The cellular and subcellular localisation was studied using β -glucuronidase (GUS) and green fluorescent protein (GFP) fusion constructs and revealed localisation of STINT in nucleus and cytosol. In order to functionally characterize STINT, gene knock down by RNAi approach was performed (Hedtmann 2005, Hedtmann 2007). Here, STINT RNAi tobacco plants were exposed to various abiotic stresses, including heat, cold and drought, revealing in the strongest phenotype after exposure to cold stress.

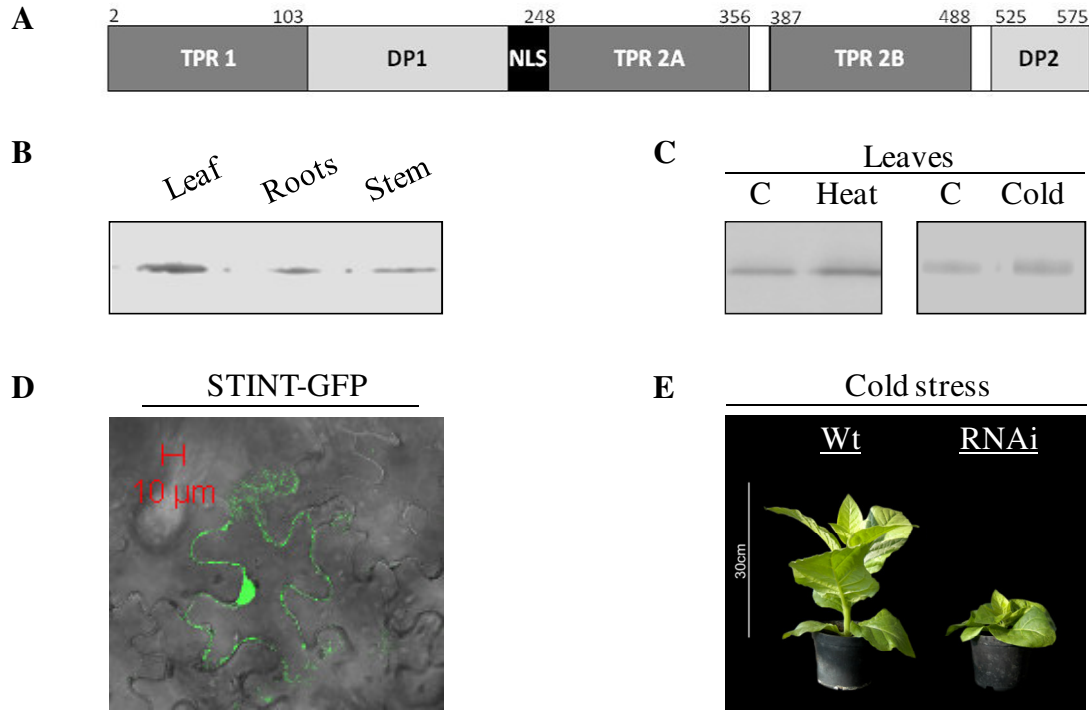


Figure 1: Initial functional characterization of STINT.

- A:** Sequence analysis of STINT protein revealed three TPR domains, two DP repeat regions and one NLS.
- B, C:** Expression analysis of STINT using immunodetection with antiserum against STINT resulted in detection in various tissues (B) and induction after heat and cold stress in leaf (C).
- D:** Confocal laser scanning microscopy of transgenic tobacco plants expressing STINT-GFP show subcellular localisation of STINT in nucleus and cytosol.
- E:** Transgenic plants containing an RNAi construct of STINT were sensitive to cold stress, resulting in a stunted phenotype and reduced leaf area.

2.2. The role of HOP/STI1 proteins in mammalia and yeast

The HOP/STI1 protein is a co-chaperone which reversibly couples to Hsp70 and Hsp90 (Chen and Smith 1998). The yeast HOP stress-inducible protein 1 (STI1) was initially identified in a genetic screen for proteins involved in heat shock response (Nicolet and Craig 1989). The human heterolog was first described as transformation-sensitive protein IEF SSP 3521 (Honore *et al.* 1992) and later referred to as HOP. Yeast STI1 and human HOP share 42 % amino acid identity and are characterized by specific structural features. They contain nine TPR motifs that are clustered in three TPR domains, namely TPR1, TPR2A and TPR2B (Scheufler *et al.* 2000) (Figure 2). A single TPR motif is a degenerate 34 amino acid sequence with higher frequency of conservation at 8 amino acid residues generating a consensus at positions 4 (W/L/F), 7 (L/I/M), 8 (G/A/S), 11 (Y/L/F), 20 (A/S/E), 24 (F/Y/L), 27 (A/S/L),

and 32 (P/K/E), especially at positions 8, 20, 24 and 27 (Blatch and Lässle 1999). The interaction with the C-terminal EEVD residues of Hsp70 and Hsp90 is mediated by TPR1 and TPR2A of HOP/STI1 (Demand *et al.* 1998, Scheufler *et al.* 2000, Young *et al.* 1998). The function of TPR2B is not yet resolved, but a binding to Hsp70 or a function as Hsp90 ligand has been suggested (reviewed in Odunuga *et al.* 2004, Song and Masison 2005). In addition to TPR motifs, HOP/STI1 contains smaller regions with conserved DP repeats, located in close proximity to the TPR motifs, that is DP1 after TPR1 (Carrigan *et al.* 2004) and DP2 after TPR2B (Chen and Smith 1998). The DP2 domain of HOP has been shown to be essential for Hsp70 binding (Carrigan *et al.* 2004), but these findings are not confirmed for yeast STI1 (Flom *et al.* 2007). A critical function of DP1 domain in Hsp70 or Hsp90 binding has not been described so far (Carrigan *et al.* 2004). These results indicate that knowledge of HOP/STI1 interactions with Hsp70 and Hsp90 is far from being complete.

Despite the high similarities between HOP and STI1, also distinctive characteristics are described. A putative NLS was found in HOP (Longshaw *et al.* 2004), which is absent in yeast STI1.

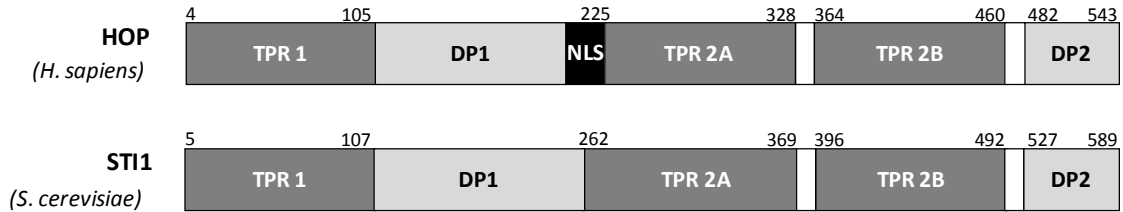


Figure 2: HOP/STI1 domain structure.

TPR, DP repeat regions and NLS are indicated. Domains stretches are indicated by amino acid residue numbers at the domain borders (scale is approximate).

HOP functions primarily as an adaptor that directs Hsp90 to Hsp70-client protein complexes in the cytoplasm (Figure 3). This interaction is best studied in the maturation pathway of hormone receptors such as glucocorticoid receptor in mammals (Chen *et al.* 1996, Dittmar *et al.* 1996). HOP binds to the ADP-bound form of Hsp90, resulting in HOP-Hsp90 complex (Johnson *et al.* 1998) and subsequently to Hsp70 with low affinity, which is increased in the presence of Hsp90 (Hernandez *et al.* 2002).

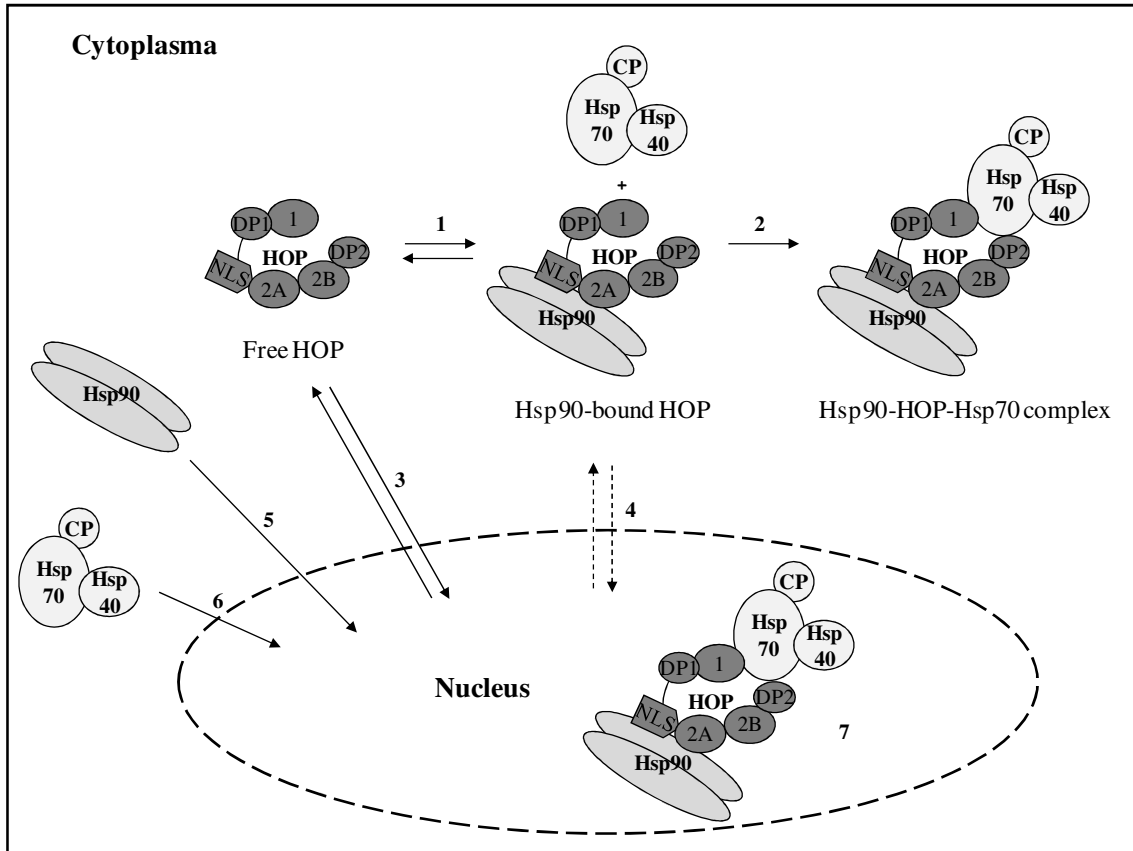


Figure 3: Model for HOP functionality and its cellular distribution in the mammalian systems (modified after Daniel *et al.* 2008). All processes are also assumed to be regulated by phosphorylation.

- 1: Location of free or reversibly Hsp90-bound HOP in cytoplasm.
- 2: Coupling of Hsp90-bound HOP with the Hsp70-Hsp40-client protein (CP) complex in the cytoplasm to mediate the transfer of a CP from Hsp70 to Hsp90, *e.g.* the steroid hormone receptor complex.
- 3: Free HOP translocates into nucleus, which increases in response to heat stress.
- 4: Translocation of Hsp90-bound HOP into nucleus is proposed, but not yet experimentally confirmed.
- 5+6: Hsp90 and Hsp70-Hsp40-CP complex translocates into nucleus under heat stress conditions.
- 7: Putative Hsp90-HOP-Hsp70-Hsp40-CP complex in nucleus, *e.g.* Octamer binding protein 1 coactivator in S phase (OCA-S), which is essential for S phase-dependent histone H2B transcription.

Annotations 1, 2A, 2B, DP1, DP2 and NLS in HOP refer to its TPR1, TPR2A and TPR2B domains, DP repeat region and NLS respectively.

HOP is also involved in binding of proteins other than Hsp90 and Hsp70 (Abbas-Terki *et al.* 2002, Abbas-Terki *et al.* 2001, Glover and Lindquist 1998) and appears to be involved in the formation of numerous Hsp90-independent complexes (Odunuga *et al.* 2004). Early studies reported the presence of HOP in Golgi apparatus and small vesicles of normal cells, and in the nucleolus of human SV40-transformed fibroblast cells (Honore *et al.* 1992). It has been proposed that HOP integrates into the plasma membrane as part of a sialoglycoprotein (alpha-

helix rich prion protein, PrPC) complex, although HOP lacks a signal peptide for membrane transport (Zanata *et al.* 2002).

The participation of HOP in a variety of cellular processes is dependent on its distribution in cytosol and nucleus. Translocation of HOP from its predominant cytoplasmic localisation (Lassle *et al.* 1997) to the nucleus increases in response to heat shock (Daniel *et al.* 2008, Longshaw *et al.* 2004). This nucleocytoplasmic shuttling is probably regulated by phosphorylation/dephosphorylation events (Daniel *et al.* 2008, Longshaw *et al.* 2004).

2.3. Plant-encoded HOP/STI1 proteins

Plant heterologs of HOP are described in soybean (Torres *et al.* 1995, Zhang *et al.* 2003), Arabidopsis (Krishna and Gloor 2001, Prasad *et al.* 2010), wheat germ lysate (Krishna and Kanelakis 2003), and rice (Chen *et al.* 2010). The number of *HOP* genes per plant species varies between one gene in soybean and three in Arabidopsis. The phylogenetic analysis of all currently known plant HOP compared to yeast STI1 and human HOP is shown in Figure 4.

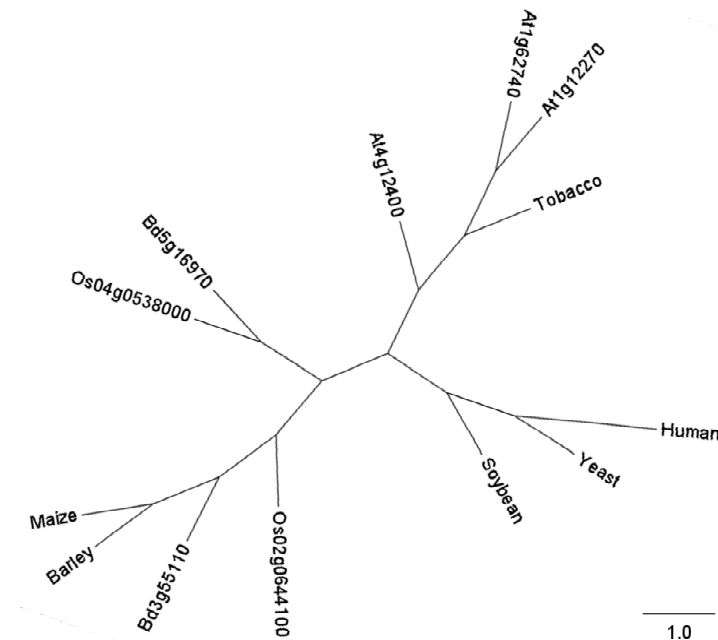


Figure 4: Phylogenetic analysis of *HOP/STI1* from plants, human and yeast drawn with Clustal X.

HOP from human and *STI1* from yeast are single-copy genes. There are three genes in the genome of Arabidopsis (At), and two in rice (Os) and Brachipodium (Bd). Only one *HOP* gene is known in soybean, maize and barley. The scale bar represents evolutionary distance (amino acid replacements).

In addition, two *HOP* genes were found in the genome of rice and *Brachipodium distachion*, and one in barley and maize using Basic Local Alignment Tool (BLAST) at National Centre for Bio**te**chnological Information (NCBI). Whether barley and maize contain *HOP* multicopy genes remains unknown until sequencing of these organisms is completed.

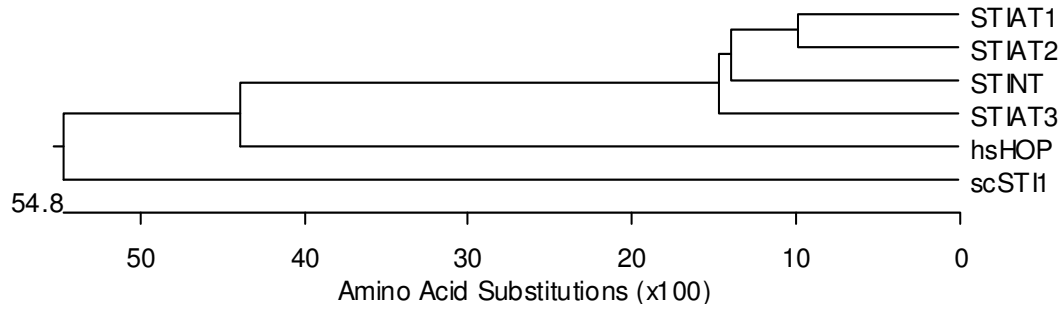
In vitro binding assays in soybean and wheat germ lysate revealed the interaction of HOP either with Hsp90 alone or with both Hsp90 and Hsp70 (Krishna and Kanelakis 2003, Zhang *et al.* 2003). The interaction of the rice HOP-Hsp90 heterocomplex with the chitin receptor CERK1 and in the Rac1 immune complex indicate a dual function in rice innate immunity (Chen *et al.* 2010). Authors suggested that the HOP-Hsp90 complex is involved in the efficient export of PAMP (*P*athogen *A*ssociated *M*olecular *P*atterns) receptors from endoplasmatic reticulum to plasma membrane (PM) and in signalling pathways in the defense at the PM. In Arabidopsis, functions of HOP homologues have not been defined so far.

2.4. The HOP/STI1 isoforms in Arabidopsis (STIAT)

As mentioned before, the Arabidopsis genome contains three genes that encode HOP, in this work referred to as STIAT (stress-induced proteins in A. thaliana). The gene product of *STIAT1* (At1g62740) on chromosome one showed highest homology to the tobacco stress-induced protein STINT (Hedtman 2007). The other two genes, one located on the same chromosome and one on the fourth chromosome, are presumably the result of duplication/triplication event. The gene product of *STIAT2* (At1g12270) has the same sequence length as *STIAT1*, while *STIAT3* (At4g12400) lacks some amino acids when compared to the other two (Hedtman 2007).

All STIAT isoforms show homology to human HOP and yeast STI1 (Figure 5) containing the characteristic protein domains described in section 2.2. So far, experimental evidences for the involvement in stress response or the functional characterisation of HOP/STI1 family in Arabidopsis are lacking.

A



B

STIAT1	---MADEAKAKGNAAFSSGDFNSAVNHFTDAINLTPT-NHVLFSNRSAAHASLNHYDEAL	56
STIAT2	---MAEEAKAKGNAAFSSGDFTTAINHFTEAIALAPT-NHVLFSNRSAAHASLHQYAEAL	56
STIAT3	---MAEEAKSKGNAAFSSGDYATAITHFTEAINLSPT-NHILYSNRSASYASLHRYEAL	56
STINT	---MADEAKAKGNAAFSAGNFTDAITHFTEAINLSPT-NHVLFSNRSAAAYASIGKYS DAL	56
scSTI1	MSLTADEYKQQGNAAF TAKDYDKAIELFTKAI EVSETPNHVLYSNRSACYTSLKKFSDAL	60
hsHOP	-MEQVNELKEKGNKALSVGNIDDALQCYSEAIKLDPH-NHVLFSNRSAAAYAKKGDYQKAY	58
TPR1		
STIAT1	SDAKKTVELKPDWGKGY SRLGAAHLGLNQFDEAVEAYS KGLEIDPSNEGLKSG LADAKAS	116
STIAT2	SDAKETIKLKPYPKGY SRLGAAHLGLNQFELAVTAYKKGLDVPDPTNEALKSG LADAEAS	116
STIAT3	SDAKKTIELKPDWSKGY SRLGAAFLGLSKFDEAVDSYKKGLEIDPSNEMLKSG LADASRS	116
STINT	SDAQKTVDLKSDWAKGY SRLGAAHLGLHHYDEAVSAYKKGLEIDPNNEALKSG LSDAQAA	116
scSTI1	NDANECVKINPSWSKGY NRLGAAHLGLGDLDEAESNYKKALELDASNKAAKEGLDQVHRT	120
hsHOP	EDGCKTVDLKPDWGKGY SRKAAALEFLNRFEEAKRTYEEGLKHEANNPQLKEGLQNMEAR	118
STIAT1	ASRSRAS--APNPF GDAFQGPEMWSKLTADPSTRG LLKQPDFVNM MKEIQRNPSNLN-LY	173
STIAT2	VARSRA---APNPF GDAFQGPEMWTKLTSDPSTRGF LQQPDFVNM MQEIQKNPSSLN-LY	172
STIAT3	RVSSKS----NPFVDAFQ GKEMWEKLTADPGTRVYLEQDDFVKTMKEIQRNPNLN-LY	170
STINT	QARSRGPASSANPF GDAFSGPEMWA KLTDSSSTRAYLNQPDFVNM MKDIQKNPSNLN-LY	175
scSTI1	QQARQAQP--DLGLTQLFADPNLIENLKKNPKTSEMMKDPQLVAKLIGYKQNPQAIGQDL	178
hsHOP	LAERK-----FMNPFNMPNLYQKLES DPTRTLLSDPT YRELIEQLRNKPSDLG-TK	169
STIAT1	LQDQRMQALGVLLNIQIR-TQQAGDDMEIGEEEMAVPSRKEPEVEKKRKP EPEPEPEP-	231
STIAT2	LKDQRMQSLGVLLNVKFRPPPPQGDEAEVPESDMQSSNEPEVEKKREPEPEPEPEVT	232
STIAT3	MKDKRVMKALGVLLNVKFG--GSSGEDTEMKEAD-----ERKEPEPEMEPEM	214
STINT	LKDQRMQALGVLLGMKLSTRMPEEEDAEMPEP---SPERKRP AEEKKRPEPEPEPEPEM	232
scSTI1	FTDPRLMTIMATLMGVLDNMDDINQSNSMPKEPETS KSTEQQKDAEPQSDSTTSKENS SK	238
hsHOP	LQDPRIMTTL SVLLGVDLG---SMDEEEIATPP-----PPPPPKKETKPE	212
STIAT1	EFGE EK-----QKKLKAQKEKELGNAAYKKKDFETAIQH YSTAMEIDDEDISY	279
STIAT2	EEKEKK-----ERKEKAKKEKELGNAAYKKKDFETAIQH YSTAIEIDDEDISY	280
STIAT3	ELTEERQK-----KERKEKALKEKEGGNVAYKKKDFGRAVEHYTKAMELDDEDISY	266
STINT	EVGEEKEI-----KERKAKAQKEKEAGNAAYKKKDFETAIQH YSKAIELDDEDISF	284
scSTI1	APQKEESESEPMEVDEDDSKIEADKEKAEGNKFYKARQFDEAIEHYNKAWELH-KDITY	297
hsHOP	PMEEDLP-----ENKKQALKEKELGNDAYKKKDFDTALKHYDKAKELDPTNMTY	261
TPR2A		
STIAT1	ITNRAAVHLEM KYDEC IKDCDKAVERGRELRSDYKMVAKALTRKGTALGKMAK VSKDYE	339
STIAT2	LTNRAAVYLEM KYNECIEDCNKAVERGRELRSDYKMVARALTRKGTALT KMAKCSKDYE	340
STIAT3	LTNRAAVYLEM KYEECIEDCKAVERGRELRSDFKMIARALTRKGSALVKMARCSKD FE	326
STINT	ITNRAAVYLEM KYEDCIKDCDQAVERGRELRSDFKMIARALTRKGTALAKMAKSSKDFE	344
scSTI1	LNNRAAAEY EKGEYETAISTLNDAVEQGREMRADYKVISKSFARIGNAYHKLGD----LK	353
hsHOP	ITNQAAVYFEKGDY NKRELCEKAIEVGNRENREDYRQIAKAYARIGNSYFKEEK----YK	317

STIAT1	PVIQTYQKALTEHRNPETLKRLNEAERAKKELEQQEYYDPNIGDEEREKGNDFKQKYP	399
STIAT2	PAIEAFQKALTEHRNPDTLKRLNDAERAKKEWEQKQYFDPKLGDEEREKGNDFKQKYP	400
STIAT3	PAIETFQKALTEHRNPDTLLKLNDAEKVKKELEQQEYFDPTIAEEEREKGNDFKQKYP	386
STINT	VAIEVFQKALTEHRNPDTLLKLNDAEKARKELEQQEYFNPQIADEEREKGNQFFKEMKYP	404
scSTI1	KTIEYYQKSLTEHRTADILTKLRNAEKELKKAEEAYVNPEKAEERLEGKEYFTKSDWP	413
hsHOP	DAIHFNKSLAEHRTDPVLKCCQQAQAEKILKEQERLAYINPDLALEEKNKGNECFQKGDYP	377
TPR2B		
STIAT1	DAVRHYTEAIKRNPKDPRAYSNRAACYTKLGAMPEGLKDAEKCIELDPTFLKGYSRKGA	459
STIAT2	EAIKHYTEAIKRNPNNDHKAYSNRAASYTKLGAMPEGLKDAEKCIELDPTFSKGYSRKAAV	460
STIAT3	EAVKHYSEAIKRNPNNDVRAYSNRAACYTKLGALPEGLKDAEKCIELDPSFTKGYSRKGA	446
STINT	EAVKHYTESIKRNPKDPRAYSNRAACYTKLAALPEGLKDAEKCIELDPTFVKGYTRKGA	464
scSTI1	NAVKAYTEMIKRAPEDARGYSNRAALAKLMSFPEAIADCNKAIKDPNFVRAYIRKATA	473
hsHOP	QAMKHYTEAIKRNPKDAKLYSNRAACYTKLLEFQLALKDCEECIQLEPTFIKGYTRKAAA	437
STIAT1	QFFMKEYDNAMETYQKG-----LEHDPNNQELLDGVKRCVQQINKANRGDLTPEELKER	513
STIAT2	QFFLKEYDNAMETYQAG-----LEHDPNQELLDGVKRCVQQINKANRGDLTPEELKER	514
STIAT3	QFFMKEYDKAMETYQEG-----LKHDPKNQEFLDGVRRCVEQINKASRGDLTPEELKER	500
STINT	QFFMKEYEKAMETYQEG-----LKHDPQNQELLDGVKRCVEQINRGRGDLTPEELKER	518
scSTI1	QIAVKKEYASALETLDAARTKDAEVNNGSSAREIDQLYKASQQRFPQPGTSNETPEETYQR	533
hsHOP	LEAMKDYTKAMDVYQKA-----LDLDSCKEAAADGYQRCMMAQYNRHD---SPEDVKRR	488
STIAT1	QAKGMQDPEIQNILTDPVMRQVLSDLQENPAAAQKHMQNPMIMNKIQKLISGIVQMK-	571
STIAT2	QAKGMQDPEIQNILTDPVMRQVLSDLQENPSAAQKHMQNPMVMNKIQKLISAGIVQMK-	572
STIAT3	QAKAMQDPEVQNILSDPVMRQVLDVDFQENPKAAQEHMKNPMVMNKIQKLVSAGIVQVR-	558
STINT	QAKGMQDPEIQNILTDPVMRQVLTDFQENPKAAQDHMKNPLVMNKIQKLINAGIVQS--	575
scSTI1	---AMKDPEVAAIMQDPVMSILQQAQONPAALQEHMKNPEVFKKIQTLIAAGIIRTGR	589
hsHOP	---AMADPEVQQIMS DPAMRLILEQMOKDPQALSEHLKNPVIAQKIQKLMVGLIAIR-	543

Figure 5: Homology analysis of the HOP/STI1 proteins from Arabidopsis and of selected eukaryotic homologues.

A: Similarity tree of HOP/STI proteins aligned by Clustal W. Yeast, human and plant HOP are clustering together. Arabidopsis HOP (STIAT1 and STIAT2) show highest homology to STINT from tobacco in comparison to STIAT3 and yeast/human HOP.

B: Alignment of HOP/STI proteins. STIAT: *A. thaliana*, STINT: *N. tabacum*, scSTI1: *S. cerevisiae*, hsHOP: *H. sapiens*. Grey shaded areas represent TPR domains. DP repeats are shown in bold.

2.5. HOP/STI1 proteins participate in plant stress response network

Plants are exposed to different kinds of abiotic stresses, such as extreme temperatures, drought, salinity, chemical toxicity and oxidative stress, that potentially reduce crop yield by more than 50 % (reviewed in Vij and Tyagi 2007, Wang *et al.* 2004, Wang *et al.* 2003).

Physiological consequences of abiotic stresses are morphological, physiological, biochemical and molecular changes affecting plant growth and productivity (Wang *et al.* 2001). Heat stress is one of the main abiotic stress factors that effects plant biomass and productivity, in particular during warm seasons and when growing boreal crops in warm climatic regions (Huang and Xu 2008). It also turns into deciding factor when plants suffer from water loss during dry spells. In addition, global warming increases the world's average ambient temperature resulting in an aggregation of that issue. In order to accelerate breeding efforts for

plant improvement moderating the adverse effects of heat stress, understanding of heat stress defence mechanisms are essential.

Despite the diversity of environmental stresses, a conserved activation of cell signalling pathways (Knight and Knight 2001) and cellular responses is known, such as the production of stress-related proteins and the accumulation of antioxidants or compatible solutes (Vierling and Kimpel 1992). A proposed model describing the complex plant response network is represented in Figure 6.

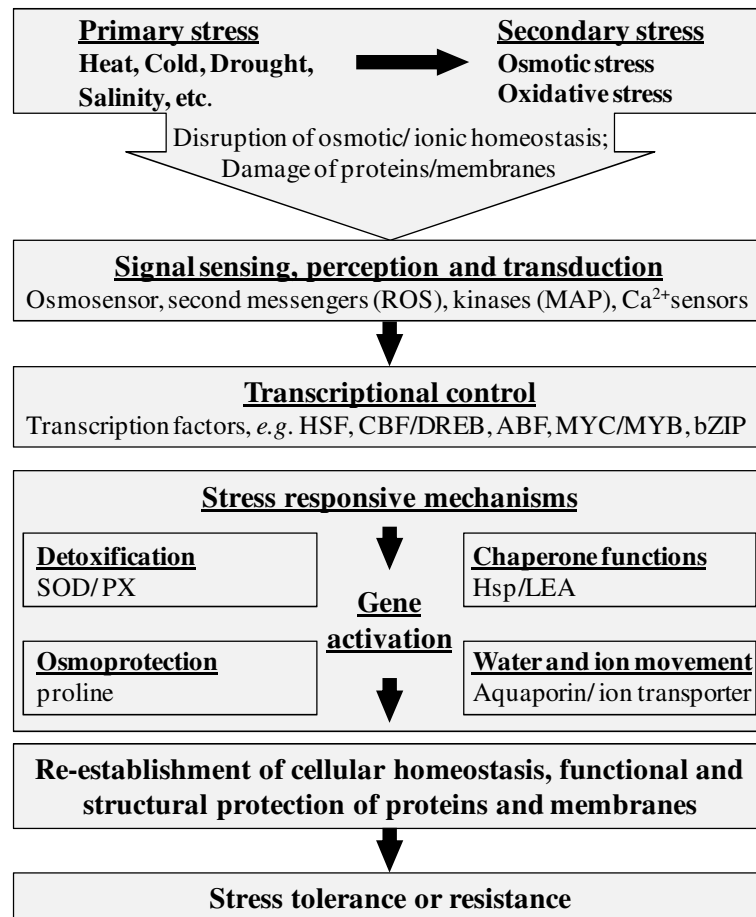


Figure 6: The complexity of plant response network to abiotic stresses (Wang, *et al.* 2003).

Initial abiotic stresses including heat, cold, drought and salinity which can be overlapping, result in the generation of secondary stresses. The primary signals trigger downstream signalling processes and activate transcription factors. The subsequent gene activation results in the re-establishment of cellular homeostasis and protection of proteins and membranes.

Abbreviations: ABF, ABRE binding factor; bZIP, basic leucine zipper transcription factor; CBF/DREB, C-repeat-binding factor/dehydration-responsive binding protein; Hsp, heat shock protein; LEA, late embryogenesis abundant; MAP, mitogen-activated protein; PX, peroxidase; ROS, reactive oxygen species; SOD, superoxide dismutase.

Initially, mostly overlapping abiotic stresses including drought, salinity, cold and heat, result in the disruption of cellular homeostasis and the generation of secondary effects like osmotic and oxidative stresses. Protein damage and distortions in ionic homeostasis represent signals that are perceived and transduced. Genes responsible for diverse stress-responsive mechanisms are activated by specific transcription factors that mainly function in detoxification, osmoprotection, water and ion movement, and chaperone network. Finally, all components of the network result, in a concerted manner, to the re-establishment of cellular homeostasis and protection or reparation of damaged proteins and membranes. However, the inappropriate response at one or more steps in this signalling cascade leads to irreversible disturbances in cellular homeostasis and damages of structural proteins, finally to cell death.

In recent years, investigations of the transcriptional control, analysis of free-radical scavengers, osmoprotectants and ion transporters were in the focus of research efforts, largely omitting the significance of stress-induced proteins (reviewed in Wang *et al.* 2003). Functional analysis of the role of stress-induced proteins during abiotic stress responses, such as heat-shock proteins and late embryogenesis abundant (LEA)-type proteins, are limited to the focus on small Hsp family (reviewed in Wang *et al.* 2003).

Many Hsp have been shown to act as molecular chaperones, responsible for protein synthesis, targeting, maturation and degradation. They are expressed under normal growth conditions, indicating contribution to cellular homeostasis, but they also respond to a wide range of unfavourable environmental conditions, such as heat, flooding, salinity, osmotic, cold and oxidative stress (Boston *et al.* 1996, Vierling 1991). They are known to be an important adaptive strategy in plant tolerance to heat stress, which is reflected by an elevated expression there (Vierling 1991).

Five major families of Hsp are described in plants and grouped, initially according to their molecular size, into small Hsp, Hsp60, Hsp70, Hsp90 and Hsp100. Current classifications, however, are based on homology and functional domains.

Except for the small Hsp family, relatively little focus has been given to the role of other Hsp in relation to plant abiotic stresses in the past (reviewed in Wang *et al.* 2003). There is still no specific information on how the two major protein chaperones Hsp70 and Hsp90 contribute to survival of heat stress in plants (Kotak *et al.* 2007) and how HOP/STI1 proteins are involved.

2.6. Hsp70 and Hsp90 protein families in Arabidopsis – the potential interaction partners of STIAT isoforms

Hsp70 proteins have an important role in preventing aggregation and in assisting refolding of native proteins under both normal and stress conditions (Hartl 1996). They also function in protein import, translocation processes and targeting of proteins to proteasomes for degradation (Frydman 2001, Hartl 1996). The latter function is mediated by inducible family members, while the general function is performed by constitutively expressed isoforms (Frydman 2001, Hartl 1996).

Structurally, Hsp70 consists of a highly conserved N-terminal ATPase domain of 44 kDa and a C-terminal peptide-binding domain of ca. 25 kDa (Zhu *et al.* 1996). Substrate binding and release are coupled to ATPase activity of Hsp70, which requires the assistance of co-chaperones.

The Hsp70 protein superfamily is divided into two subfamilies: the *Escherichia coli* DnaK subfamily, and mammals and yeast Hsp110/SSE subfamily (reviewed in Wang *et al.* 2004).

The genome of the model plant *A. thaliana* contains 18 genes encoding Hsp70 family members, including one pseudogene (Lin *et al.* 2001). The DnaK subfamily in Arabidopsis contains 13 members with diverse subcellular localisations implying both functional specificity and phylogenetic divergence (Vierling 1991). AtHsp70-1 to AtHsp70-5 are predicted to be located to the cytosol and nucleus, AtHsp70-6 and AtHsp70-7 to plastids (Su and Li 2008), AtHsp70-9 and AtHsp70-10 to mitochondria and AtHsp70-11 to AtHsp70-13 to endoplasmic reticulum (ER) (Lin *et al.* 2001). AtHsp70-8 represents an exception, because it shows large sequence variation with similarity of only 25 % to most other AtHsp70s (Lin *et al.* 2001). The 4 members of Hsp110/SSE subfamily AtHsp70-14 to AtHsp70-17 are predicted to be localized in cytosol, with exception of AtHsp70-17 expected to reside to ER.

In recent years, specific functions of single Hsp70 isoforms in Arabidopsis have been studied. Overexpression of the major cytosolic Hsp70 isoform (Hsp70-1) resulted in an improved tolerance to heat and cadmium stress but in sensitivity to pathogens (Cazalé *et al.* 2009, Noël *et al.* 2007, Sung and Guy 2003). The involvement of the cytosolic and stress-inducible Hsp70-4 isoform in protein degradation and embryogenesis has been demonstrated using Hsp70-4 RNAi plants (Lee *et al.* 2009). Knock down of stromal Hsp70-6 and Hsp70-7 isoforms revealed an abnormal plastid structure and an impaired root growth after heat shock treatment of germinating seeds indicating essential role in chloroplast development and thermotolerance of germinating seeds (Latijnhouwers *et al.* 2010, Su and Li 2008). Very

recently, Hsp70-15 deficient *Arabidopsis* plants showed growth reduction after heat stress and improved tolerance to turnip mosaic virus, indicating essential function of Hsp70-15 during thermotolerance and virus infection process (Jungkunz *et al.* 2011). Moreover, authors suggested that Hsp70-15 may function as nucleotide exchange factor for cytosolic members of the DnaK subfamily because Hsp70-15-deficient *Arabidopsis* resulted in an equal up-regulation of genes coding for Hsp as seen in a study with L-azetidine-2-carboxylic acid (AZC), which is used to induce the cytosolic Hsp70 protein response (Jungkunz *et al.* 2011). Thus, these findings indicate that Hsp70 isoforms have specific functions in cellular response to different environmental stresses.

Hsp90 is one of the most abundant proteins under normal physiological conditions and a highly conserved molecular chaperone found in all organisms with key roles in cell viability. In general, Hsp90 has major functions in folding, translocation, activation and degradation of proteins involved in a wide range of processes, from signal transduction to cell cycle control (Buchner 1999, Richter and Buchner 2001, Young *et al.* 2001). As for the Hsp70 family some members of the Hsp90 family are stress-inducible, while others are constitutively expressed.

All Hsp90 share a conserved N-terminal ATP-binding domain and a C-terminal dimerisation domain which are connected by a highly charged linker of variable length (Buchner 1999, Richter and Buchner 2001, Young *et al.* 2001). Cytoplasmatic Hsp90 isoforms from both animals and plants contain the C-terminal pentapeptide MEEVD, which is used as a diagnostic marker (Buchner 1999, Krishna and Gloor 2001, Richter and Buchner 2001, Young *et al.* 2001).

Cytosol, ER- and plastid-localized Hsp90 genes have been isolated from several plant species, sharing 63-71 % amino acid sequence similarity with Hsp90 of yeast and animal origin and 88-93 % within Hsp90 from plants (Krishna and Gloor 2001). The *Arabidopsis* genome contains seven members of Hsp90 family: AtHsp90-1 to AtHsp90-4 constitute the cytoplasmatic subfamily, while AtHsp90-5, AtHsp90-6 and AtHsp90-7 are predicted to be localized to plastids, mitochondria or ER, respectively (Krishna and Gloor 2001).

Genes of Hsp90-2/3/4 are located as a cluster on chromosome five and show 97 % homology, indicating gene duplication and redundant function. They are constitutively expressed, whereas Hsp90-1 is only induced after heat shock and arsenite treatment (Haralampidis *et al.* 2002). An essential function of Hsp90-1 was reported in pathogen resistance by binding to resistance proteins RAR1 and SGT1 (Takahashi *et al.* 2003), whereas the complex of Hsp90-

1 with ROF1 is modulating thermotolerance in Arabidopsis (Meiri and Breiman 2009). Overexpression of Hsp90-2 and Hsp90-3 in Arabidopsis enhanced plant sensitivity to both salt, drought and heat stress, but improved tolerance to high Ca^{2+} (Song *et al.* 2010, Xu *et al.* 2010), suggesting that proper balance of Hsp90 is critical for cellular stress response and/or tolerance in plants.

Overexpression of cytosolic Hsp90-2 and organellar Hsp90-5 and Hsp90-7 resulted in an improved tolerance towards oxidative stress (Song *et al.* 2009a, Song *et al.* 2009b). However, the comparison of cytosolic and organellar Hsp90 overexpression led to reduced resistance towards oxidative stress and a higher sensitivity under salt and drought conditions of the organellar Hsp90, indicating different functional roles of cytosolic and organellar Hsp90 (Song *et al.* 2009a, Song *et al.* 2009b). Since the detailed functional mechanism of Hsp90 during abiotic stress is still unresolved, studying Hsp90 in plants has great potential to reveal yet unknown important roles which are specific for plants.

2.7. Aims of the work

The functional investigation of HOP/STI1 protein family in plants by means of molecular and biochemical analysis was addressed in this thesis to clarify the roles during control and stress conditions. The analyses were performed in Arabidopsis as it encodes three STIAT genes (Krishna and Gloor 2001), but all information available so far is based on *in silico* data (Krishna and Gloor 2001, Prasad *et al.* 2010) or found during untargeted large-scale proteomic analysis (Benschop *et al.* 2007, Conde *et al.* 2011, Sugiyama *et al.* 2008). Partly studies were conducted in tobacco on the homologous protein STINT, which was detected earlier in leaf trichomes of tobacco during the characterisation of the protein complement (Amme *et al.* 2005).

In order to clarify the roles of the different STIAT isoforms in Arabidopsis the following group of topics were analysed: the characterisation of STIAT isoform expression (1), the verification of their intracellular distribution (2) and the isolation and characterisation of their potential interaction partners and their molecular status (3). For the expression analysis of STIAT isoforms Arabidopsis T-DNA insertion lines were selected. STIAT isoform expression has been investigated in these mutants, during abiotic stress treatments and in different organs by immunoblotting using the antiserum against STINT.

As the knowledge of the subcellular localisation on STIAT isoforms is limited to the localisation of STIAT1 in cytosol and nucleus when fused to GFP (Hedtmann 2005), subcellular compartments of Arabidopsis and tobacco leaves were isolated and analysed by immunoblotting.

Last, for the isolation and identification of putative interaction partners of STIAT/STINT and the analysis of the molecular status a combination of chromatographic and gel based separation methods as well as mass spectrometry analysis has been applied. Therefore Arabidopsis leaf material, tobacco and Arabidopsis cell cultures, a STI1-TAP yeast strain as well as the recombinant produced proteins were used, *e.g.* in immunoprecipitation experiments of STIAT isoforms from Arabidopsis leaf material and in tandem affinity purifications of STINT overexpressed in an Arabidopsis cell culture.

3. Material and Methods

3.1. Plant material and plant growth

Arabidopsis thaliana ecotype Columbia-0 plants were grown on soil under short-day conditions (8h light, 16h dark), at approximately 60 % humidity and 22 °C/18 °C day/night temperature. They were transferred to long-day conditions (16 h light, 8 h dark) were applied to allow flowering.

Wild-type Columbia-0 line N1072 and T-DNA insertion lines GABI_399G03 (*stiat1-1*), GABI_028A04 (*stiat1-2*) and GABI_420A10 (*stiat2-1*) (Rosso *et al.* 2003) and SALK_023494 (*stiat3-1*) (Alonso *et al.* 2003) were ordered from Nottingham Arabidopsis Stock Center (Nottingham, United Kingdom).

For *in vitro* cultivation, seeds were surface sterilized by treatment with 70 % ethanol for 2 min, 7 % NaOCl for 8 min and three washing steps with sterile water. Seeds were placed on ¼ MS medium (Murashige and Skoog 1962) (1.1 g L⁻¹ MS medium including vitamins (Duchefa, Haarlem, Netherlands), 5 g L⁻¹ sucrose, 8 g L⁻¹ agar, pH 5.8) and selective marker. Stratification of seeds was performed at 4 °C for 4 days in the dark prior to growth under controlled conditions.

Abiotic stress experiments were performed with 5 weeks old plants at 10 °C and 30 °C, representing cold and heat stress, respectively under short day conditions. Water was not restricted.

Tobacco root cell suspension culture *N. tabacum* L. cv Havana SR1 (Maliga *et al.* 1973) was maintained in 20 ml modified Linsmeier-Skoog medium LS-3 (Linsmeier and Skoog 1965) (4,4 g L⁻¹ LS medium (Duchefa, Haarlem, Netherlands), 30 g·L⁻¹ sucrose, 2 mg·L⁻¹ α -naphthalene acetic acid, 0.3 mg·L⁻¹ kinetin, pH 6.0) at 25 °C in the dark by gentle agitation (110 rpm). The cells were subcultured in fresh medium at a 1:10 dilution every 7 days.

3.2. Antibodies

3.2.1. Preparation of STINT specific antibody

Immunisation of rabbits with purified, recombinant STINT-Protein and collection of bleed samples was done as a service by Dr. Udo Conrad (Research Group Phytoantibodies, IPK Gatersleben).

Recombinant STINT protein was produced as His-fusion protein using pQE32 expression vector following manufacturer's instructions (Qiagen, Hilden, Germany). Therefore, a 1,728 bp *SmaI-HindIII* fragment of STINT was obtained by PCR using primers 5-ATCCCGGGGCCGACGAAGCTAAG-3 and 5-CGCGAAGCTTTTATTTAACTTGGACA-ATTCC-3, ligated into *SmaI-HindIII* digested pQE32 and transformed into *Escherichia coli* strain XL1 Blue cells (Bullock *et al.* 1987). The expression clone was sequenced to confirm the identity (MWG Biotech, Martinsried, Germany). The recombinant STINT was purified using affinity chromatography with 1 ml Ni sepharose high performance (HP) column in ÄktaExplorer System (GE Healthcare, Freiburg, Germany) according to manufacturer's instructions and confirmed by SDS-PAGE.

The antiserum was purified with ÄktaExplorer System using a 5 ml HiTrap-NHS column (GE Healthcare, Freiburg, Germany) following instruction of manufacturer. Initially, isopropanol was removed from the column manually by washing three times with ice cold 1 mM HCl (drop by drop). The washed column was incubated with 5 ml recombinant STINT for 30 min at RT. Unspecific bounded protein was removed by washing with 25 ml PBS buffer (140 mM NaCl, 10 mM KCl, 6.4 mM Na₂HPO₄, 2 mM KH₂PO₄). Washing and deactivation of the column was performed by alternate incubation with buffer A (0.5 M ethanolamine, 0.5 M NaCl, pH 8.3) and buffer B (0.1 M acetate, 0.5 M NaCl, pH 4). Antiserum was desalted against PBS buffer using PD-10 columns (GE Healthcare, Freiburg, Germany) before loading to the HiTrap-NHS column at a flow rate of 0.3 ml min⁻¹, which was equilibrated with 50 mL PBS buffer. After removing unspecific bounded proteins from the column with 40 mL washing buffer (0.01 M Tris, 1 M NaCl, pH 7.5) the elution was carried out with 0.1 M glycine, pH 2.8. The purity of the lysate was confirmed by Western blot analysis.

3.2.2. Other antibodies

An Arabidopsis Hsp90 antibody was produced in this thesis as described above with minor modification. Recombinant Hsp90-1 protein was produced as HIS protein using pDEST17 expression vector (Invitrogen, Karlsruhe, Germany). The Hsp70 specific antibody recognizing cytosolic Arabidopsis isoforms Hsp70-1 to Hsp70-5, the anti-H⁺-ATPase- and anti-V-ATPase polyclonal antisera were obtained by Agrisera (Vännäs, Sweden). Anti-polyHistidine mouse monoclonal antibody HIS-1, anti-GOAT donkey antiserum and alkaline phosphatase-coupled secondary mouse and rabbit antibodies were purchased from Sigma-Aldrich (Taufkirchen,

Germany). Infrared dye-coupled secondary rabbit antibody was obtained by Li-Cor (Bad Homburg, Germany).

3.3. Preparation of total proteins extracts, determination of protein concentration, SDS-PAGE and immunodetection

3.3.1. Preparation of total proteins extracts and determination of protein content

Total protein extracts were prepared by homogenisation of one part of frozen, ground plant material with two parts of extraction buffer [50 mM Hepes pH 7.5, 150 mM NaCl, 1 mM DTT, 1 mM PMSF, 1 X protease inhibitor cocktail (Roche, Mannheim, Germany)]. After centrifugation at 16,000 x g for 30 min at 4 °C, supernatants were subjected to Bradford protein assay (Bradford 1976) to determine the protein content. Bovine serum albumin (BSA) served as a reference protein.

3.3.2. SDS-PAGE and immunodetection

Defined protein amounts were separated by SDS-PAGE according to Laemmli (1970) using the Mini Protean II (Biorad, Munich, Germany) or Perfect Blue Twin ExW S apparatus (Peqlab, Erlangen, Germany). The aluminium-based staining protocol of Kang *et al.* (2002) was applied for colloidal Coomassie staining of proteins. After electrophoresis, gels were washed twice with water for 10 min and subsequently incubated in staining solution (5 % aluminium sulfate-(14-18)-hydrate, 0.02 % CBB-G250, 10 % ethanol, 2 % ortho-phosphoric acid) for 1-3 h and destaining solution (10 % ethanol, 2 % ortho-phosphoric acid) for 30 min to visualize the proteins.

Protein transfer to polyvinylidene fluoride (PVDF) membrane and immunodetection using alkaline phosphatase-coupled secondary antibodies was performed as described in Amme *et al.* (2005). Subsequent to SDS-PAGE, proteins were transferred to a PVDF membrane (Immobilon-P, pore size 0.45 µm, Millipore, Eschborn, Germany) using a semidry apparatus (Schütt, Göttingen, Germany). Immunodetection was performed using the respective antibodies and alkaline phosphatase color reagents 5-bromo-4-chloro-3-indolyl phosphate (BCIP), and nitroblue tetrazolium chloride (NBT).

Gels and membranes visualized with alkaline phosphatase-coupled secondary antibodies were documented using a UMAX Power Look III scanner (UMAX Systems GmbH, Willich,

Germany) with the MagicScan software (v.4.5). Li-Cor scanner (Li-Cor, Bad Homburg, Germany) with the Odyssey software (v3.0) was used for documentation of membranes decorated with infrared dye-coupled secondary antibody and densitometric evaluation of protein bands.

3.3.3. Two-dimensional protein gel electrophoresis and immunodetection

Protein extraction for 2-D gel electrophoresis was performed according to the procedure described by Amme *et al.* (2005). Frozen plant material was homogenized under liquid nitrogen to a fine powder. Ten parts of TCA/acetone solution [10 % (w/v) TCA, 0.07 % (w/v) 2-mercaptoethanol in acetone] were added to one part of ground material (approximately 1 g) and incubated 45 min at -20 °C. The precipitate was pelleted by centrifugation at 36,000 x *g* for 15 min at 4 °C (Eppendorf centrifuge 5417R with FA45-24-11 rotor, Eppendorf, Hamburg, Germany) and washed twice with 0.07 % (w/v) 2-mercaptoethanol in acetone. After drying the pellet in a vacuum centrifuge for 10 min at RT (Concentrator 5301, Eppendorf, Hamburg, Germany), it was solubilized in rehydration buffer (8 M urea, 2 % CHAPS, 20 mM DTT, 0.5 % IPG buffer) for 1 h at 37 °C under shaking conditions. Solid residues were removed by an additional centrifugation step and clarification through 0.45 µm filter units (Ultrafree-MC, Millipore, Eschborn, Germany). The protein concentration was determined using 2-D Quant-Kit (GE Healthcare, Freiburg, Germany) according the manufacturer's instructions. BSA served as a reference protein.

2-D gel electrophoresis was performed following the procedure described by Schlesier and Mock (2006). Fifteen µg total protein extract were loaded on immobilized pH gradient (IPG) strip of 7 cm in length (GE Healthcare, pH 4-7) by rehydration. Isoelectric focussing (IEF) was performed on IPGphor II unit (GE Healthcare) with following parameters: 14 h rehydration, 30 min Gradient to 250 V, 30 min Gradient to 500 V, 30 min Gradient to 3,000 V and 4.40 h 3,000 V with a total of about 15 kVh. After IEF, IPG-strips were equilibrated in 50 mM Tris-HCl, pH 8.8, 6 M urea, 30 % (v/v) glycerin, 2 % (w/v) SDS, 20 mM DTT, 0.01 % bromphenol blue for 15 min. Then, the equilibrated strips were placed on top of an 11.25 % SDS gel, covered with 0.5 % agarose and second dimension was performed using Mini Protean II (Biorad, Munich, Germany). 2-D gel was subsequently subjected to Western blot analysis as described in section 3.3.2.

3.4. Transcriptional analysis using Genevestigator

Genevestigator (Hruz *et al.* 2008) (www.genevestigator.com, V3) was employed to extract the transcriptional data of STIAT isoforms in Arabidopsis. Standard settings using Affymetrix ATH1 22k genome array with high quality as quality control was applied, resulting in a total number of 6100 arrays.

3.5. Identification and characterisation of STIAT T-DNA insertion mutants

T-DNA insertion lines GABI_399G03 (*stiat1-1*), GABI_028A04 (*stiat1-2*) and GABI_420A10 (*stiat2-1*) (Rosso *et al.* 2003) were screened for homozygous plants by PCR-based genotyping. Using the gene-specific primers 5'-GGCGGACGAAGCAAAAGCTAAAG-3'/ 5'-CTTTCCCATCTCTAGATGAACAGCAG-3' for *stiat1-1*, 5'-GAAAGGGGTAGAGAGCTTAGGTCTG-3'/ 5'-GAATAATCTCCCCGTGACTTAACACC-3' for *stiat1-2* and 5'-ATGGCAGAAGAAGCTAAAGCTAAAGGAAA-3'/ 5'-TTATTTTCATCTGGACGATCC-CAGCGCTAATAA-3' for *stiat2-1* Wt-like allele was detected. For detection of T-DNA allele Primer for left border of T-DNA insertion (5'-CCCATTTGGACGTGAATGTAGACAC-3') was combined with 5'-CTTTCCCATCTCTAGATGAACAGCAG-3' (*stiat1-1*), 5'-GAATAATCTCCCCGTGACTTAACACC-3' (*stiat1-2*) and 5'-ATGGCAGAAGAAGCTAAAGCTAAAGGAAA-3' (*stiat2-1*). Knock out was confirmed by Western blot analysis using antiserum directed against the recombinant tobacco protein STINT.

The resulting T-DNA insertion lines were subjected to abiotic stress treatments cold and heat as described in section 3.1. The growth parameters “diameter of rosette”, “number” and “fresh weight of leaves” were determined for 15 plants for each line grown under control and stress conditions in three independent experiments. Means of 15 plants per line, treatment and experiment were calculated and statistical analysis of mutant lines compared to control line Columbia-0 for each treatment and experiment was performed using ANOVA followed by Tukey-test with a significance level at $p < 0.05$.

3.6. Methods for subcellular localisation of proteins

3.6.1. *In silico* analysis tools

The subcellular localisation analysis of STIAT isoforms was performed using the tools TargetP (Emanuelsson *et al.* 2000) and WoLF PSORT (Horton *et al.* 2007). Mitoprot (Claros and Vincens 1996) and Predotar (Small *et al.* 2004) were used for verification of mitochondrial targeting peptides based on the assumed localisation in mitochondria. The prediction of transmembrane domains in STIAT isoforms was employed by using the tools SOSUI (Hirokawa *et al.* 1998), HMMTop (Tusnady and Simon 2001) and DAS (Cserzo *et al.* 1997) with standard parameters.

3.6.2. Fractionation of all nuclei

Nuclei isolation was performed according to Shen *et al.* (2007) with an additional purification step. 1.5 g fresh leaf tissue was homogenized with 3 ml of Honda buffer [2.5 % Ficoll 400, 5 % dextran T40, 0.4 M sucrose, 25 mM Tris-HCl pH 7.4, 10 mM MgCl₂, 1 mM DTT, 1 mM PMSF, 1 X protease inhibitor cocktail (Roche, Mannheim, Germany)] using pre-cooled mortar and filtered through a 62 µm nylon mesh. Filtrate (total protein) was incubated with Triton X-100 at a final concentration of 0.5 % on ice for 15 min and centrifuged at 1,500 x g for 5 min (Hereaus Multifuge 1S-R with TTH400 rotor, Schütt, Göttingen, Germany). The supernatant represented the soluble fraction. The pellet was washed with 2.5 ml Honda buffer containing 0.1 % Triton X-100, centrifuged, resuspended with 2.5 ml Honda buffer without Triton X-100 and transferred to two microcentrifuge tube. Starch and remaining cell debris were spun down at 100 x g for 5 min. The supernatant was centrifuged at 2,000 x g for 5 min (Eppendorf centrifuge 5417R with FA45-24-11 rotor, Eppendorf, Hamburg, Germany) to pellet the nuclei. Additional purification was achieved by resuspending the nuclei in buffer G [1.7 M sucrose, 10 mM Tris-HCl pH 8.0, 0.15 % Triton-X100, 2 mM MgCl₂, 5 mM DTT, 1 X protease inhibitor cocktail (Roche, Mannheim, Germany)], overlaying an equal amount of buffer G and centrifugating at 16,000 x g for 1 h. This pellet was resuspended in 100 µl Honda buffer. All centrifugation steps were carried out at 4 °C. If necessary, this procedure was scaled up to 3 or 6 g fresh leaf tissue.

3.6.3. Enrichment of leaf plasma membrane proteins

Plasma membrane enrichment was performed by two-phase partitioning method described by Santoni (2007). Fifty g fresh leaf tissue was vacuum infiltrated with two volumes homogenisation buffer [50 mM MOPS, 5 mM EDTA, 0.33 M sucrose, pH 7.5 with KOH; added before use: 5 mM DTT, 5 mM ascorbate, 0.6 % (w/v) polyvinylpolypyrrolidone, 1 X protease inhibitor (Roche, Mannheim, Germany)]. After filtration through two layers of Miracloth (Calbiochem, Darmstadt, Germany), the solution was centrifuged at 4,200 x g for 30 min at 4 °C (Hereaus Multifuge 1S-R with TTH400 rotor, Schütt, Göttingen, Germany) to remove debris. The supernatant was ultracentrifuged at 55,000 x g for 50 min at 4 °C (Beckman ultracentrifuge with Ti770 rotor, BeckmanCoulter, Fullerton, USA) to pellet the microsomes. The supernatant (cytosolic fraction) was removed and microsomal pellet was homogenized in resuspension buffer (5 mM potassium phosphate pH 7.8, 0.33 M sucrose; added before use: 1 mM DTT, 0.1 mM EDTA) using a brush. The two-phase partitioning was performed on three two-phase systems containing 6.4 % (w/w) dextran T500 and 6.4 % (w/w) PEG 3350, 5 mM potassium phosphate, 5 mM KCl, 0.3 M sucrose and water to a final weight of 27 g. Nine g microsomal fraction or resuspension buffer were added to two systems, 1 and 2 respectively, mixed by inverting and centrifuged at 1,000 x g for 7 min at 4 °C. The upper phase of system 2 was removed and upper phase of system 1 was transferred to lower phase of system 2. Resuspension buffer was added to system 3 and all three systems were centrifuged. The lower phase of system 1 resulted in endomembrane fraction. The upper phase of system 3 was removed and upper phase of system 2 was transferred to lower phase of system 3. After phase separation by centrifugation, the upper phase of system 3 displayed the plasma membrane fraction. Both membrane fractions were mixed with one volume resuspension buffer and ultracentrifuged at 100,000 g for 60 min at 4 °C. Pellets of plasmamembrane and endomembrane were resolved in 400 and 1000 µl resuspension buffer using a brush, respectively, and stored at -80 °C. All steps were carried out at 4 °C.

3.7. Size exclusion chromatography of the putative STINT complex

Total protein extracts were prepared from tobacco cell culture by mixing 200 mg lyophilized cell culture with 600 µl 0.05 M Hepes pH 8.5 supplemented with 1 X protease inhibitor cocktail (Roche, Mannheim, Germany). After centrifugation at 16,000 g for 30 min at 4 °C (Eppendorf centrifuge 5417R with FA45-24-11 rotor, Eppendorf, Hamburg, Germany), supernatants were clarified through 0.45µm filter units (Ultrafree-MC, Millipore, Eschborn,

Germany) and concentrated by Viaspin 6 column with exclusion size of 10 kDa (Sartorius, Göttingen, Germany) to 1.5 ml. 500 μ l of total protein extracts was separated on a Superdex 200 size exclusion column in ÄktaExplorer System (GE Healthcare, Freiburg, Germany) at a flow rate of 0.5 ml min⁻¹ pre-equilibrated in gel filtration buffer (0.05 M Hepes, 0.2 M NaCl pH 8.5). Fractions of 500 μ l were collected and 10 μ l of each fraction was analyzed by immunoblotting with antiserum directed against the recombinant STINT.

Ferritin (440 kDa), catalase (232 kDa), aldolase (160 kDa) and bovine serum albumin (66 kDa) (Serva, Heidelberg, Germany) were used as molecular mass references. 150 μ l of each reference protein (2 mg ml⁻¹ diluted in 0.05 M Hepes pH 8.5) was pooled and 500 μ l (1.2 mg protein) were loaded on the Superdex 200 column in ÄktaExplorer System using the same running conditions as described above.

3.8. Blue native PAGE and native immunodetection of the STINT complex

Blue native PAGE (BN-PAGE) and subsequent native immunodetection was performed with precasted 4-16 % Bis-Tris Native PAGE gels (Invitrogen, Karlsruhe, Germany) using a Höfer miniVE complete (GE Healthcare, Freiburg, Germany) according to the manufacturer's conditions. As recommended, the dark blue cathode buffer was replaced by light blue cathode buffer after one third of separation for Western blot analysis.

3.9. Protein identification methods

3.9.1. Peptide mass fingerprinting by MALDI-TOF MS

Relevant SDS-PAGE lanes were excised manually from the gels and incubated with 400 μ l wash buffer [10 mM ammonium bicarbonate (ABC), 10 % acetonitrile (ACN)] for 30 min under vigorous shaking. After buffer removal, gel plugs were dried for 15 min at RT in a vacuum centrifuge (Concentrator 5301, Eppendorf, Hamburg, Germany) and proteins were incubated with 7.5 μ l trypsin solution (Sequencing Grade Modified Trypsin V511, Promega, Mannheim, Germany, 10 ng μ l⁻¹ in 5 mM ABC, 5 % ACN) for 5 h at 37 °C. The digest was terminated by addition of 1 μ l 1 % TFA and peptides eluted from the gel plug at 4 °C overnight.

For MALDI-TOF mass spectrometry (MS), 0.5 μl of the digests were deposited onto the MALDI target (MTP 384 target plate AnchorChip 800um, Bruker Daltonics, Bremen, Germany) and subsequently covered with 1 μl matrix solution (0.7 mg/ml *a*-cyano-4-hydroxycinnamic-acid (HCCA) in 90 % ACN, 0.1 % TFA, 1 mM $(\text{NH}_4)_2\text{H}_2\text{PO}_4$). A MALDI tandem MS instrument (Ultraflextreme, Bruker Daltonics) was used to acquire peptide mass fingerprints (PMF). Peptide calibration standard covering a mass range from 1,000-4,000 Da were used for external calibration and trypsin autolysis peaks (m/z 842.509, 2211.104) for internal calibration.

PMF were subjected to protein homology identification using Mascot search engine (Matrix Science, London, United Kingdom) in Biotools 3.0 software (Bruker Daltonics) by searching for *Viridiplantae* in the NCBI non-redundant protein database. The following parameter settings were used: 50 ppm monoisotopic mass accuracy, one missed cleavage, oxidation (Met), propionamide (Cys) and carbamidomethyl (Cys) as allowed variable modifications.

3.9.2. *De novo* sequencing of peptides by nanoLC-ESI-Q-TOF MS/MS

When the identification described in section 3.9.1 failed, 5 μl of tryptic digest was used for nanoLC-ESI-Q-TOF MS/MS analysis and *de novo* sequencing (Witzel *et al.* 2007). Peptides were separated on a C18 pre-column (180 μm x 20 mm Symmetry, 5 μm) coupled to a C18 column (100 mm x 100 μm BEH, 1.7 μm) (Waters Corporation, Manchester, United Kingdom) at a flow rate of 0.6 $\mu\text{l min}^{-1}$ with 40 °C column temperature and an increasing ACN gradient from 3 % to 35 % in 30 min with solvent A (0.1 % formic acid in water) and solvent B (0.1 % formic acid in ACN). Mass spectrometry was performed using Q-TOF Premier with MassLynx 4.1 software (Waters, Eschborn, Germany) in a positive ion V-mode. The resulting mass spectra were integrated over 1 s intervals with internal calibration using Glu-Fibrinopeptide B (Sigma-Aldrich, Taufkirchen, Germany). Automatic data directed analysis (DDA) on doubly- and triply-charged precursor ions was applied for MS/MS analysis. Mass spectra were collected from m/z range of 400 to 1,600, and product ion MS/MS spectra were collected from m/z 50 to 1,600. Lock mass correction of the precursor and the product ions was conducted with 500 pmol μl^{-1} Glu-Fibrinopeptide B in 0.1 % formic acid in ACN/water (50:50, v/v), respectively. Mass spectra for the reference mass were acquired in continuous fragmentation mode at collision energy of 22 eV. ProteinLynx GlobalSERVER v2.3 (PLGS) software was used for data processing and database searches. The MS/MS spectra searches were conducted against the protein index of the non-redundant

SwissProt database and the UniProtKB index for *Viridiplantae* complemented with human keratin, porcine trypsin, and yeast enolase sequences. The following parameter settings were used: 10 ppm peptide, 0.1 Da fragment tolerance, one miss cleavage, oxidation (Met), carbamidomethyl (Cys) and phosphorylation (STY) as allowed variable modifications. The false positive rate was set to 4 %. Results for positive protein identification were accepted when at least two peptides per protein were identified with a peptide score of > 50 %.

3.10. Immunoprecipitation of STIAT isoforms

Immunoprecipitations were performed with Dynabeads Protein G (Invitrogen, Karlsruhe, Germany) according to manufacturer's instructions. One to ten µg purified STINT antibody diluted in 200 µl PBST was coupled to 50 µl dynabeads Protein G for 30 min at RT with gentle rotation with an RM5 apparatus (Karl-Hecht GmbH & Co KG, Sondheim). Unbound antibody was removed by binding of the Dynabeads Protein G to the magnet and antibody coupled Dynabeads were washed once with equal volume PBST by gentle mixing with an RM5 apparatus. After removal of wash buffer, total protein extracts as described in section 3.3.1 were incubated with the antibody coupled Dynabeads for 1h at RT with gentle rotation. Supernatant containing unbound protein was removed and three wash steps with 200 µl PBS followed as described before. The fourth wash fraction of 100 µl PBS was transferred to a new reaction tube. Precipitated proteins and antibody were eluted from the Dynabeads under denaturing conditions by incubation with 100 µl 1 X DTE sample buffer at 94 °C for 10 min. Eluate fractions were analyzed by SDS-PAGE either by Coomassie staining or immunoblotting with antiserum directed against the recombinant STINT.

3.11. Expression and purification of proteins in *E. coli*

Full-length cDNA gateway clones G67849 (At1g62740/ STIAT1), G21235 (At1g12270/ STIAT2), G16132 (At1g16030/ Hsp70-5) and G22186 (At5g52640/ Hsp90-1) were obtained from Arabidopsis Biological Resource Center (ABRC, Columbus, USA) and sequenced to confirm identities. RAFL21-02-C06 (At4g12400/ STIAT3), RAFL09-22-P16 (At3g12580/ Hsp70-4), RAFL09-88-H11 (At1g79930/ Hsp70-14) and RAFL09-76-I24 (At5g56030/ Hsp90-2) were obtained from RIKEN BioResource Center (Tsukuba, Japan) and used to amplify full-length coding sequences by PCR. Using gene specific primers 5-CACCATGGCGGAAGAAGCAAAATCC-3/ 5-TTACCGGACCTGAACAATTCCGG-3 for

STIAT3, 5-CACCGCGGGTAAAGGTGAAGGTCC-3/ 5-TTAATCAACTTCTTCAATCTT-TGGGCCAGC-3 for Hsp70-4, 5-CACCAGTGTAGTCGGGTTTGATTTTGG-3/ 5-TTAGGTACTACCTTCCGCGGGATTC-3 for Hsp70-14 and 5-CACCGCGGACGCTGAAACCTTTGC-3/ 5-TTAGTCGACTTCCTCCATCTTGCTACC-3 for Hsp90-2, full-length coding cDNA were subsequently inserted into pENTR/D-TOPO vector (Invitrogen, Karlsruhe, Germany). Sequencing of entry clones confirmed the identity (Eurofins MWG Operon, Ebersberg, Germany). Then, the coding sequences were introduced into pDEST17 vector (Invitrogen) by LR recombination and transformed to *E. coli* strains TOP10F' and B121AI (Invitrogen) for plasmid propagation and expression, respectively. The recombinant His-tagged fusion proteins were expressed according to instructions of manufacturer, but the *E. coli* lysates were prepared under native conditions as described in QIAexpressionist handbook (Qiagen, Hilden, Germany) with a modification. Lysis buffer (50 mM NaH₂PO₄, 300 mM NaCl pH 8) without imidazol was used, because of higher binding capacity of HIS tagged proteins in the subsequent purification procedure.

This was performed by affinity chromatography with 1 ml Ni-sepharose high performance (HP) column in ÄktaExplorer System (GE Healthcare, Freiburg, Germany) according to manufacturer's instructions. The purities of the recombinant generated proteins were confirmed by SDS-PAGE.

3.12. *In vitro* interaction studies of STIAT isoforms with its putative interaction partners

The *in vitro* interaction studies were performed according to Wegele *et al.* (2003) with total protein extracts from Arabidopsis described in section 3.3.1 and with purified recombinant proteins STIAT1, STIAT2 and Hsp70-5 in a volume of 200 µl. Reaction mixes were incubated at RT for 1 h with gentle rotation. One to ten µg purified STINT antibody diluted in 200 µl PBST was coupled to 50 µl Dynabeads Protein G (Invitrogen, Karlsruhe, Germany) for 30 min at RT with gentle rotation on a. Unbound antibody was removed by binding of the Dynabeads Protein G to the magnet and antibody coupled Dynabeads were washed once with equal volume PBST by gentle mixing. After removal of wash buffer, *in vitro* binding studies were incubated with the antibody coupled Dynabeads for 1 h at RT with gentle rotation. Supernatant containing unbound protein was removed and three wash steps with 200 µl PBS followed as described before. The fourth wash fraction of 100 µl PBS was transferred to a

new reaction tube. Precipitated proteins and antibody were eluted from the Dynabeads under denaturing conditions by incubation with 100 μ l 1 X DTE sample buffer at 94 °C for 10 min. All fractions were analyzed by SDS-PAGE and subsequent immunoblotting with both antiserum directed against the recombinant STINT and Hsp70.

3.13. Tandem affinity purifications of STINT and STII

3.13.1. Tandem affinity purification of heterologous STINT in Arabidopsis

Tandem affinity purification of heterologous STINT protein in Arabidopsis was performed in collaboration with Functional Proteomics Group at VIB/ University Gent, Belgium and was conducted as described in Van Leene *et al.* (2007).

Full-length coding sequences of *STINT* containing a stop codon for N-terminal fusion and lacking a stop codon for C-terminal fusion were amplified from Plasmid-DNA by PCR, respectively. Subsequently, attB sites were attached to the PCR fragments using primers 5'-GGGGACAAGTTTGTACAAAAAAGCAGGCT-3'/ 5'-GGGGACCACTTTGTACAAGAAAGCTGGGT-3' in a second PCR. These fragments were inserted into entry vector pDONR221 and *E. coli* strain Top10F' (Invitrogen, Karlsruhe, Germany) by BP reaction according to manufacturer instructions. Sequencing confirmed the identities of PCR products (Eurofins MWG Operon, Ebersberg, Germany). Coding sequences were then introduced into destination vectors pKNTAP and pKCTAP (Van Leene *et al.* 2007) by LR reaction according to manufactory's protocol and transformed to *Agrobacterium tumefaciens* strain C58C1RifR (pMP90) by electroporation.

Transformation of cell culture *A. thaliana* ecotype Landsberg *erecta* (PSB-D), tandem affinity purification and protein identification was performed following Van Leene *et al.* (2007).

3.13.2. Tandem affinity purification of STII in yeast

Tandem affinity purification was performed as described by Rigaut *et al.* (1999) with some modifications. The *S. cerevisiae* strain expressing STII-TAP from its natural chromosomal location (MATa his3 Δ 1 leu2 Δ 0 met15 Δ 0 ura3 Δ 0) was obtained by Biocat (Heidelberg, Germany). Yeast cells were grown at 30 °C in YPD [1 % (w/v) yeast extract, 2 % (w/v) peptone, 2 % (w/v) glucose] or minimal medium lacking specific amino acids (0.67 % yeast nitrogen base without amino acids, 2 % glucose, supplemented with all required amino acids)

to an optical density at 600 nm of 2 to 3. Cells of 200 ml culture were harvested (approximately 2 g), washed with water and resuspended in TAP lysis and IgG binding buffer [50 mM Tris-HCl pH 8, 150 mM NaCl, 0.1 % Tween-20, added before use: 1 mM PMSF, 1 mM DTT, 1 X protease inhibitor (Roche, Mannheim, Germany)]. Cells were disrupted twice in the presence of glass beads (0.25-0.3 mm, Roth, Karlsruhe, Germany) for 45 sec at 5,000 rpm in Precellys (Peqlab, Erlangen, Germany) and centrifuged at 16,000 x g for 10 min at 4 °C (Eppendorf centrifuge 5417R with FA45-24-11 rotor, Eppendorf, Hamburg, Germany). Supernatants were transferred to 100 µl IgG-Sepharose 6 Fast Flow beads (GE Healthcare, Freiburg, Germany) in Poly-Prep columns (Biorad, München, Germany) pre-equilibrated with 10 ml of IPP150 buffer (10 mM Tris-Cl pH 8.0, 150 mM NaCl, 0.1 % Tween-20), supplemented with 1 mM PMSF and 1 X protease inhibitor (Roche). After incubation for 2 h at 4 °C under gentle rotation the IgG-Sepharose beads were washed three times with 10 ml IPP150 buffer and once with 10 ml TEV cleavage buffer (IPP150 buffer, added before use: 0.5 mM EDTA, 1 mM DTT). Bound bait protein with its interaction partners was eluted with TEV protease (100 U, Invitrogen, Karlsruhe, Germany) in 1 ml TEV cleavage buffer for 1 h at 21 °C under gentle rotation followed by gravity flow. An aliquot of IgG eluate fraction was retained for SDS-PAGE. One volume of IgG eluate fraction was mixed with three volume of calmodulin binding buffer (CBB) (10 mM Tris-Cl pH 8.0, 150 mM NaCl, 0.1 % NP-40, 1 mM Mg-acetate, 1 mM imidazole, 2 mM CaCl₂, added before use: 10 mM β-mercaptoethanol, 1 mM PMSF) and CaCl₂ concentration was adjusted to 2 mM. This fraction was transferred to 100 µl calmodulin sepharose (GE Healthcare, Freiburg, Germany) in Poly-Prep columns pre-equilibrated with 10 ml CBB. After incubation over night at 4 °C under gentle rotation, calmodulin sepharose beads were washed three times with 10 ml CBB. Bound bait protein and its interaction partners were eluted 5 times with 200 µl calmodulin elution buffer (10 mM Tris-Cl pH8.0, 150 mM NaCl, 0.1 % NP-40, 1 mM Mg-acetate, 1 mM imidazole, 2 mM EGTA, added before use: 10 mM β-mercaptoethanol). Fractions were analyzed by SDS-PAGE and protein visualized by Coomassie staining.

3.14. Enrichment of phosphorylated peptides

3.14.1. Immobilized metal ion affinity chromatography

Protein reduction, alkylation, digestion with trypsin, desalting of peptides and immobilized metal ion affinity chromatography (IMAC) followed by phosphopeptide enrichment was

performed for the reference protein casein as described in Villen and Gygi (2008). A 20 μM casein solution was prepared by dissolving casein in lysis buffer [8 M urea, 75 mM NaCl, 50 mM Tris-HCl pH 8.2, 1 X protease inhibitor (Roche, Mannheim, Germany), 50 mM NaF, 50 mM β -glycerophosphate, 1 mM sodium orthovanadate, 10 mM sodium pyrophosphate, 1 mM PMSF]. The casein solution was incubated for 25 min at 56 °C in the presence of 5 mM DTT to reduce the disulfide bonds. Alkylation of free cysteines was performed in the presence of 14 mM iodoacetamide at room temperature for 30 min in the dark. The unreacted iodoacetamide was quenched by adding 5 mM DTT and incubating 15 min at RT in the dark. The urea concentration in the protein mixture was reduced to 1.6 M by dilution of 1:5 in 25 mM Tris-HCl, pH 8.2. CaCl_2 was added to a final concentration of 1 mM before proteins were digested with 0.2 $\mu\text{g } \mu\text{l}^{-1}$ trypsin (Sequencing Grade Modified Trypsin V511, Promega, Mannheim, Germany) in a enzyme:substrate ratio of 1:200 overnight at 37 °C. The digest was terminated by adjusting the pH to ~2 with TFA to 0.4 % (v/v) and the resulting pellet was removed by centrifugation at 20 min for 18,000 g at 4 °C (Eppendorf centrifuge 5415C, Eppendorf, Hamburg, Germany).

Peptides were desalted using SepPak with 50 mg of tC18 beads (Waters, Eschborn, Germany). The cartridge was conditioned using 3 ml ACN followed by 1 ml 50 % ACN, 0.5 % HAcO. Three ml 0.1 % TFA were used for equilibration before sample was applied. Desalting of the peptides was performed with 3 ml 0.1 % TFA. Remaining TFA was removed by adding 300 μl 0.5 % HAcO, before peptides were eluted with 1 ml 50 % ACN, 0.5 % HAcO. The eluted peptides were dried for 2.5 h at RT in a vacuum centrifuge (Concentrator 5301, Eppendorf, Hamburg, Germany).

One hundred μl of IMAC bead suspension (PhosSelect, Sigma-Aldrich, Taufkirchen, Germany) were prepared by adding of 1 ml IMAC binding buffer [40 % (v/v) ACN, 25 mM FA in H_2O], shaking and discarding the supernatant, three times each. Finally, the beads were resuspended in 100 μl IMAC binding buffer. Ten μl of the prepared IMAC bead suspension was incubated with the desalted peptides diluted in 120 μl IMAC binding buffer for 60 min at RT. The supernatant was transferred to a new reaction tube for MS analysis. The IMAC beads were washed twice with 120 μl IMAC binding buffer and wash fractions were subjected to MS analysis. Elution was performed twice by incubation with 40 μl IMAC elution buffer A (50 mM K_2HPO_4 pH 10) at RT. The eluates were neutralized by addition of 40 μl 10 % FA and dried for 1 h at RT in a vacuum centrifuge (Concentrator 5301, Eppendorf, Hamburg, Germany).

StageTips for phosphopeptide desalting were prepared according to Rappsilber *et al.* (2001). A first 200 μ l tip was cut directly behind the bottom with a razor-blade. A second 200 μ l tip was cut the same way, but with a wider opening. The second tip was used for cutting out the C18 Empore material (3M Germany, Neuss, Germany). By putting the second tip into the first one, the C18 material was directly transferred to the first tip using a 10 μ l gel loader tip. StageTips were positioned into an adaptor for centrifugation consisting of an on the bottom cutted 0.5 ml reaction tube within a 2 ml reaction tube. StageTips were equilibrated by passing each time 20 μ l MeOH, 20 μ l 50 % (v/v) ACN, 0.5 % (v/v) HAcO and 20 μ l 1 % FA through. The last step was performed twice. The dried eluate of IMAC was solubilized in 20 μ l 1 % FA and passed through the StageTip. After one wash step using 20 μ l 1 % FA, peptides were eluted by passing 40 μ l 50 % (v/v) ACN, 0.5 % (v/v) HAcO through. All samples were dried for 30 min at RT in a vacuum centrifuge (Concentrator 5301, Eppendorf, Hamburg, Germany) and stored at -20 °C until MS analysis. Samples were solubilized in 10 μ l 5 % (v/v) ACN, 4 % (v/v) FA. Flow-through and wash fractions of IMAC and StageTips were diluted 1:100 in 5 % (v/v) ACN, 4 % (v/v) FA.

0.5 μ l of each fraction were deposited onto the MALDI target, but subsequently covered with 1 μ l matrix solution [2 mg/ml 2.5-dihydroxybenzoic acid (DHB) in 50 % (v/v) MeOH, 0.2 % (v/v) TFA]. MALDI-TOF mass spectrometry was performed as described in section 3.9.1.

3.14.2. Phos-tag agarose

Casein reduction, alkylation, digestion with trypsin and desalting of peptides was performed as described in section 3.14.1.

For STIAT isoform, a 1.5 nM protein solution was prepared in 50 mM ammonium bicarbonate (ABC). Reduction and alkylation was performed as described for casein. As the protein was dissolved in ABC, protein was directly digested with 0.2 μ g μ l⁻¹ trypsin (Sequencing Grade Modified Trypsin V511, Promega, Mannheim, Germany) in a enzyme:substrate ratio of 1:200 overnight at 37 °C. The termination of the digest and the desalting of peptides was performed as described for casein in section 3.14.1.

Phosphopeptide enrichment using Phos-tag agarose was performed according to Kinoshita *et al.* (2005).

Zebra desalt columns (Thermo Fisher Scientific, Braunschweig, Germany) were filled with 60 μ l Phos-tag agarose and centrifuged for 20 sec at 2,000 g. Phos-tag agarose was incubated

with balancing buffer (10 mM MES, 0.1 M NaCl, 5 mM sodium oxalate, pH 6.0 with NaOH; added before use: 10 mM Zn acetate) for 5 min at RT. Balancing buffer was removed by centrifugation as described before and agarose was incubated twice with binding buffer (10 mM MES, 0.1 M NaCl, 5 mM sodium oxalate, pH 6.0 with NaOH). One hundred μ l of desalted peptides (40 μ g of casein, 20 μ g of STIAT) were incubated with Phos-tag agarose for 5 min at RT and removed by centrifugation. After three washing steps with 100 μ l binding buffer, peptides were eluted four times using 5 % (w/v) NH_3 . 0.5 μ l of each fraction were deposited onto the MALDI target, but subsequently covered with 1 μ l matrix solution (20 mg/ml 2,5-dihydroxybenzoic acid (DHB) in 50 % (v/v) MeOH, 0.2 % (v/v) TFA). MALDI-TOF mass spectrometry was performed as described in section 3.9.1.

3.15. Preparative IEF of STIAT isoforms

Protein extraction was performed as described in section 3.3.3, but the pelleted precipitate was solubilized in 1.25 X sample buffer [8.4 M urea, 2.4 M thiourea, 78 mM DTT, 6 % (v/v) glycerol, 1.2 % IPG buffer, 0.005 % (v/v) bromphenol blue] for 1 h at 37 °C under shaking conditions.

Preparative IEF was performed following the user protocol (Agilent, Böblingen, Germany). The device was set up for the 12 fractions separation by using a 12 cm in length IPG gel strip (GE Healthcare, Freiburg, Germany, pH 4-7). IPG strip was swelled in rehydration solution (1 X sample buffer) for 15 min at RT. One mg total protein extract (corresponding to 1.8 ml) was loaded. Preparative IEF was performed on Offgel fractionator 3100 unit (Agilent) with the following parameters: maximum current of 50 μ A, total voltage of 20 kVh. After focusing, 50 to 200 μ l of sample was recovered for each well and transferred in individual micro tubes. Fractions were precipitated using MeOH/chloroform (Wessel and Flügge 1984) and analysed by SDS-PAGE either by Coomassie staining or immunoblotting with antiserum directed against the recombinant STINT.

3.16. Ion exchange chromatography of STIAT isoforms

Total protein extracts were prepared from Arabidopsis leaves as described in section 3.7 with minor modifications. Four g intact frozen leaf material was homogenized prior to extraction and incubated with 11.2 ml 0.05 M HEPES pH 8.5 supplemented with 1 X protease inhibitor cocktail (Roche, Mannheim, Germany) for 30 min at 4 °C with mixing every 5 min. When

influence of phosphorylation was investigated, extraction buffer contained additionally 1 X phosphatase inhibitor cocktail (Roche, Mannheim, Germany). After centrifugation at 16,000 g for 10 min at 4 °C, proteins were reextracted. The supernatants obtained after a second centrifugation step were desalted against anion exchange running buffer (0.05 M HEPES pH 7.5) using PD10 desalting units (GE Healthcare, Freiburg, Germany).

Ten to 14 ml of total protein extracts (referring 6 to 14 mg total protein) were loaded on a 1 ml Hi Trap Resource Q anion exchange column in ÄktaExplorer System (GE Healthcare, Freiburg, Germany) at a flow rate of 0.25 ml min⁻¹ pre-equilibrated in anion exchange running buffer (0.05 M HEPES pH 7.5). After loading of the sample chromatography was continued at a flow rate of 0.5 ml min⁻¹. Elution of proteins was performed as following: direct 10 % anion exchange elution buffer (0.05 M HEPES, 1 M NaCl pH 7.5) for 12 ml, 35 % anion exchange elution buffer in 15 min and holding for 10 ml, 100 % anion exchange elution buffer in 10 min. Fractions of 1 ml were collected and 10 µl of each fraction was analyzed by immunoblotting with antiserum directed against the recombinant STINT.

4. Results

The STINT protein was originally found in a comparative proteomic approach between leaf and trichome preparations in tobacco and identified based on homology to a stress-induced protein of *A. thaliana* (Amme *et al.* 2005). The functional characterisation of STINT in tobacco was initiated by analysing the protein expression using immunoblotting, the cellular and subcellular localisation using GUS and GFP fusion constructs and knock down of gene by RNAi approach (Hedtmann 2005, Hedtmann 2007). In order to gain further insight into the biochemical and functional properties of this protein, the characterisation of stress-induced protein in *A. thaliana* (STIAT) was initiated. Three genes encode for STIAT protein family in the genetic model system Arabidopsis. The gene product of the gene located on chromosome one, named *STIAT1* (At1g62740), showed highest homology of 76.3 % to tobacco stress-induced protein STINT (Hedtmann 2007). The other two genes, one located on the same chromosome and one on the fourth chromosome, are named *STIAT2* (At1g12270) and *STIAT3* (At4g12400) and are presumably the result of two duplication events. The gene products of *STIAT1* (571 aa) and *STIAT2* (572 aa) have the same sequence length, while *STIAT3* (558 aa) lacks some amino acids when compared to the other two (Figure 5).

4.1. Characterisation of STIAT isoform expression

Four different Arabidopsis lines, Columbia-0 ecotype with T-DNA insertion in exons of *STIAT1*, *STIAT2* and *STIAT3* genes, were identified from www.gabi-kat.de and signal.salk.edu. In the following, the lines GABI_399G03, GABI_028A04, GABI_420A10 and SALK_023494 are named *stiat1-1*, *stiat1-2*, *stiat2-1* and *stiat3-1*, respectively.

4.1.1. Identification and analysis of *stiat1-1* and *stiat2-1* T-DNA insertion lines

The relative positions of T-DNA insertions in *STIAT1* and *STIAT2* genes are indicated in Figure 7A. Plants homozygous for the respective knock-out were identified by PCR-based genotyping. Immunoblots using the antiserum directed against the recombinant tobacco protein STINT are shown for one representative plant per line compared to Columbia-0 as control with colloidal Coomassie Brilliant Blue (cCBB) stained gels as loading control (Figure 7B). T-DNA insertion lines for *STIAT1* (*stiat1-1*, *stiat1-2*) showed absence of the lower band in leaf extracts compared to Columbia-0, demonstrating the knock-out of *STIAT1*.

The STIAT2 (*stiat2-1*) mutant line resulted in absence of upper band, indicating STIAT2 protein deletion there. Further isoforms were not detected in all lines under these conditions.

The identity of STIAT isoforms in leaves of Columbia-0 grown under control conditions was further proven by mass spectrometric analysis after immunoprecipitation (see section 4.1.4).

The T-DNA insertion line for STIAT3 (*stiat3-1*) was also analysed, but indicated no functional T-DNA insertion for STIAT3 (Figure A 1) and was not further investigated.

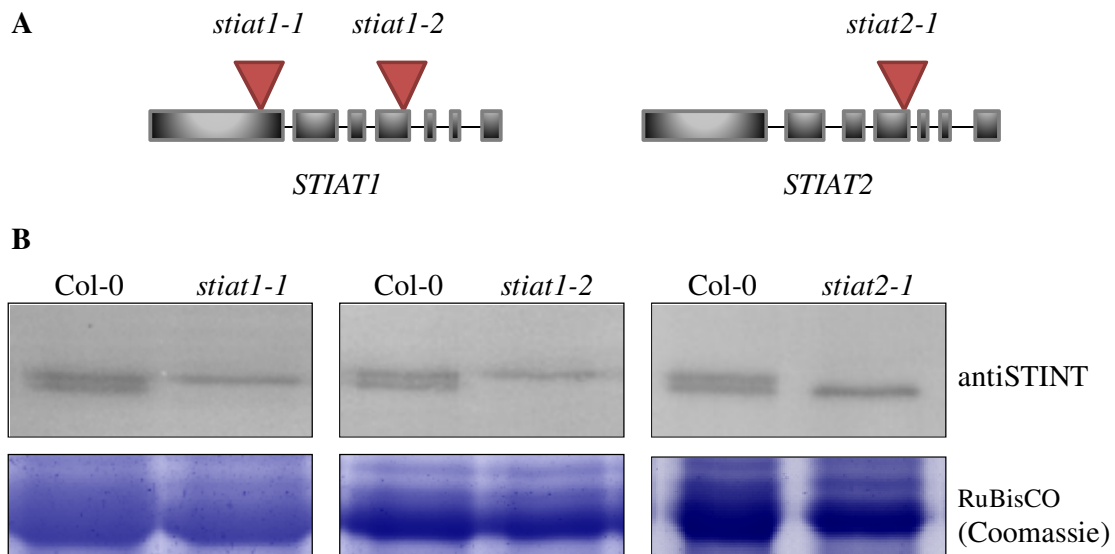


Figure 7: Analysis of T-DNA insertion lines of *STIAT1* and *STIAT2* in Columbia-0 ecotype.

A: Relative positions of T-DNA insertions in *STIAT1* and *STIAT2* genes, indicated by red triangles.

B: Immunodetection of STIAT isoforms in T-DNA insertion lines and Col-0. Five μ g of total leaf protein extracts were separated on SDS-PAGE and probed with antiserum against STINT. Knock-out lines of *STIAT1* (*stiat1-1*, *stiat1-2*) showed the absence of lower band, indicating depletion of *STIAT1* there. In contrast, *STIAT2* deletion resulted in absence of upper band. The Coomassie staining of ribulose-1,5-bisphosphate carboxylase-oxygenase (RuBisCO) was used as loading control.

4.1.2. Morphological characterisation of *stiat1-1* and *stiat2-1* during abiotic stresses

In order to elucidate the potential significance of *STIAT1* and *STIAT2*, analyses of their T-DNA insertion lines during control and abiotic stress conditions was performed. Previous data showed that gene silencing of STINT in tobacco lead to a stunted phenotype after exposition to long term cold stress with impact on the growth parameters plant height and leaf area. (Figure 1E, Hedtmann 2007). To confirm this in Arabidopsis, the identified T-DNA insertion lines for *STIAT1* and *STIAT2* were used and subjected to comparable stress conditions (Figure 8). Five-week-old plants were grown for two weeks at 10 °C or 30 °C, representing cold and heat treatments, respectively. Plants serving as control were grown at 20 °C. No

obvious differences regarding leaf anatomy were observed between STIAT1 and STIAT2 T-DNA insertion lines compared to Columbia-0 under control or stress conditions (Figure 9).

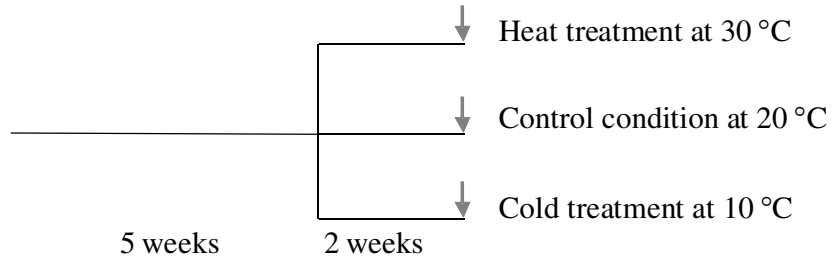


Figure 8: Schematic presentation of the experimental set-up of the stress experiments performed with T-DNA insertion lines for STIAT1 and STIAT2 and Columbia-0 as control line.

Five-week-old plants grown under control conditions at 20 °C were further grown under heat treatment at 30°C or cold treatment at 10°C for two weeks. Plants grown at 20 °C represent control conditions.

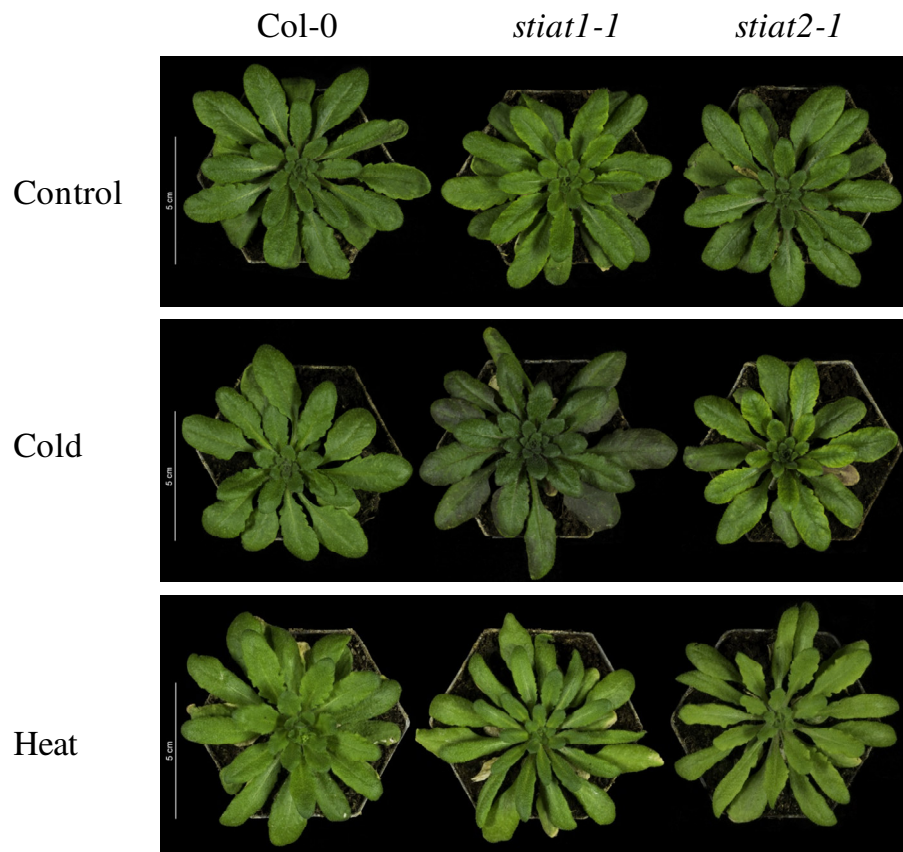


Figure 9: Phenotype of *stiat1-1* and *stiat2-1* T-DNA insertion lines after cold or heat stress treatment. Five-week-old plants were subjected to 10 °C or 30 °C for two weeks. Growth at 20 °C represents control conditions. No phenotypic difference was observed between T-DNA insertion lines of STIAT1 and STIAT2 compared to Columbia-0 under all conditions.

Different biometric parameters for leaves were measured, including ‘diameter of rosette’, ‘number’ and ‘fresh weight of leaves’ to obtain quantitative morphological data. In three independent experiments 15 plants per line and condition were analysed for these parameters. Statistical analysis was done by ANOVA followed by Tukey test with a significance level $p < 0.05$. The summary of the statistical analysis among all three experiments is shown in Table 1. No differences between mutants and control line in all three experiments were observed for parameter ‘fresh weight of leaves’. Significant decreases of ‘number of leaves’ and ‘diameter of rosettes’ of both mutant lines compared to Columbia-0 under cold stress were only observed in one of three experiments. Furthermore, parameter ‘diameter of rosette’ showed significant changes for both mutants in all treatments, but again in most cases only in one of three experiments.

Table 1: Statistical analysis of *stiat1-1* and *stiat2-1* leaf growth parameters compared to Columbia-0, cultivated at 10 °C (cold) or 30 °C (heat) for two weeks.

Means of $n = 15$ plants were analysed by ANOVA followed by Tukey-test with $p < 0.05$.

↔: No significant changes compared to Columbia-0.

↓/↑: Significant decrease/ increase in comparison to Columbia-0.

1, 2, 3: Number of experiment.

Parameter	Control		Cold		Heat	
	<i>stiat1-1</i>	<i>stiat2-1</i>	<i>stiat1-1</i>	<i>stiat2-1</i>	<i>stiat1-1</i>	<i>stiat2-1</i>
Fresh weight of rosette	↔	↔	↔	↔	↔	↔
Number of leaves	↔	↔	↔ ^{2,3} ↓ ¹	↔ ^{2,3} ↓ ¹	↔	↔
Diameter of rosette	↑ ¹ ↓ ² ↔ ³	↔ ^{1,3} ↓ ²	↔ ^{1,2} ↓ ³	↔ ^{2,3} ↓ ¹	↑ ^{1,3} ↔ ²	↔

Figure 10 shows the graphical data for one of the three experiments. Here, no statistical differences between *stiat* mutant lines compared to Columbia-0 under control and stress conditions were observed for any of the measured parameters.

In summary, knocking down either STIAT1 or STIAT2 alone results in no strong phenotypic alterations under the chosen experimentally conditions, indicating redundant functionality of STIAT1 and STIAT2.

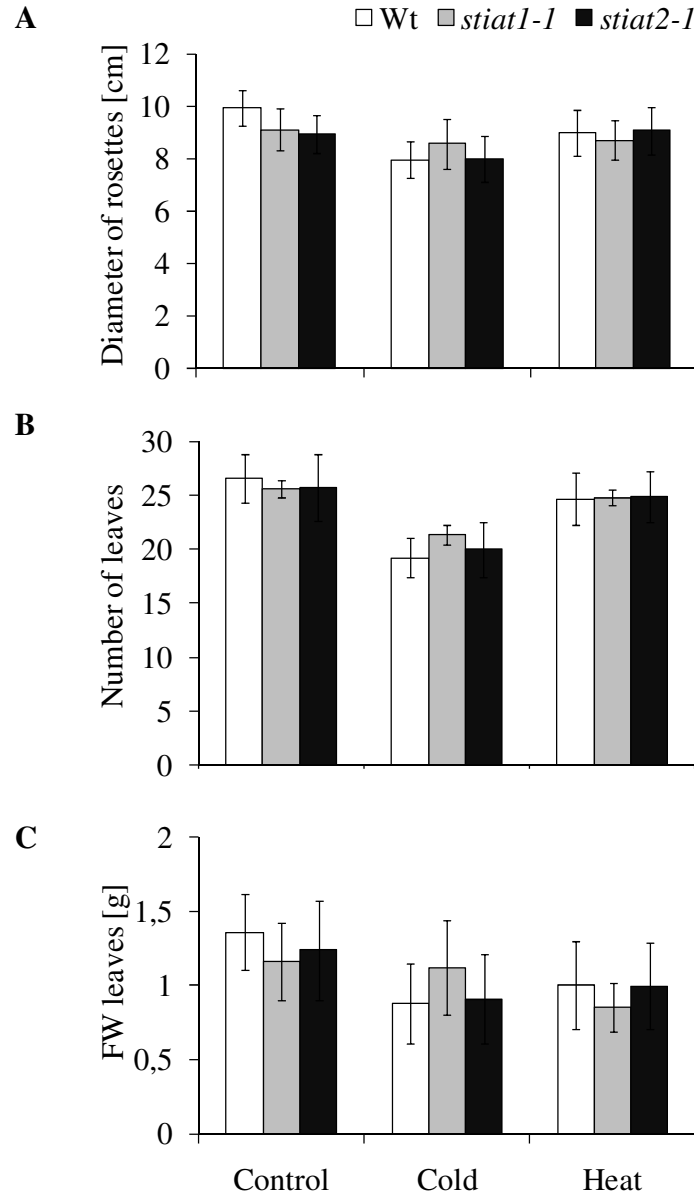


Figure 10: Measurements of leaf growth parameters of five-week-old *stiat1-1* and *stiat2-1* mutants, cultivated at 10 °C (cold) or 30 °C (heat) for two weeks.

A: Diameter of rosette. B: Number of leaves. C: Fresh weight (FW) of leaves.

Means of $n = 15$ plants per treatment of one representative harvest are shown. Statistical analysis between mutant lines and Columbia-0 per treatment were analysed by ANOVA followed by Tukey-test with a significance level at $p < 0.05$. No significant differences were detected.

4.1.3. STIAT isoform expression in *stiat1-1* and *stiat2-1* during abiotic stresses

The annotation of *STIAT* genes and homologues in other species as stress-induced was based on gene expression data (Zimmermann *et al.* 2004). Therefore, the expression of *STIAT* proteins during stress experiments was investigated. Previous data showed that *STINT* protein expression in tobacco was induced after heat and cold stress (Hedtmann 2007). To confirm

this finding in Arabidopsis, Columbia-0 and T-DNA insertion lines were subjected to identical stress conditions as described in 4.1.2 and used to detect differences in STIAT isoform expression. Protein extracts from Arabidopsis leaves were separated by SDS-PAGE and STIAT isoform expression was verified by Western blot analysis using antiserum directed against the recombinant tobacco protein STINT (Figure 11). Columbia-0 showed co-expression of STIAT2 and STIAT1 in all treatments with higher abundance after cold and heat stress. In mutant lines *stiat1-1* and *stiat2-1*, where only one of the two isoforms was expressed, the same tendency was observed. After heat stress treatment, both knock-out lines and Columbia-0 revealed an expression of an additional band, indicating STIAT3, the heat-inducible isoform. The identity of that additional band in leaves of Columbia-0 after heat stress was later proven by mass spectrometric analysis after immunoprecipitation (4.1.4).

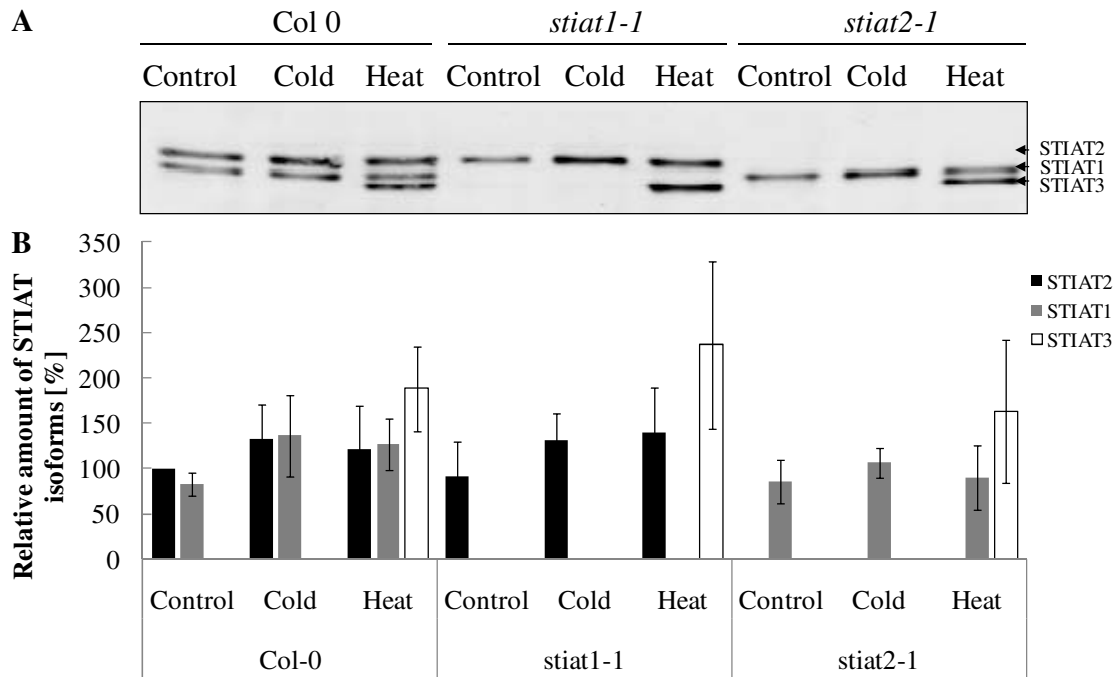


Figure 11: Analysis of STIAT isoform expression in leaves of T-DNA insertion mutants and Columbia-0 ecotype after cold and heat stress. The experiments were performed triply to ensure technical reproducibility.

A: Western blot analysis of two μg of total leaf protein extracts were separated on SDS-PAGE and probed with antiserum against STINT. One representative figure of the results obtained in at least three independently conducted experiments is shown.

B: Relative protein amount of STIAT isoforms. STIAT2 isoform of Col-0 grown under control conditions was set to 100 % and all other isoforms were calculated in relation to that isoform. Means of three biological replicates are shown.

STIAT2 and STIAT1 were co-expressed under control conditions and are higher abundant after cold and heat stress in Columbia-0. The same tendency is observed in the mutants with only one of the two isoforms. Both T-DNA insertion lines and Columbia-0 revealed an expression of a third band after heat treatment indicating the expression of the STIAT3 isoform (for confirmation by MS, see 4.1.4).

The STIAT isoform composition in leaves of heat stressed Columbia-0 ecotype and T-DNA insertion lines were additionally analysed by 2-D Western blot. Total proteins extracted under native conditions were analysed in the first dimension using isoelectric focussing (IEF) and in the second dimension by SDS-PAGE coupled to immunoblotting using antiserum directed against the recombinant tobacco protein STINT (Figure 12). In 2-D Western blot analysis, Columbia-0 and the knock-out lines for STIAT1 and STIAT2 showed expression of the additional spot, STIAT3, after heat stress treatment compared to control conditions. This isoform is detected the closest to pH 7, indicating the more basic isoform of the three.

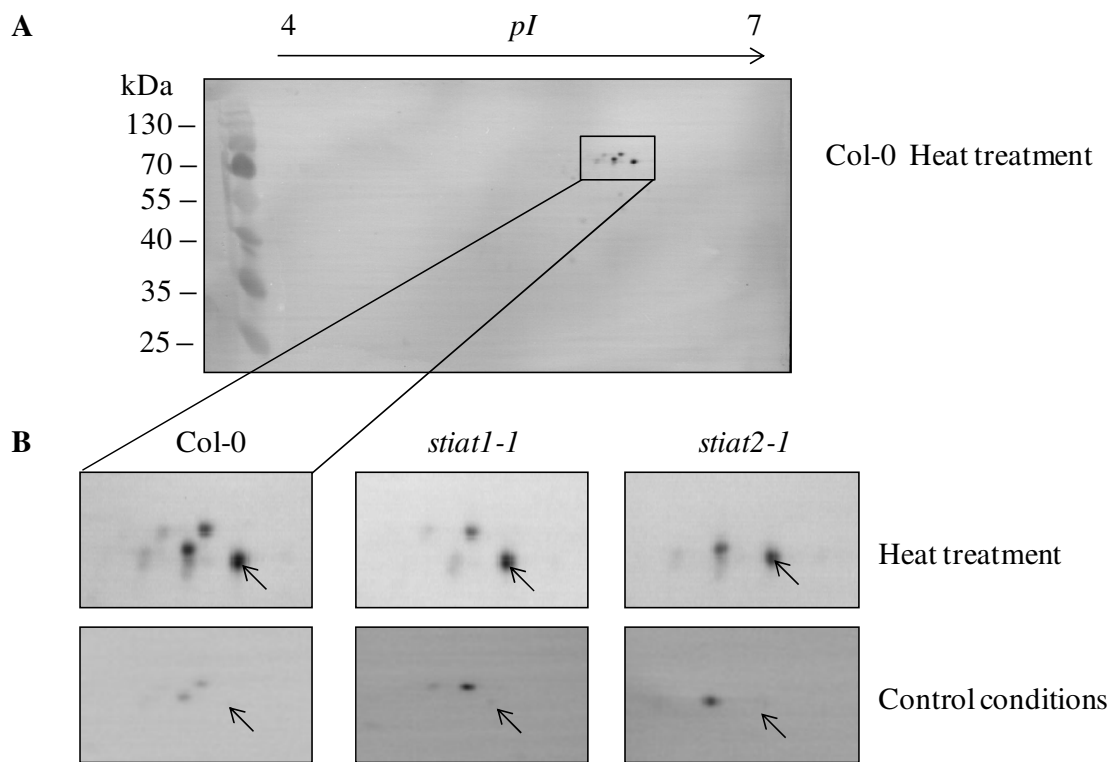


Figure 12: Characterization of STIAT isoform composition in leaves of Columbia-0 ecotype and T-DNA insertion mutants after heat stress. This experiment was performed from one biological harvest.

A: 2-D Western blot analysis of 15 μ g of total protein extract from heat stressed Columbia-0 leaves was separated on 7 cm pH gradients 4-7 and SDS-PAGE and probed with antiserum against STINT.

B: The indicated area of the immunoblot is reproduced with higher magnification, showing a protein pattern of three spots. The other five panels show total protein extract prepared from T-DNA insertion lines that were heat stressed as Columbia-0 (top) or remained under control conditions (bottom).

Arrowheads indicate the additional expression of STIAT3 in Columbia-0 and T-DNA insertion lines after heat treatment.

4.1.4. Identification of STIAT isoforms under control and heat conditions

Immunoprecipitation (IP) experiments of STIAT isoforms from leaves of *Arabidopsis* grown under control and heat stress conditions were performed to enrich the isoforms from total protein extracts and to ease their identification by MS analysis. Total protein extracts were precipitated by antibody raised against STINT and antiGoat serving as a negative control. Eluate fractions were separated by SDS-PAGE and either stained by cCBB or transferred to PVDF membrane and probed with antiserum directed against the recombinant tobacco protein STINT (Figure 13). The Coomassie stained gel showed detection of two and three protein bands in control and heat stressed leaf samples precipitated by anti-STINT antibody, respectively. Precipitation using the anti-goat antibody revealed no protein bands indicating specific binding during immunoprecipitation. Immunoblot analysis for the STIAT isoforms using antiSTINT antibody confirmed the findings obtained by the cCBB staining.

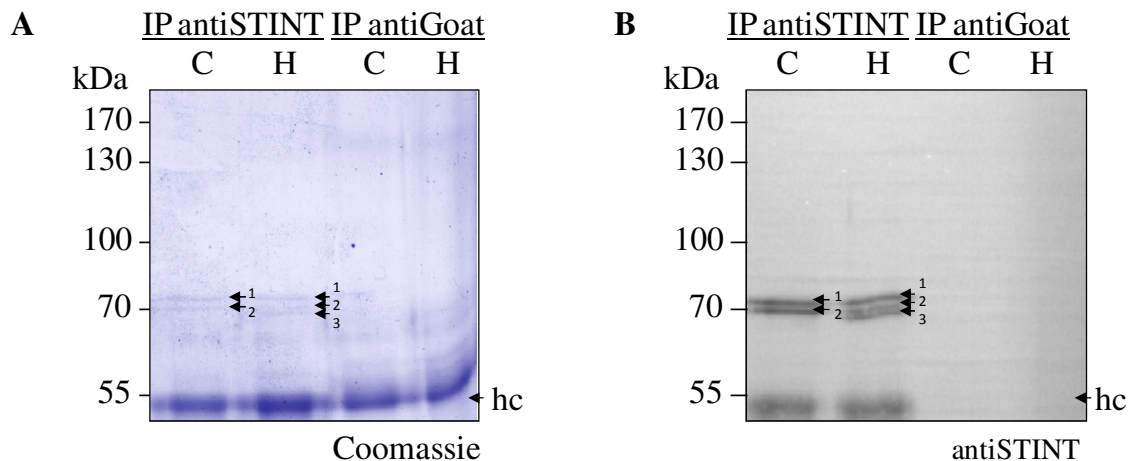


Figure 13: Immunoprecipitation of STIAT isoforms from Columbia-0 leaf samples using antiSTINT and antiGoat antibodies.

A: Precipitated fractions from control (C) or heat stressed leaves (H) were separated by SDS-PAGE and visualized by cCBB staining. Two and three bands (black arrowheads with numbers) were detected using the antiSTINT antibody, respectively, while no bands were found in IP experiments using the anti-goat antibody.

B: Immunodetection with antiserum against STINT confirmed exclusive detection of STIAT isoforms in precipitated fractions using antiSTINT antibody.

Hc represents the heavy chain of the antibodies, respectively.

These five detected bands were excised manually from the cCBB stained gels in order to verify the isoform identity. The gel bands were incubated with trypsin and peptide eluates were subjected to MS. Analysis by LC-ESI-Q-TOF MS/MS using the derived *de novo* sequences of tryptic peptides for homology-based database search led to distinct identification

of STIAT isoforms (summarized in Table 2). For each sample and each STIAT isoform the total and isoform-specific peptides are listed. The STIAT isoform with highest number of diagnostic peptides per sample is shown in bold, representing the STIAT isoform identified per sample. The identified peptides were analysed for their diagnostic properties by matching them to the complete protein sequences of the three isoforms (examples in Figure 14 to Figure 18). All peptides found in the first band derived from IP of control leaves were aligned to the protein sequences of the three isoforms (Figure 14). Four of five peptides were found to be diagnostic for STIAT2. ESI-MS/MS spectra of peptide ions for one diagnostic (SGLARAEASVAR) and one conserved peptide (GDLTPEELKER) are presented. The Figure 15 shows the identification of STIAT1 in band #2 derived from IP of control leaves, while identification of STIAT2, STIAT1 and STIAT3 in bands # 1, #2 and #3 derived from IP of heat stressed leaves is presented in Figure 16 to Figure 18.

In summary, the first and second band of control and heat stressed leaves revealed the identification of STIAT2 and STIAT1, respectively. The third band was detected in heat stressed leaves solely, and this band was reliably identified as STIAT3.

Table 2: Identification of precipitated STIAT isoforms from control and heat-stressed leaves by LC-ESI-Q-TOF MS/MS. Given are the sample as indicated in Figure 13, the protein name and accession number, the detected total and isoform-specific peptides revealed by ESI MS/MS. Overlapping peptide sequences occurred. The isoforms with maximum of diagnostic peptides are shown in bold.

Sample	Protein	Accession	Total peptides	Diagnostic peptides
Control 1	STIAT2	Q9LNB6	5	4
	STIAT1	Q5XEP2	2	1
	STIAT3	B9DG66	1	0
Control 2	STIAT1	Q5XEP2	11	9
	STIAT2	Q9LNB6	2	0
	STIAT3	B9DG66	1	0
Heat 1	STIAT2	Q9LNB6	9	6
	STIAT1	Q5XEP2	4	2
	STIAT3	B9DG66	2	0
Heat 2	STIAT1	Q5XEP2	5	3
	STIAT3	B9DG66	4	2
	STIAT2	Q9LNB6	2	0
Heat 3	STIAT3	B9DG66	10	8
	STIAT1	Q5XEP2	2	0
	STIAT2	Q9LNB6	2	0

A ...

STIAT1	KTVELKPDWGKGY SRLGAAHLGLNQFDEAVEAYSKGLEIDPSNEGLKSGLADAKASASRS	120
STIAT2	ETIKLKPYPWPKGY SRLGAAHLGLNQFELAVTAYKK GLDVDP TNEALKSGLADAEASVAR	120
STIAT3	KTIELKPDWSKGY SRLGAAFI GLSKFDEAVDSYKKGLEIDPSNEMLKSGLADASRSRVSS	120
STIAT1	RASAPNPFGDADFQGPPEMWSKLTADPSTRGLKQPDFVNMMEIQRNPSNLNLYLQDQVRM	180
STIAT2	RA-APNPFGDADFQGPPEMWTCLTSDPSTRGF LQQPDFVNMMEIQK NPS SLNLYL KDQVRM	179
STIAT3	KS---NPFVDAFQ GKEMWEKLTADPGTRVY LEQDDFVKTMKEIQRNPNLNLYLKMKDKRVM	177
...		
STIAT1	YSNRAACYTKLGAMPEGLKDAEKC IELDPTFLKGYSRKGA VQFFMKEYDNAMETYQKGLE	478
STIAT2	YSNRAASYTKLGAMPEGLKDAEKC IELDPTFSKGYSRK AAVO FLK EYDNAMETYQAGLE	479
STIAT3	YSNRAACYTKLGALPEGLKDAEKC IELDPSFTKGYSRKGA IQFFMKEYDKAMETYQEGLEK	465
STIAT1	HDPNNQELLDGVRKCVQQ INKANR GDLTPEELKER QAKGMQDPEIQNI LTDPVMRQVLSD	538
STIAT2	HDPSNQELLDGVRKCVQQ INKANR GDLTPEELKER QAKGMQDPEIQNI LTDPVMRQVLSD	539
STIAT3	HDPKNQEFLDGVRRCVEQ INKASR GDLTPEELKER QAKAMQDPEVQNI LSDPVMRQVLVD	525
STIAT1	LQENPAAQKHMQNPMIMNKIQK LISSGIVQMK	571
STIAT2	LQENPSAAQKHMQNPMVMNKIQKLISAGIVQMK	572
STIAT3	FQENPKAAQEHMKNPMVMNKIQKLVSAGIVQVR	558

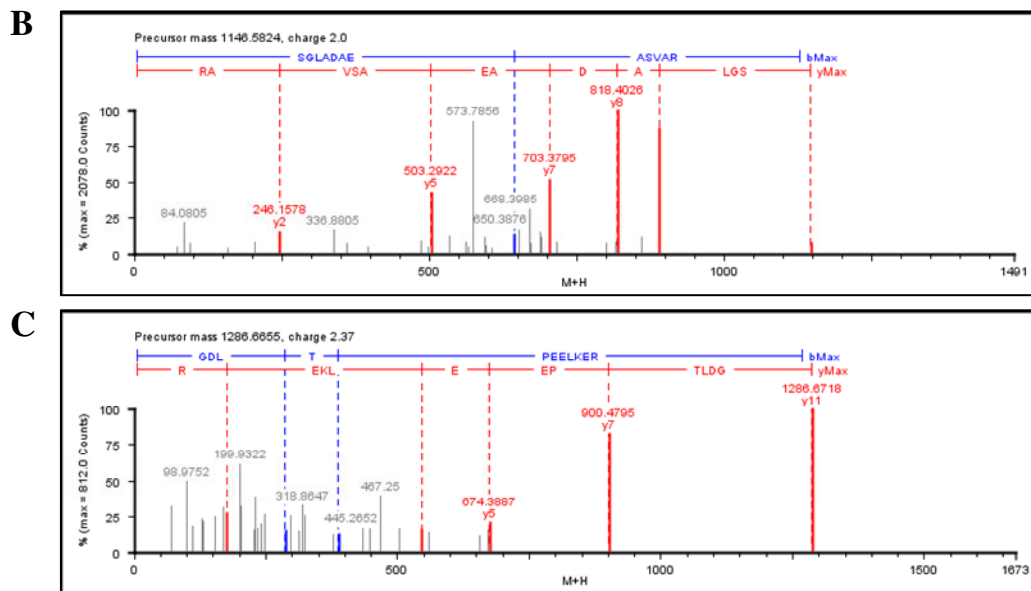


Figure 14: Identification of band #1 of control leaves after STINT-IP from Figure 13A as STIAT2 using LC-ESI-Q-TOF MS/MS.

A: Sequence alignment of STIAT isoforms and matching tryptic peptides sequenced by LC-ESI-Q-TOF MS/MS (**bold**) are displayed representing diagnostic (red underlined) or conserved peptides (red) for STIAT2. Additionally, one peptides diagnostic for STIAT1 was detected (*italics*).

B: ESI-MS/MS spectra of the diagnostic peptide SGLARAEASVAR (m/z 1146.5824 $[M+H]^+$).

C: ESI-MS/MS spectra of the conserved peptides GDLTPEELKER (m/z 1286.6655 $[M+H]^+$).

B (red) and Y (blue) ion series are shown as fragmentation products of the C-N bond leading to charge either the N-terminus (B ions) or C-terminus (Y ions).

STIAT1	MADEAKAKGNAAFSSGDFNSAVNHFTDAINLTPTNHVLFVSNR SAAHASLNHYDEALS DAK	60
STIAT2	MABEAKAKGNAAFSSGDFTTAINHFTFAIALAPTNNHVLVSNR SAAHASLHQYAEALS DAK	60
STIAT3	MABEAKSKGNAAFSSGDYATAITHFTFAINLSPTNNILYSNRSASYASLHRYEEALSDAK	60
STIAT1	KTVELKPDWGK GY SRLGAAHLGLNQFDEAVEAYSK GLEIDPSNEGLK SGLADAKASASRS	120
STIAT2	ETIKLKPYPWPKGY SRLGAAHLGLNQFELAVTAYKKGLDVPDPTNEALKSGLADAEASVARS	120
STIAT3	KTIELKPDWSKGY SRLGAAFI GLSKFDEAVDSYKKGLEIDPSNEMMLKSGLADASRSRVSS	120
STIAT1	RASAPNPFGDAFQGPEMWSKLTADPSTRGLLKQPDFVNMMEIQR NPSNLNLYLQDOR VM	180
STIAT2	RA-APNPFGDAFQGPEMWTCLTSDPSTRGF LQQPDFVNMMEIQK NPSNLNLYLKDQR VM	179
STIAT3	KS---NPFVDAFQ GKEMWEKLTADPGTRVY LEQDDFVKTMKEIQRPNNNLNLYMKDKRVM	177
...		
STIAT1	DCDKAVERGRELRSYKYMVAKALTRKGTALGKMAKVSK DYEPVIOTYOKALTEHRNP ETL	358
STIAT2	DCNKAVERGRELRSYKYMVARALTRKGTALTKMAKSKDYEP AIEAFQKALTEHRNP DTL	359
STIAT3	DCDKAVERGRELRSDFKMIARALTRKGSALVKMARC SKDFEP AIE TFQKALTEHRNPDTL	345
...		
STIAT1	YSNRAACYTK LGAMPEGLK DAEK IELDPTFLKGYSRKGAVQFFMKEYDNAMETYQK GLE	478
STIAT2	YSNRAASYTK LGAMPEGLK DAEK IELDPTFSKGYSRKA AVQFFLKEYDNAMETYQAGLE	479
STIAT3	YSNRAACYTKLGALPEGLKDAEK IELDPSFTKGYSRKGAIQFFMKEYDKAMETYQEGLK	465
STIAT1	HDPNNOELLDGVKR CVQQ INKANR GDLTPEELK ERQAKGMQDPEIQNI L TDPVMR QVLS D	538
STIAT2	HDPSNQELLDGVKRCVQQ INKANR GDLTPEELK ERQAKGMQDPEIQNI L TDPVMR QVLS D	539
STIAT3	HDPKNQEF LDGVRRCVEQ INKASR GDLTPEELK ERQAKAMQDPEVQNI L S D P V M R Q V L V D	525
STIAT1	LOENPAAQK HMQNPMIMNKIQKL ISSGIVQMK	571
STIAT2	LQENPSAAQKHMQNPMVMNKIQKLISAGIVQMK	572
STIAT3	FQENPKAAQEHMKNPMVMNKIQKLVSAGIVQVR	558

Figure 15: Identification of band #2 of control leaves after STINT-IP from Figure 13A as STIAT1 using LC-ESI-Q-TOF MS/MS. The sequence alignment of STIAT isoforms and matching tryptic peptides sequenced by LC-ESI-Q-TOF MS/MS are shown (bold). Nine peptides identified were diagnostic (red underlined) for STIAT1, two peptides were conserved (red) at least within two of three isoforms. Overlapping peptide sequences occurred.

STIAT1	KTVELKPDWGKGY SRLGAAHLGLNQFDEAVEAYSK GLEIDPSNEGLK SGLADAKASASRS	120
STIAT2	ETIKLKPYPWPKGY SRLGAAHLGLNQFELAVTAYKK GLDVPDPTNEALKSGLADAEASVARS	120
STIAT3	KTIELKPDWSKGY SRLGAAFI GLSKFDEAVDSYKKGLEIDPSNEMMLKSGLADASRSRVSS	120
STIAT1	RASAPNPFGDAFQGPEMWSKLTADPSTRGLLKQPDFVNMMEIQRNPNSLNLYLQDQRVM	180
STIAT2	RA-APNPFGDAFQGPEMWTCLTSDPSTRGF LQQPDFVNMMEIQK NPSNLNLYLKDQR VM	179
STIAT3	KS---NPFVDAFQ GKEMWEKLTADPGTRVY LEQDDFVKTMKEIQRPNNNLNLYMKDKRVM	177
...		
STIAT1	KKLKAQKEKELGNAAYKKKDFETA IQHYSTAMEIDDEDISYI TNRAAVHLEMGYDECIK	298
STIAT2	RKEKAKKEKELGNAAYKKKDFETA IQHYSTAI EIDDEDISYL TNR AAVYLEMGK YNECIE	299
STIAT3	RKEKALKEKGEVNAVYKKKDFGRAVEHYTKAMELDDEDI SYL TNR AAVYLEMGK YEECIE	285
STIAT1	DCDKAVERGRELRSYKYMVAKALTRKGTALGKMAKVSKDYEPVIQTYQKALTEHRNPETL	358
STIAT2	DCNKAVERGRELRSYKYMVARALTRKGTALTKMAKSK DYEP AIEAFOKALTEHRNPDTL	359
STIAT3	DCDKAVERGRELRSDFKMIARALTRKGSALVKMARC SKDFEP AIE TFQKALTEHRNPDTL	345
...		
STIAT1	YSNRAACYTK LGAMPEGLK DAEK IELDPTFLKGYSRKGAVQFFMKEYDNAMETYQKGLE	478
STIAT2	YSNRAASYTK LGAMPEGLK DAEK IELDPTFSKGYSR AAVOFFLK KEYDNAMETYQAGLE	479
STIAT3	YSNRAACYTKLGALPEGLKDAEK IELDPSFTKGYSRKGAIQFFMKEYDKAMETYQEGLK	465
STIAT1	HDPNNOELLDGVKRCVQQ INKANR GDLTPEELK ERQAKGMQDPEIQNI L TDPVMR QVLS D	538
STIAT2	HDPSNQELLDGVKRCVQQ INKANR GDLTPEELK ERQAKGMQDPEIQNI L TDPVMR QVLS D	539
STIAT3	HDPKNQEF LDGVRRCVEQ INKASR GDLTPEELK ERQAKAMQDPEVQNI L S D P V M R Q V L V D	525
STIAT1	LQENPAAQKHMQNPMIMNKIQKL ISSGIVQMK	571
STIAT2	LOENPSAAQK HMQNPMVMNKIQKLISAGIVQMK	572
STIAT3	FQENPKAAQEHMKNPMVMNKIQKLVSAGIVQVR	558

Figure 16: Identification of band #1 of heat stressed leaves after STINT-IP from Figure 13A as STIAT2 using LC-ESI-Q-TOF MS/MS. The sequence alignment of STIAT isoforms and matching tryptic peptides sequenced by LC-ESI-Q-TOF MS/MS are shown (bold). Six peptides identified were diagnostic for STIAT2 (red underlined), three peptides were conserved at least within two of three. Additionally, two peptides diagnostic for STIAT1 were detected (italics).

...

STIAT1	KTVELKPDWGKGY SRLGAAHLGLNQFDEAVEAYS K GLEIDPSNEGLK SGLADAKASASRS	120
STIAT2	ETIKLKPYPWPKGY SRLGAAHLGLNQFELAVTAYKKGLDVPDPTNEALKSGLADAEASVARS	120
STIAT3	KTIELKPDWSKGY SR LGAAFIGLSK FDEAVDSYKKGLEIDPSNEMLSGLADASRSRVSS	120

...

STIAT1	DCDKAVERGRELRS DYKMVAKALTRKGTALGKMAKVS K DYEPVIOTYOK ALTEHRNPETL	358
STIAT2	DCNK AVERGRELRS DYKMVARALTRKGTALTKMAKCS KDYEP AIEAFQKALTEHRNPDTL	359
STIAT3	DCDKAVERGRELRSDFKMIARALTRKGSALVKMARC SKDFEPAIETFQKALTEHRNPDTL	345

...

STIAT1	HDPNNQELLDG VKRCVQQ INKANR GDLTPEELKER QAKGMQDPEIQNILTDPV MRQVLS D	538
STIAT2	HDPSNQELLDG VKRCVQQ INKANR GDLTPEELKER QAKGMQDPEIQNILTDPV MRQVLS D	539
STIAT3	HDPK NOEFLDGVR RCVEQ INKASR GDLTPEELKER QAKAMQDPEVQNILSDPVMRQV LVD	525

STIAT1	LOENPAAQK HMQNPMIMNKIQKL ISSGIVQMK	571
STIAT2	LQENPSAAQKHMQNPMVMNKIQKL ISAGIVQMK	572
STIAT3	FQENPKAAQEHMKNPMVMNKIQKLVSAGIVQVR	558

Figure 17: Identification of band #2 of heat stressed leaves after STINT-IP from Figure 13A as STIAT1 using LC-ESI-Q-TOF MS/MS. The sequence alignment of STIAT isoforms and matching tryptic peptides sequenced by LC-ESI-Q-TOF MS/MS are shown (bold). Three peptides identified were diagnostic isoforms (red underlined) for STIAT1, one peptide was conserved for all isoforms. Additionally, two peptides diagnostic for STIAT3 were detected (italics).

...

STIAT1	KTVELKPDWGKGY SRLGAAHLGLNQFDEAVEAYS K GLEIDPSNEGLK SGLADAKASASRS	120
STIAT2	ETIKLKPYPWPKGY SRLGAAHLGLNQFELAVTAYKKGLDVPDPTNEALKSGLADAEASVARS	120
STIAT3	KTIELKPDWSKGY SR LGAAFIGLSK FDEAVDSY K GLEIDPSNEMLSGLADASRSRVSS	120

STIAT1	RASAPNPF GDAF QGPEMWSKLTADPSTRGLKQPDFVNMME IQRNPSNLNLYLQDQVRM	180
STIAT2	RA-APNPF GDAF QGPEMWTKLTS DPSTRGFLQQPDFVNMME IQKNPSNLNLYLKDQVRM	179
STIAT3	KS---NPFVDAF QGKEMWEKLTADPGTR VYLEODDFVK TMKE IQRNPNLNLYMCKDKRVM	177

...

STIAT1	DCDKAVERGRELRS DYKMVAKALTRKGTALGKMAKVS KDYEPVIQTYQKALTEHRNPETL	358
STIAT2	DCNK AVERGRELRS DYKMVARALTRKGTALTKMAKCS KDYEP AIEAFQKALTEHRNPDTL	359
STIAT3	DCDKAVERGRELRSDFKMIARALTRKGSALVKMARC SK DFEPAIETFOK ALTEHRNPDTL	345

...

STIAT1	YSNRAACYTKLGAMPEGLKDAEKC IELDPTFLKGY SRKAVQFFMKEYDNAMETYQKGLE	478
STIAT2	YSNRAASYTKLGAMPEGLKDAEKC IELDPTFSKGY SRKAAVQFFLKEYDNAMETYQAGLE	479
STIAT3	YSNRAACYTK L GALPEGLKDAEK IELDPSFTKGY SRKGAIQFFMKEYDKAMETYQEGLK	465

STIAT1	HDPNNQELLDG VKRCVQQ INKANR GDLTPEELKER QAKGMQDPEIQNILTDPV MRQVLS D	538
STIAT2	HDPSNQELLDG VKRCVQQ INKANR GDLTPEELKER QAKGMQDPEIQNILTDPV MRQVLS D	539
STIAT3	HDPK NOEFLDGVR RCVEQ INKASR GDLTPEELKER QAKAMQDPEVQNILSDPVMRQV LVD	525

STIAT1	LQENPAAQKHMQNPMIMNKIQKL ISSGIVQMK	571
STIAT2	LQENPSAAQKHMQNPMVMNKIQKL ISAGIVQMK	572
STIAT3	FOENPK AAQEHMKNPMVMNKIQKLVSAGIVQVR	558

Figure 18: Identification of band #3 of heat stressed leaves after STINT-IP from Figure 13A as STIAT3 using LC-ESI-Q-TOF MS/MS. The sequence alignment of STIAT isoforms and matching tryptic peptides sequenced by LC-ESI-Q-TOF MS/MS (red) are shown. Eight peptides identified were diagnostic isoforms (underlined), two peptides were conserved for all isoforms.

4.1.5. Gene and protein of STIAT3 isoform is induced after heat stress and present over the time of elevated temperature

Information on transcriptional alteration of STIAT isoforms during cold and heat stress was obtained from microarray data analysis using Genevestigator tool (Hruz *et al.* 2008) (Figure 19). Cold and heat stress studies performed on green tissue were selected. All cold treatment studies were performed with 4-week-old plants grown on soil and stress application varied in temperature and duration of stress ranging from 4 °C to 17 °C and 6 h to 14 d. STIAT1 showed strong upregulation at 4 °C for 24 h, which decreased during length of stress until 14 d. The same slight upregulation of STIAT1 at 4 °C for 14 d was observed at higher temperatures but shorter time (8 °C and 10 °C for 78 h). In the other cold stress treatments STIAT1 was not upregulated. STIAT2 showed a similar regulation during cold stress as STIAT1, but to a lesser extent. Cold stress had no influence on the expression of STIAT3. Transcriptional expression data of STIAT isoforms obtained after heat stress application on green tissue was less detailed compared to cold stress data. Heat treatment was performed only at one temperature and for a short time, 37 °C for either 30 min or 2 h. Plants differed in their age and growth conditions. Plants treated for 30 min were 3 weeks old and grown *in vitro*, whereas the plants incubated for 2 h were 8 weeks old and grown on soil. Both experiments showed upregulation of all three STIAT isoforms with highest abundance of STIAT3. When plants, grown *in vitro*, were shifted to control conditions after heat application, upregulation of the STIAT isoforms was diminished.

A time course experiment with Columbia-0 ecotype was performed to investigate the induction of STIAT3 isoform by heat and its expression during heat stress. Plants were subjected to comparable stress condition as described before, but the influence of heat treatment on STIAT3 expression in leaves was examined ranging from short term stress of 30 minutes up to long term stress of 14 days of heat stress. Protein extracts from Arabidopsis leaves were separated by SDS-PAGE and STIAT isoform expression was verified by Western blot analysis using antiserum directed against the recombinant tobacco protein STINT (Figure 20). Immunoblotting revealed an increased expression of STIAT3 after 1 day of heat stress and its continuous presence until 14 days of stress. Analysis of STIAT isoform expression in leaves without stress application served as control, showing only expression of STIAT1 and STIAT2.

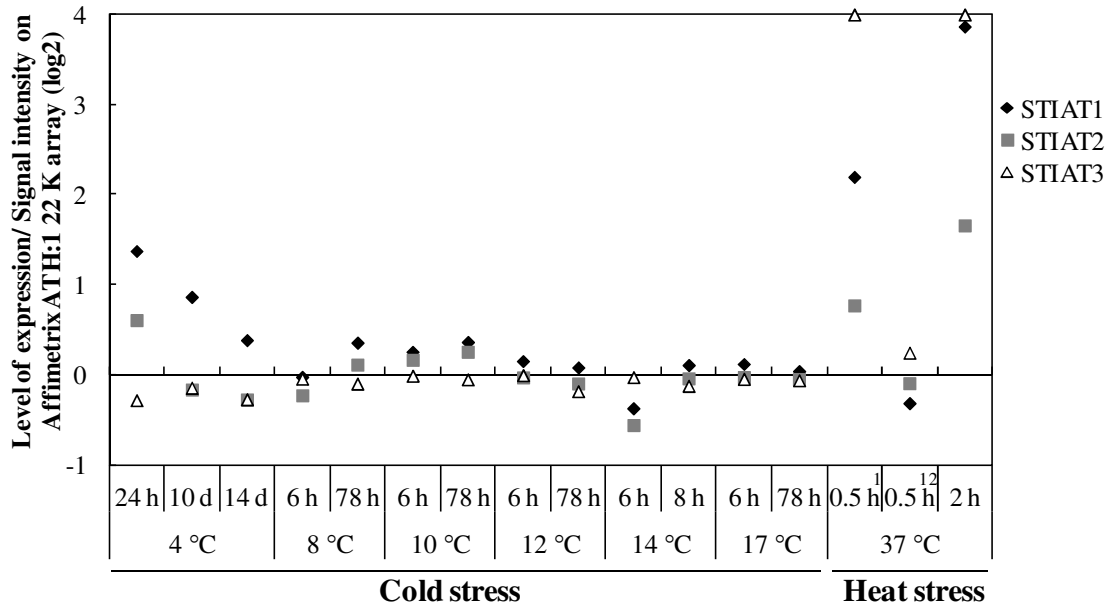


Figure 19: Transcriptional expression of STIAT isoforms in rosette tissue of Columbia-0 ecotype during cold and heat stress studies obtained from microarray data using Genevestigator tool (www.genevestigator.com, Hruz *et al.* 2008).

Microarray data analysis revealed respectable upregulation of STIAT1 and STIAT2 after short time cold stress at 4 °C for 24 h, which decreased over the time of stress. Slight induction of these isoforms was observed at higher temperatures, 8 °C and 10 °C, whereas STIAT3 showed no or even downregulation under cold stress. All three STIAT isoforms are highly upregulated after short time heat stress at 37 °C, from which STIAT3 showed the highest increase.

¹: Plants were grown *in vitro*. ²: Plants were re-shifted to control conditions for 48 h.

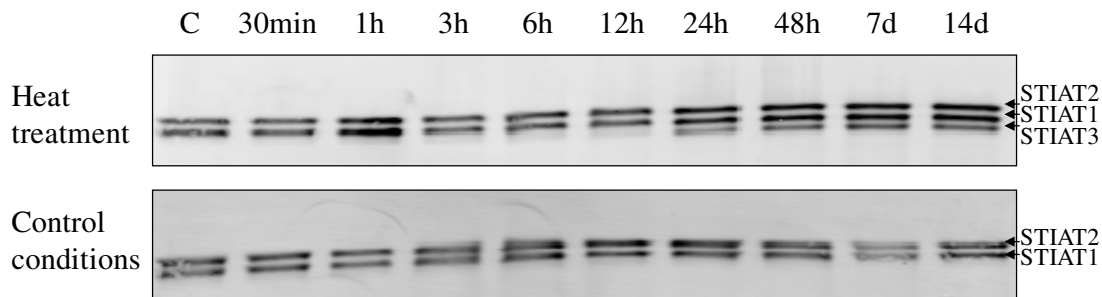


Figure 20: Characterisation of STIAT3 expression in leaves of Columbia-0 ecotype during heat stress. This experiment was performed only once.

Western blot analysis of five µg of total leaf protein extracts were separated on SDS-PAGE and probed with antiserum against STINT. STIAT3 protein was slightly induced after 1 day of heat stress and continuously expressed until the end of the treatment.

4.1.6. Organ-dependent expression of STIAT isoforms in Columbia-0

Localisation of the STIAT protein family in different tissue types of Arabidopsis was performed on total protein extracts of eight-week-old Arabidopsis Columbia-0 tissues,

separated by SDS-PAGE and subjected to Western blot analysis using antiserum directed against the recombinant tobacco protein STINT (Figure 21A). The cCBB stained gel served as a control (Figure 21B). Two STIAT isoforms were expressed in rosette leaves, whereas the third isoform was detectable in stem and flower. No STIAT isoform was present in roots under these conditions. Determination of the absolute protein amount revealed the presence of the STIAT isoforms in the range of 2-6 ng per μg total protein (Figure 21C). STIAT2 isoform showed the highest expression in the analyzed tissues, while STIAT1 and STIAT3 were detected with lower quantities.

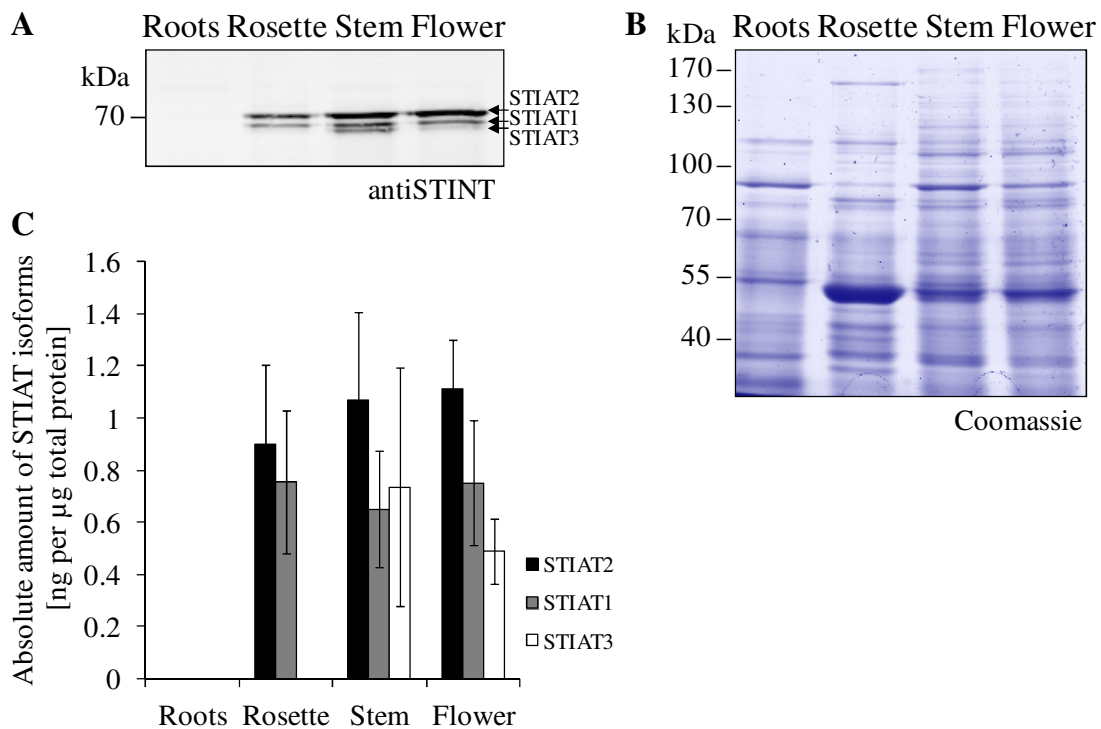


Figure 21: Protein expression of STIAT isoforms in different tissues of eight-week-old Columbia-0. Two biological replicates were performed.

A: Five μg of protein extracts from roots, leaf, stem or flower were separated by SDS-PAGE and subjected to Western blot analysis using antiserum directed against the recombinant tobacco protein STINT. STIAT2 and STIAT1 were detected in rosette, stem and flower. STIAT3 was also expressed in stem and flower. No expression level was found in roots. One technical replicate is shown.

B: The colloidal Coomassie Brilliant Blue staining of root protein served as a loading control.

C: Absolute protein amount of STIAT isoforms. STIAT isoforms of Col-0 tissues grown under control conditions are expressed in the range of 2 to 6 ng. Means of two biological replicates are shown.

Proteomic results were compared with microarray data obtained by Genevestigator tool (Hruz *et al.* 2008) (Figure 22) and revealed distinct differences. Here, STIAT1 showed the highest

expression and STIAT2 a medium level of expression in all organs analyzed including roots. STIAT3 transcripts pointed low signal intensity in stem and flower, whereas the protein was detectable in these organs using immunodetection.

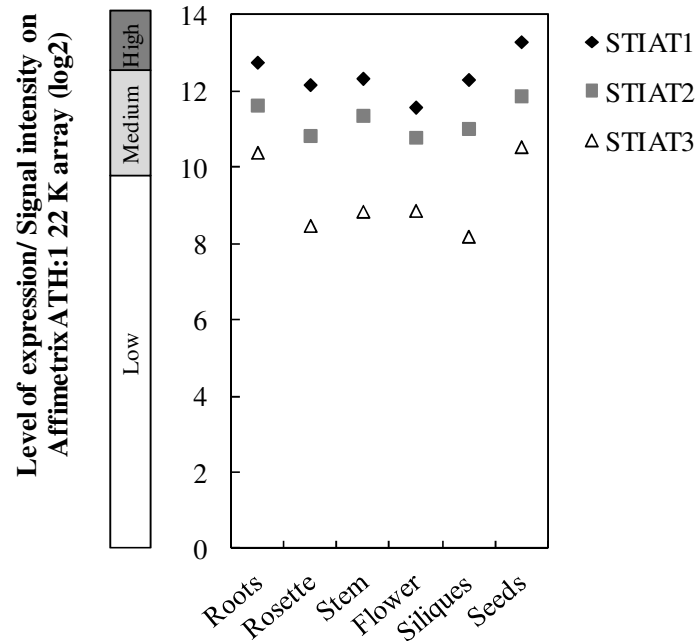


Figure 22: Transcriptional expression of STIAT isoforms in different organs obtained from microarray data using Genevestigator tool (www.genevestigator.com, Hruz *et al.* 2008).

Microarray data analysis revealed high and medium signal intensities for STIAT1 and STIAT2 in respective tissues. For STIAT3 low or medium signal intensities were detected.

4.2. Intracellular distribution of STIAT isoforms

4.2.1. Prediction of STIAT isoform localisation using *in silico* tools

Localisation of the STIAT1 isoform to cytosolic, nuclear and plasma membrane compartments was suggested according to the genomic database TAIR (The Arabidopsis Information Resource). The cytosolic and nuclear localisation of that isoform has been shown in earlier studies using GFP fusion construct (Hedtmann 2005). To obtain further evidences for the subcellular localisation and a possible association to membranes of STIAT isoforms, *in silico* analysis was performed using different software tools. Subcellular localisation of STIAT isoforms was analysed using the tools TargetP (Emanuelsson *et al.* 2000) and WoLF PSORT (Horton *et al.* 2007). Both programs analyse amino acid sequences for targeting sequences necessary for correct protein guidance to their compartments. While TargetP only

searches for targeting sequences of chloroplast, mitochondrial and secretory localisation, WoLF PSORT predicts also a cytosolic and nuclear localisation. TargetP detected neither chloroplast transit peptide, mitochondrial targeting peptide nor a signal peptide for secretory pathway in all three isoforms, indicating another localisation than in these organelles (Table A 1). The predicted subcellular localisation of STIAT isoforms using WoLF PSORT is shown in Table 3. The output was ranked according to a calculated likelihood score and highest numbers represent the predominant localisation. Whereas STIAT1 and STIAT2 were predicted to be mainly localised in the cytosol, the localisation of STIAT3 was predicted to be mainly in mitochondria. A lower prediction score for STIAT3 was found for the cytosol, while further STIAT1 and 2 predictions included mitochondria and nucleus, respectively. The assumed localisation of STIAT3 in mitochondria was verified by two more *in silico* tools. Mitoprot (Claros and Vincens 1996) and Predotar (Small *et al.* 2004) revealed no mitochondrial targeting peptides for all three isoforms (Table A 2). A possible localisation of STIAT isoforms in Arabidopsis mitochondria was not further investigated.

Table 3: *In silico* prediction of STIAT isoform localisation using WoLF PSORT (Horton *et al.* 2007).

Ranking of likelihood scores revealed a main predicted subcellular localisation of STIAT1 in cytosol, while STIAT2 is either localised there or in mitochondria. For STIAT3 the tool predicted a predeominant localisation in mitochondria.

Isoform	Cytosol	Nucleus	Mitochondria	Chloroplast	Plastids
STIAT1	7.0	2.0	4.0	-	-
STIAT2	5.0	2.0	5.0	-	1.0
STIAT3	3.0	1.0	7.0	1.0	1.0

The STIAT isoforms and the plasma membrane-type H⁺-ATPase from Arabidopsis (At2g18960) as reference were examined for transmembrane domains using the tools SOSUI (Hirokawa *et al.* 1998), HMMTop (Tusnady and Simon 2001) and DAS (Cserzo *et al.* 1997) to elucidate possible association to membranes. Earlier studies indicated the presence of the human HOP in Golgi apparatus and plasma membrane (Honore *et al.* 1992, Zanata *et al.* 2002). Transmembrane alpha-helices consist of around 15-30 amino acids, which are predominantly hydrophobic and necessary for anchoring the membrane. Algorithms of SOSUI and HMMTop did not predict such a transmembrane domain for STIAT isoforms. However, *in silico* analysis using DAS revealed one transmembrane domain between amino acids 183 to 187 for STIAT1 and 181 to 184 for STIAT3, respectively (Figure 23). The

transmembrane domain for STIAT2 was predicted between amino acids 180 to 187 at a lower threshold.

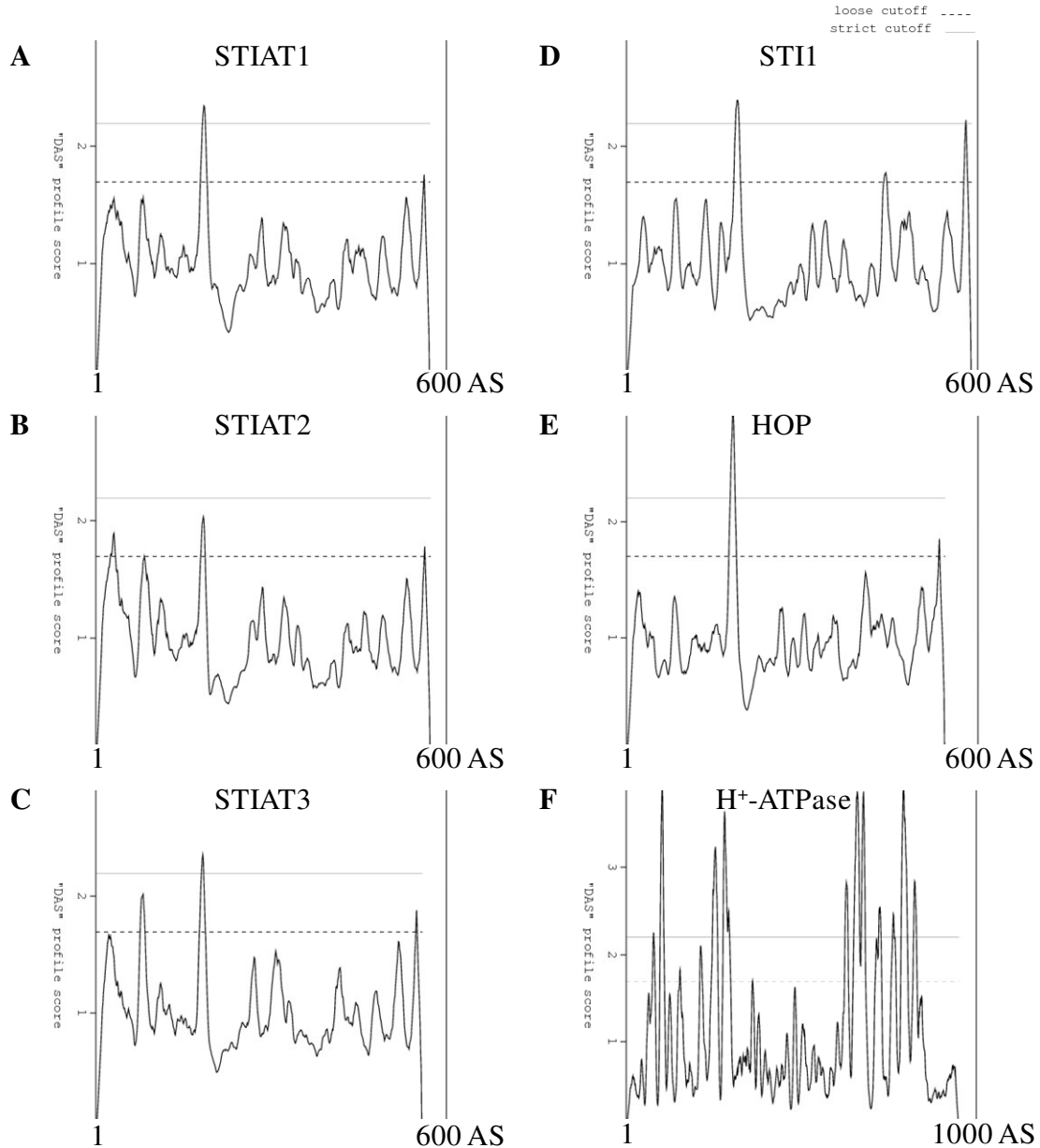


Figure 23: Prediction of transmembrane regions of STIAT isoforms (A-C) in comparison to yeast STI1 (D), human HOP (E) and the Arabidopsis plasmamembrane protein H⁺-ATPase1 (F) using *in silico* tool DAS (Cserzo *et al.* 1997).

Dashed and continuous lines represent a loose and a strict threshold at DAS scores of 1.7 and 2.2 for transmembrane domain respectively. They give the actual location or are informative in terms of the number of matching segments of the transmembrane segment. STIAT1 and STIAT3 contain one transmembrane domain at the strict threshold, while STIAT2 comprises that at a loose threshold. In comparison, STI1 and HOP contain a transmembrane domain at the strict threshold in the same region as the STIAT isoforms. Only STI1 has a second transmembrane domain at the strict threshold at the C-terminus. The transmembrane protein H⁺-ATPase1 was used to validate the accuracy of transmembrane domain prediction by *in silico* tool DAS.

In comparison, yeast STI1 and human HOP contain a transmembrane domain in the same region as the STIAT isoforms, while STI1 has a second transmembrane domain at the C-terminus. Ten transmembrane domains were predicted for the plasma membrane-type H⁺-ATPase, which is in accordance to the literature (Pedersen *et al.* 2007) and suggests the accuracy of the prediction algorithm. Although only one transmembrane domain was detected based on hydrophobic amino acid sequences at described positions, an association of STIAT isoforms to membranes is possible.

4.2.2. STIAT1 and STIAT2 are localised in cytosol and nucleus.

In order to obtain experimental evidences for the subcellular distribution of the STIAT2 isoform and additional support for STIAT1 localisation, subcellular fractionations of *Arabidopsis* leaves grown under control conditions were examined.

First, nuclei isolation was performed following the protocol of Shen *et al.* (2007). The resulting protein fractions were separated by SDS-PAGE and quality of nuclei preparation was verified by immunoblotting using marker proteins for nuclei, cytosol and chloroplasts (Figure 24). Western blot analysis of STIAT isoforms using antiserum directed against the recombinant tobacco protein STINT revealed detection of STIAT1 and STIAT2 predominantly in cytosol compared to nuclei fraction. STIAT3 isoform was not present in leaves of *Arabidopsis* plants grown under control conditions as already depicted in Figure 11 and Figure 20. The enrichment of nuclei was validated by marker protein Histon3. This was detected in all fractions, indicating remaining nuclei in the soluble nuclei-depleted fraction. Monodehydroascorbate reductase (MDAR) and cytochrome F were used as marker proteins for contamination with cytosolic and plastidic proteins in the nuclei fraction, respectively. Signals for both proteins were observed in total and soluble fraction, whereas no signal of them was detected in nuclei, indicating low contamination with cytosolic and plastidic proteins there. Similar results were obtained in nuclei isolations of tobacco leaves (Figure A 2).

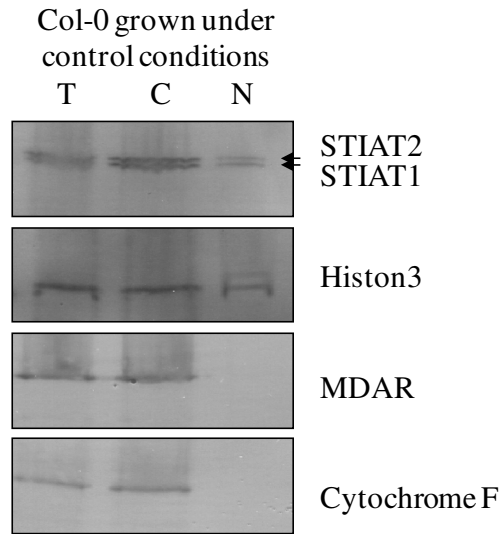


Figure 24: Distribution of STIAT isoforms in nuclei separated fractions of Columbia-0 leaves. The experiments were performed three times to ensure technical reproducibility.

Equal amounts of total (T), cytosolic (C) and nuclear (N) extracts were separated on SDS-PAGE and transferred to PVDF membrane. Immunological detection with antiserum against STINT and marker for nuclei (Histon3), cytosol (monodehydroascorbate reductase MDAR) and chloroplasts (cytochrome F) revealed a predominantly cytoplasmatic localisation of STIAT1 and STIAT2 compared to its amount in the nucleus.

4.2.3. STIAT1 and STIAT2 can partially associate with membranes.

Experimental evidences for a possible association of STIAT isoforms to membranes were collected by using aqueous two-phase partitioning method (Schindler *et al.* 2008). Leaf tissue from Arabidopsis grown under control conditions was used to fractionate the material into endomembrane- (EM) and plasma membrane (PM)-enriched extracts. The resulting protein fractions were separated by SDS-PAGE and the quality of PM preparation was assessed by Western blot analysis using marker proteins for cytosol, endomembrane and plasma membranes (Figure 25). Immunoblot analysis of STIAT isoforms using antiserum directed against the recombinant tobacco protein STINT showed detection of STIAT1 and STIAT2 in all fractions analysed with a predominant signal in the cytoplasmatic fraction. STIAT3 isoform was not present in leaves of Arabidopsis plants grown under control conditions as already depicted in Figure 11 and Figure 20. The detection of STIAT1 and STIAT2 in EM and PM fractions indicates a possible association with membranes. The enrichment of PM was confirmed by marker protein H^+ -ATPase which was detected only in the PM fraction. Contamination of PM fraction by endomembrane and soluble proteins was verified by visual inspection of immunoblot analysis of marker proteins V-ATPase and MDAR. The abundance of V-ATPase was similar in EM and microsomal fraction, but lower in PM fraction. This

demonstrates a depletion of endosomal proteins in this fraction. The signal intensity of the MDAR was highest in the cytosolic fraction, as expected for a marker for cytosolic proteins. Only traces of MDAR were found in EM and PM preparations, indicating low amounts of cytosolic proteins in those fractions. Similar results were obtained in PM fractionations of tobacco leaf and barley root tissue (Figure A 3).

In summary, STIAT1 and STIAT2 were co-localised in cytosol with higher abundance in cytosol and they partially associate with membranes.

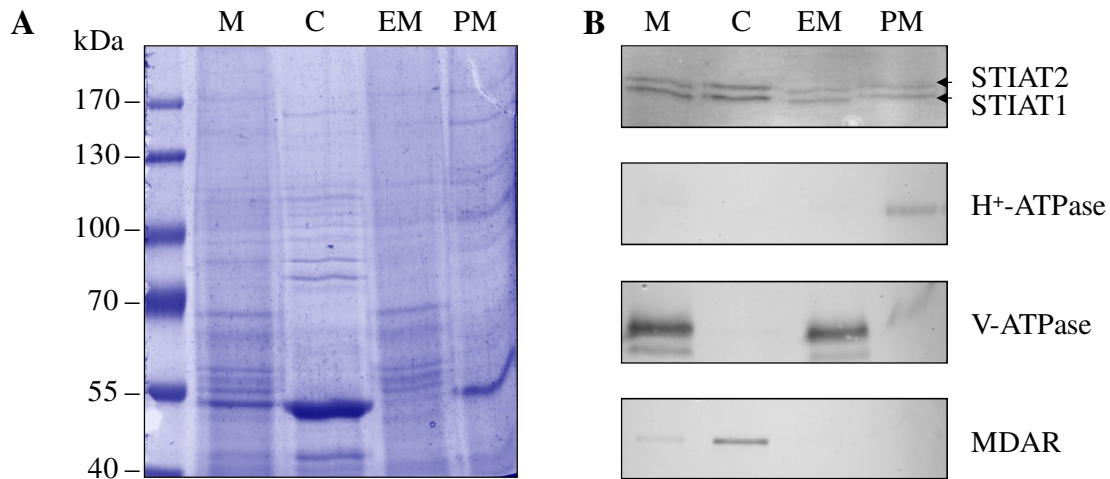


Figure 25: Subcellular distribution of STIAT isoforms in membrane fractions of Columbia-0 leaves.

A: Five μg of protein of microsomal (M), cytosolic (C), endomembrane (EM) and plasma membrane (PM) fractions were separated by SDS-PAGE and visualized by cCBB staining. The specific band patterns indicate the fractionation using aqueous two-phase partitioning.

B: The quality of membrane preparations was assessed using immunoblotting with antibodies against the subcellular marker proteins H⁺-ATPase, MDAR and V-ATPase. Western blot analysis with antiserum against STIAT revealed a predominantly cytoplasmic localisation of STIAT1 and STIAT2 and a partial association to membranes.

4.3. *In silico* analysis of regulatory elements of STIAT isoforms

Transcriptional activation or repression of genes is one important step in the control of stress responses. To obtain further evidences for the STIAT isoform regulation by stress application their promoter were analysed for cis-acting regulatory DNA elements using different *in silico* tools. Cis-acting regulatory DNA elements consist typically of 4-20 nucleotides, which are DNA-binding domains for one or more transcription factors. The programs PLACE (Higo *et al.* 1999), Athena (O'Connor *et al.* 2005) and AGRIS AtcisDB (Davuluri *et al.* 2003) were used for analysis of cis-elements in *STIAT* promoter sequences. Only cis-elements for the

putative promoter regions of the *STIAT* isoforms are listed, which were found with at least two of the programs (Table 4 to Table 6). The detection of DNA-binding domain HSE (heat shock element) in the *STIAT3* promoter comprised an exception, because it was only found by AGRIS AtcisDB. Furthermore, this cis-element was only detected in *STIAT3* promoter, suggesting regulation of *STIAT3* gene by heat shock transcription factors.

Table 4: List of potential cis-regulatory elements in *STIAT1* promoter.

Cis-element, signal sequence, function and reference are given.

Cis-element	Sequence	Function	Reference
ARF	TGTCTC	Induction by auxin and brassinosteroids	(Ulmasov <i>et al.</i> 1999)
ATB2	ACTCAT	Induction by hypoosmolarity	(Sato <i>et al.</i> 2002)
Box II/ GT1	GGTTAA	Regulation by light	(Green <i>et al.</i> 1988)
CARGCW8GAT	C(W) ⁸ G	Embryo-specific expression	(Tang and Perry 2003)
DRE	RCCGAC	Induction by drought, high-light, cold	(Kasuga <i>et al.</i> 1999)
DPBF	ACACNNG	Induction by abscisic acid, Embryo-specific expression	(Kim <i>et al.</i> 1997)
E2F	TTTCCCGC	Regulation by cell cycle	(Chaboute <i>et al.</i> 2000)
E2FAT	TYTCCCGCC	Regulation by cell cycle	(Ramirez-Parra <i>et al.</i> 2003)
GAREAT	TAACAAR	Induction by gibberellic acid	(Ogawa <i>et al.</i> 2003)
GATABOX	GATA	Regulation by light	(Teakle <i>et al.</i> 2002)
HEXAMER	CCGTCG	Meristem-specific expression	(Chaubet <i>et al.</i> 1996)
IBOX	GATAAG	Regulation by light	(Giuliano <i>et al.</i> 1988)
LEAFYATAG	CCAATGT	Flower-specific expression	(Lohmann <i>et al.</i> 2001)
MYB1AT	WAACCA	Induction by ABA	(Abe <i>et al.</i> 2003)
MYBATRD22	CTAACCA	Induction by ABA and drought	(Abe <i>et al.</i> 1997)
MYBPLANT	MACCWAMC	Regulation of phenylpropanoid and lignin biosynthesis	(Tamagnone <i>et al.</i> 1998)
MYCATERD1	CATGTG	Induction by dehydration	(Simpson <i>et al.</i> 2003)
MYCATRD22	CACATG	Induction by ABA and drought	(Abe <i>et al.</i> 1997)
RAV1A	CAACA	Induction by cold	(Kagaya <i>et al.</i> 1999)
SORLIP1	GCCAC	Regulation by light	(Hudson <i>et al.</i> 2003)
SV40CORE	GTGGWWHG	Enhancer, Regulation by light	(Green <i>et al.</i> 1987)
TATABOX	TATAAA	Transcriptionstart	(Shirsat <i>et al.</i> 1989)
TBOX	ACTTTG	Regulation by light	(Chan <i>et al.</i> 2001)

Table 5: List of potential cis-regulatory elements in *STIAT2* promoter.

Cis-element, signal sequence, function and reference are given.

Cis-element	Sequence	Function	Reference
ARF	TGTCTC	Induction by auxin and brassinosteroids	(Ulmasov <i>et al.</i> 1999)
ATB2	ACTCAT	Induction by hypoosmolarity	(Satoh <i>et al.</i> 2002)
ATHB2	TAATMATTAA	Regulation by light	(Ohgishi <i>et al.</i> 2001)
CARGCW8GAT	C(W) ⁸ G	Embryo-specific expression	(Tang and Perry 2003)
CBF2 (ABRE)	CCACGTGG	Induction by abscisic acid and water-stress	(Pla <i>et al.</i> 1993)
DRE	RCCGAC	Induction by drought, high-light, cold	(Kasuga <i>et al.</i> 1999))
DPBF	ACACNNG	Induction by abscisic acid, Embryo-specific expression	(Kim <i>et al.</i> 1997)
GAREAT	TAACAAR	Induction by gibberellic acid	(Ogawa <i>et al.</i> 2003)
GATABOX	GATA	Regulation by light	(Teakle <i>et al.</i> 2002)
GBOX	CACGTG	Induction by diverse stimulatory pathways	(Menkens <i>et al.</i> 1995)
HEXAMER	CCGTCG	Meristem-specific expression	(Chaubet <i>et al.</i> 1996)
L1BOX	TAAATGYA	L1 layer-specific expression	(Abbas-Terki <i>et al.</i> 2001)
LTRE	ACCGACA	Regulation by low temperature	(Nordin <i>et al.</i> 1993)
MYB1AT	WAACCA	Induction by ABA	(Abe <i>et al.</i> 2003)
MYB1LEPR	GTTAGTT	Pathogen defence	(Chakravarthy <i>et al.</i> 2003)
MYBATRD22	CTAACCA	Induction by ABA and drought	(Abe <i>et al.</i> 1997)
MYBPLANT	MACCWAMC	Regulation of phenylpropanoid and lignin biosynthesis	(Tamagnone <i>et al.</i> 1998)
MYCATERD1	CATGTG	Induction by dehydration	(Simpson <i>et al.</i> 2003)
MYCATRD22	CACATG	Induction by ABA and drought	(Abe <i>et al.</i> 1997)
RAV1A	CAACA	Induction by cold	(Kagaya <i>et al.</i> 1999)
RAV1B	CACCTG	Induction by cold	(Kagaya <i>et al.</i> 1999)
RYREPEAT	CATGCATG	Tissue-specific expression	(Bäumlein <i>et al.</i> 1992)
SORLIP1	GCCAC	Regulation by light	(Hudson <i>et al.</i> 2003)
SORLIP2	GGGCC	Regulation by light	(Hudson <i>et al.</i> 2003)
SV40CORE	GTGGWWHG	Enhancer, Regulation by light	(Green <i>et al.</i> 1987)
TATABOX	TATAAA	Transcription start	(Shirsat <i>et al.</i> 1989)
TBOX	ACTTTG	Regulation by light	(Chan <i>et al.</i> 2001)
UPRMOTIFII	CC(N) ¹² CCACG	Protein folding response	(Martinez and Chrispeels 2003)
WBOX	TTTGACY	Pathogen defence	(Eulgem <i>et al.</i> 2000)

Table 6: List of potential cis-regulatory elements in *STIAT3* promoter.

Cis-element, signal sequence, function and reference are given.

Cis-element	Sequence	Function	Reference
Box II/ GT1	GGTTAA	Regulation by light	(Green <i>et al.</i> 1988)
CARGCW8GAT	C(W)8G	Embryo-specific expression	(Tang and Perry 2003)
CCA1	AAMAATCT	Induction by light	(Wang <i>et al.</i> 1997))
DRE	RCCGAC	Induction by drought, high-light, cold	(Kasuga <i>et al.</i> 1999)
DPBF	ACACNNG	Induction by abscisic acid, Embryo-specific expression	(Kim <i>et al.</i> 1997)
GAREAT	TAACAAR	Induction by gibberellic acid	(Ogawa <i>et al.</i> 2003)
GATABOX	GATA	Regulation by light	(Teakle <i>et al.</i> 2002)
HSE	AGAACATTCT	Regulation by heat	(Hubel <i>et al.</i> 1995)
IBOX	GATAAG	Regulation by light	(Giuliano <i>et al.</i> 1988)
MYB1AT	WAACCA	Induction by ABA	(Abe <i>et al.</i> 2003)
MYBATRD22	CTAACCA	Induction by ABA and drought	(Abe <i>et al.</i> 1997)
MYBPLANT	MACCWAMC	Regulation of phenylpropanoid and lignin biosynthesis	(Tamagnone <i>et al.</i> 1998)
MYCATERD1	CATGTG	Induction by dehydration	(Simpson <i>et al.</i> 2003)
MYCATRD22	CACATG	Induction by ABA and drought	(Abe <i>et al.</i> 1997)
RAV1A	CAACA	Induction by cold	(Kagaya <i>et al.</i> 1999))
SORLIP1	GCCAC	Regulation by light	(Hudson <i>et al.</i> 2003)
SV40CORE	GTGGWWHG	Enhancer, Regulation by light	(Green <i>et al.</i> 1987)
TATABOX	TATAAA	Transcription start	(Shirsat <i>et al.</i> 1989)
TBOX	ACTTTG	Regulation by light	(Chan <i>et al.</i> 2001))
WBOX	TTTGACY	Pathogen defence	(Eulgem <i>et al.</i> 2000)

In general, many cis-elements found in the putative promoter regions of *STIAT* isoforms were described to be regulated either by phytohormones like abscisic acid (ABA), auxin and brassinosteroids or by (a)biotic factors like cold, drought and pathogens. This indicates a multiple regulation of all *STIAT* genes, with similar features. One difference was found concerning the cis-element RAV1 (Related to *ABI3/VP1*), which is bound by cold responsive transcription factor RAV1 (Fowler and Thomashow 2002, Yamasaki *et al.* 2004). Only *STIAT2* promoter contained bipartite RAV1A and B binding site (Table 5), whereas among *STIAT1* and *STIAT3* promoters only the RAV1A motif was detected (Table 4, Table 6). However, T-DNA insertion lines for RAV1 were analysed under cold stress and did not show differences in *STIAT* isoform expression (not shown).

4.4. Isolation and characterisation of STIAT/STINT interaction partners

Investigations of the interacting proteins of STINT/STIAT are important for the functional categorisation. Despite the knowledge of the homology to the co-chaperones HOP from human and STI1 from yeast, both acting as linker between Hsp90 and Hsp70 in these organisms, the knowledge of interaction partners of HOP/STI1 proteins in plants was restricted to HOP/STI1 in rice (Chen *et al.* 2010).

Several chromatographic and gel based separation methods as well as mass spectrometry analysis were combined to isolate STIAT/STINT with their interacting proteins from leaf material and cell culture in Arabidopsis and tobacco.

4.4.1. *In silico* prediction of STIAT isoform interaction partners

To obtain first indications for the putative interaction partner of the three STIAT isoforms, *in silico* analysis was performed using Arabidopsis interaction viewer (Geisler-Lee *et al.* 2007). The program predicts the interaction of Arabidopsis proteins based on interacting orthologs in yeast, nematode worm, fruit fly and human. Partial interactions have been experimentally examined for these four species (Gandhi *et al.* 2006, Giot *et al.* 2003, Li *et al.* 2004, Rual *et al.* 2005). An interaction in Arabidopsis could be predicted when orthologs existed for both interacting proteins in one of these four established interactomes. A confidence value (CV) for each interaction is displayed, which was generated on the amount of supporting evidence for each interaction being a product of amount in different datasets, different kinds of experiments and number of species. A medium confidence interaction is displayed by CV of 2 to 10, while lower and higher CV describe lower and higher confidence interactions, respectively.

All three STIAT isoforms were analysed for their putative interaction partner (Table 7 to Table 9). The highest numbers of interactions predicted were found for STIAT1 and STIAT2. The list of predicted interactions for STIAT3 was rather limited. Hsp90 and Hsp70 isoforms were suggested to interact with the three STIAT isoforms. Interactions of STIAT isoforms were predicted to three cytosolic Hsp90 isoforms, which differed in the isoform and the confidence levels of interaction predicted. STIAT1 and STIAT2 were predicted to have a high confidence interaction to Hsp90-1, whereas STIAT3 does not. Instead, a medium interaction of STIAT3 to Hsp90-4 was predicted. Four cytosolic Hsp70 isoforms were suggested to interact with STIAT1 and STIAT2, while no interaction to Hsp70 proteins was found for

STIAT3, indicating a special function of that compared to the other two isoforms. Table 10 shows the comparison of putative interacting proteins of STIAT isoforms regarding members of Hsp90 and Hsp70 protein families.

Table 7: STIAT1 interaction partners using *in silico* prediction tool Arabidopsis interaction viewer (Geisler-Lee *et al.* 2007).

Confidence interactions (CV) are shown for each interaction. High: CV >10. Medium: CV: 2 – 10. Low: CV = 1.

Interaction protein of STIAT1		Interolog Confidence	
Locus	Annotation	Value	Level
At5g52640	Hsp90-1	504	High
At3g12580	Hsp70-4	20	High
At5g56030	Hsp90-2	12	High
At1g74310	HOT1 (HSP101)	6	Medium
At5g41370	ATP-dependent helicase	6	Medium
At4g16970	ATP binding / protein serine/threonine kinase	4	Medium
At1g04980	PDI10 protein disulfide isomerase	2	Medium
At1g79930	Hsp70-14	2	Medium
At1g79990	coatamer protein complex, subunit beta 2 (beta prime)	2	Medium
At2g30110	ATUBA1 ubiquitin activating enzyme	2	Medium
At2g41500	LIS nucleotide binding	2	Medium
At3g58560	endonuclease/exonuclease/phosphatase family protein	2	Medium
At5g22060	ATJ2 (Hsp40)	2	Medium
At5g40820	ATRAD3 inositol/ phosphatidylinositol kinase/ phosphotransferase	2	Medium
At5g58290	RPT3 ATPase	2	Medium
At1g16030	Hsp70-5	1	Low
At1g18040	CDKD1;3 cyclin-dependent kinase D;3	1	Low
At1g44170	ALDH3H1 aldehyde dehydrogenase 3H1	1	Low
At1g65040	protein binding / zinc ion binding	1	Low
At1g77720	protein kinase family protein	1	Low
At1g79530	GAPCP-1 glyceraldehyde-3-phosphate dehydrogenase of plastid 1	1	Low
At3g09920	PIP5K9 phosphatidyl inositol monophosphate 5 kinase	1	Low
At3g22830	HSFA6B transcription factor	1	Low
At3g47460	ATSMC2; transporter	1	Low
At4g02450	glycine-rich protein (p23)	1	Low
At4g04940	transducin family protein / WD-40 repeat family protein	1	Low
At5g05560	ubiquitin-protein ligase	1	Low
At5g07590	WD-40 repeat protein family	1	Low

Table 8: STIAT2 interaction partners using *in silico* prediction tool Arabidopsis interaction viewer (Geisler-Lee *et al.* 2007).

Confidence interactions (CV) are shown for each interaction. High: CV >10. Medium: CV: 2 – 10. Low: CV = 1.

Interaction protein of STIAT2		Interolog Confidence	
Locus	Annotation	Value	Level
At5g52640	HSP90-1	30	High
At1g16030	HSP70-5	20	High
At1g74310	HOT1 (HSP101)	4	Medium
At5g41360	ATP-dependent DNA helicase	4	Medium
At1g11660	HSP70-16	2	Medium
At3g44110	ATJ3; protein binding	2	Medium
At1g10900	phosphatidylinositol-4-phosphate 5-kinase family protein	1	Low
At1g18040	CDKD1;3 cyclin-dependent kinase D;3	1	Low
At1g44170	ALDH3H1 aldehyde dehydrogenase 3H1	1	Low
At1g52360	coatomer protein complex	1	Low
At1g65040	protein binding / zinc ion binding	1	Low
At1g77720	protein kinase family protein	1	Low
At2g30110	ATUBA1 ubiquitin activating enzyme	1	Low
At2g41500	LIS nucleotide binding	1	Low
At3g47460	ATSMC2; transproter	1	Low
At3g58560	endonuclease/exonuclease/phosphatase family protein	1	Low
At4g04940	transducin family protein / WD-40 repeat family protein	1	Low
At4g18880	HSFA6A transcription factor	1	Low
At5g40820	ATRAD3 inositol/ phosphatidylinositol kinase/ phosphotransferase	1	Low
At5g58290	RPT3 ATPase	1	Low

Table 9: STIAT3 interaction partners using *in silico* prediction tool Arabidopsis interaction viewer (Geisler-Lee *et al.* 2007).

Confidence interactions (CV) are shown for each interaction. High: CV >10. Medium: CV: 2 – 10. Low: CV = 1.

Interaction protein of STIAT3		Interolog Confidence	
Locus	Annotation	Value	Level
At5g56000	HSP90-4	8	Medium
At3g04120	GAPC-1 glyceraldehyde-3-phosphate dehydrogenase C subunit 1	1	Low
At4g02450	glycine-rich protein (p23)	1	Low
At4g36250	ALDH3H1 aldehyde dehydrogenase 3H1	1	Low
At5g07590	WD-40 repeat protein family	1	Low
At5g63310	NDPK1A nucleoside diphosphate kinase 2	1	Low

Table 10: Selection of STIAT interaction partners belonging to Hsp90 and Hsp70 families using *in silico* prediction tool Arabidopsis interaction viewer (Geisler-Lee *et al.* 2007).

Confidence interactions (CV) are shown for each interaction. High: CV >10. Medium: CV: 2 – 10. Low: CV = 1.

Interaction partner	STIAT1	STIAT2	STIAT3
Hsp90-1	High	High	No
Hsp90-2	High	No	No
Hsp90-4	No	No	Medium
Hsp70-4	High	No	No
Hsp70-5	Low	High	No
Hsp70-14	Medium	No	No
Hsp70-16	No	Medium	No

4.4.2. Co-localisation of STIAT1 and STIAT2 isoforms with specific members of the Hsp90 and Hsp70 families in cytosol and nucleus

Putative interacting proteins are often co-expressed or co-localised in the same compartment. In order to obtain first indications of STIAT isoform interactions with members of the major interaction partners Hsp70 and Hsp90 the co-expression of them with the STIAT isoforms was analysed in different compartments.

Nuclei and cytosol protein fractions of Arabidopsis leaves grown under control conditions were separated by SDS-PAGE and subsequent immunoblotting of STIAT isoforms and their putative interaction partner were performed using antisera against Hsp90-1 from Arabidopsis, an Hsp70 antibody recognizing Arabidopsis Hsp70-1 to Hsp70-5 and antisera against STINT (Figure 26). Western blot analysis of the major putative STIAT isoform interaction partners revealed detection of specific members of Hsp70 and Hsp90-1 predominantly in the cytosol, but also in the nuclei fraction with minor signal intensity for Hsp90-1 in nuclei. For STIAT1 and STIAT2 the same subcellular localisation was already observed (4.2.2), indicating the co-localisation of STIAT isoforms with specific members of its putative interaction partners Hsp70 and Hsp90 in same compartments.

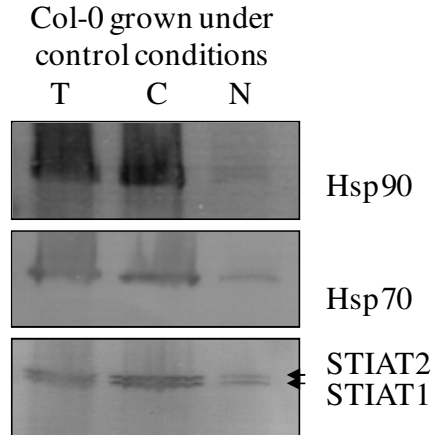


Figure 26: Cellular distribution of STIAT isoforms with the putative interaction partner Hsp70 and Hsp90.

Equal amounts of total (T), cytosolic (C) and nuclear (N) extracts were separated on SDS-PAGE and transferred to PVDF membrane. Immunological detection with antisera against AtHsp90-1, an Hsp70 antibody specific for AtHsp70-1 to AtHsp70-5 and antisera against STINT illustrated similar subcellular localisation of them, predominantly cytoplasmatic with minor accumulation in nucleus.

4.4.3. Size exclusion chromatography revealed participation of STINT in high molecular weight fraction and occurrence as a dimer in tobacco

Evidences for the participation of a protein in protein complexes can be obtained by analysing elution profiles of the protein of interest using size exclusion chromatography (SEC). The total protein extract from a tobacco cell culture was separated by Superdex 200 column to elucidate the participation of STINT in protein complexes. The resulting fractions were analysed by subsequent Western blot analysis using antiserum directed against STINT (Figure 27). Densitometric evaluation of signal intensities revealed elution of STINT across fractions of 10 to 15 ml with two maxima at 10 and 14 ml. The comparison of STINT elution profile with molecular weight marker proteins illustrated the detection of STINT in fractions ranging from 67 to 440 kDa. This result suggests the participation of the STINT protein in protein complexes. However, the highest signal intensity was found in the second peak of around 140 kDa indicating the occurrence of STINT as a dimer, whereas the monomeric form of 67 kDa was detected with lower intensity.

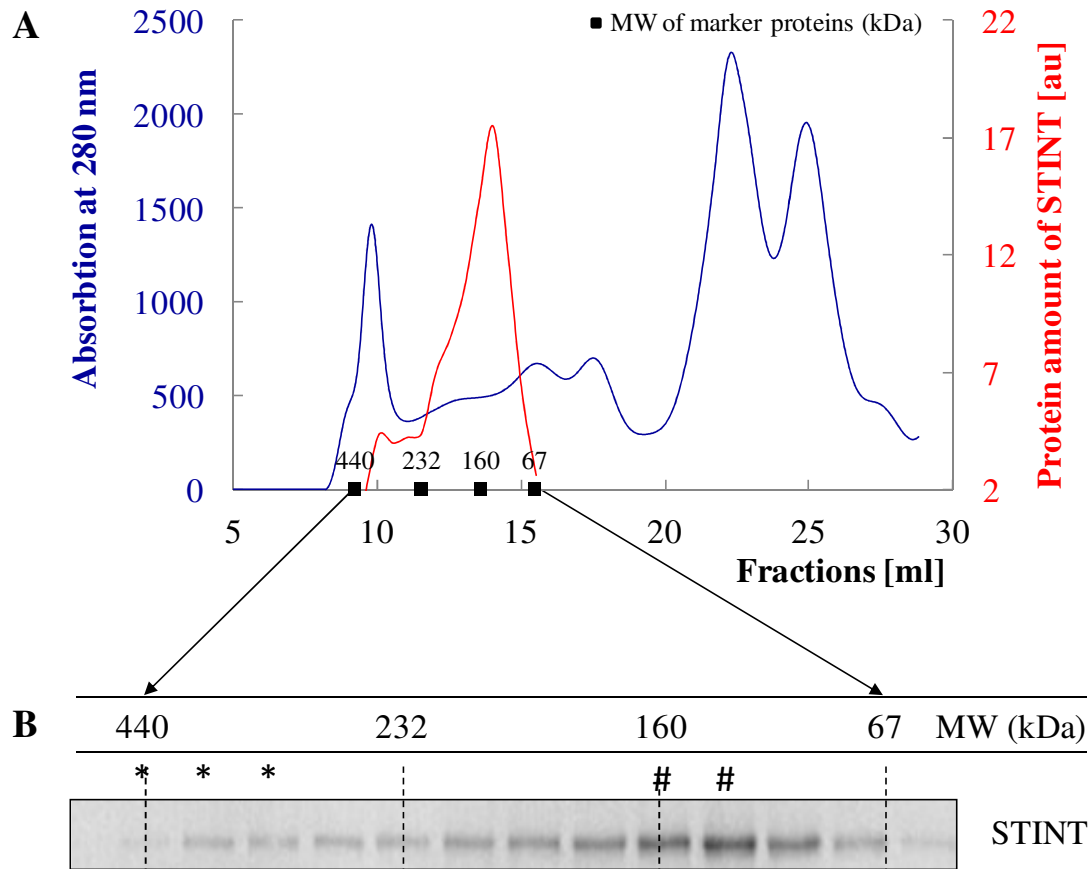


Figure 27: Size exclusion chromatography of STINT isolated from the tobacco cell culture S2LS3. The experiments were performed in triplicate to ensure technical reproducibility.

A: Separation profile of gel filtration using Superdex 200 column.

Blue: Absorption at 280 nm. **Green:** Calibration curve using marker proteins of different molecular weight (MW) in kDa. **Red:** Quantification of STINT protein amount from Western blot analysis of fractions in arbitrary units (au).

B: Western blot analysis of fractions using antiserum against STINT. Signal detection in high (440 kDa) to low (67 kDa) molecular weight protein fractions pointed to the presence of STINT in protein complexes.

High (*) and low (#) molecular weight fractions selected for BN-PAGE in Figure 29.

4.4.4. Blue native PAGE confirmed the occurrence of the STINT protein as a dimer

After obtaining indications of monomeric and dimeric molecular forms of STINT protein and its participation in protein complexes by size exclusion chromatography, all findings were verified using Blue native (BN) PAGE.

First, the recombinant STINT protein was separated either by denaturing SDS-PAGE or native BN-PAGE and additionally subsequent Western blot analysis using antiserum directed against STINT were performed (Figure 28). The separation of STINT by SDS-PAGE resulted in detection of STINT at a size of 72 kDa in both the Coomassie-stained gel and by

immunodetection. In comparison, the separation of recombinant STINT by BN-PAGE illustrated the detection of STINT at a size of 146 kDa. This result suggests occurrence of STINT as a monomer under denatured conditions and as a dimer under native conditions.

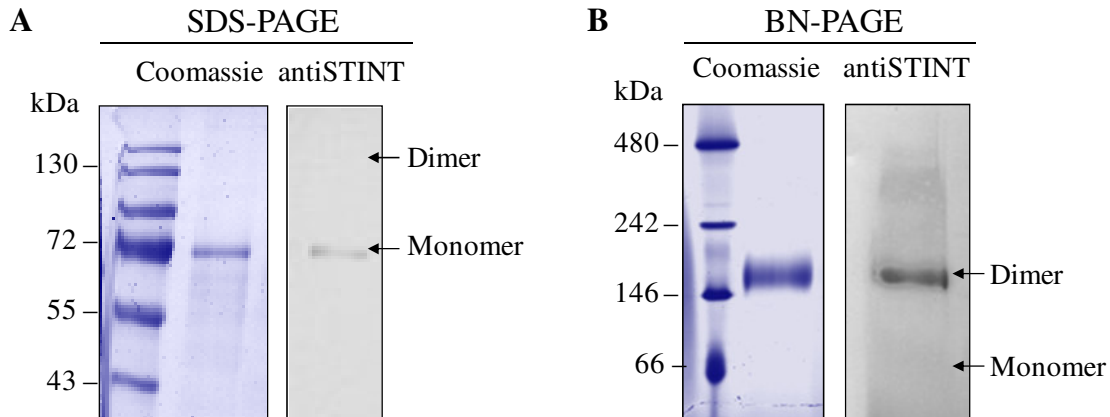


Figure 28: Determination of molecular weight of recombinant STINT protein in denatured and native PAGE.

A: Separation of 20 ng recombinant STINT by SDS-PAGE and subsequent visualisation by both Coomassie staining and immunodetection with antiserum against STINT resulted in detection of STINT of 72 kDa, indicating a Monomer.

B: Separation of 500 ng recombinant STINT by BN-PAGE with or without immunodetection using antiserum against STINT depicted detection of STINT of 146 kDa, illustrating the dimeric form.

The participation of STINT in protein complexes was analysed by BN-PAGE. Therefore, high and low molecular weight fractions of size exclusion chromatography from section 4.4.3 and recombinant STINT as loading control were subjected to BN-PAGE with subsequent Western blot analysis using antiserum directed against STINT (Figure 29). The immunodetection of STINT revealed the detection in the low molecular weight fraction at the same size as detected for the recombinant STINT, each with 146 kDa. The separation of high molecular weight fractions by BN-PAGE and subsequent Western blot analysis showed a signal for the STINT protein in the size of an apparent MW of about 720 kDa. In comparison to the largest protein signal obtained in the gel filtration experiments using the Superdex 200 column (4.4.3) the size of the protein band obtained in BN-PAGE was approximately 300 kDa higher.

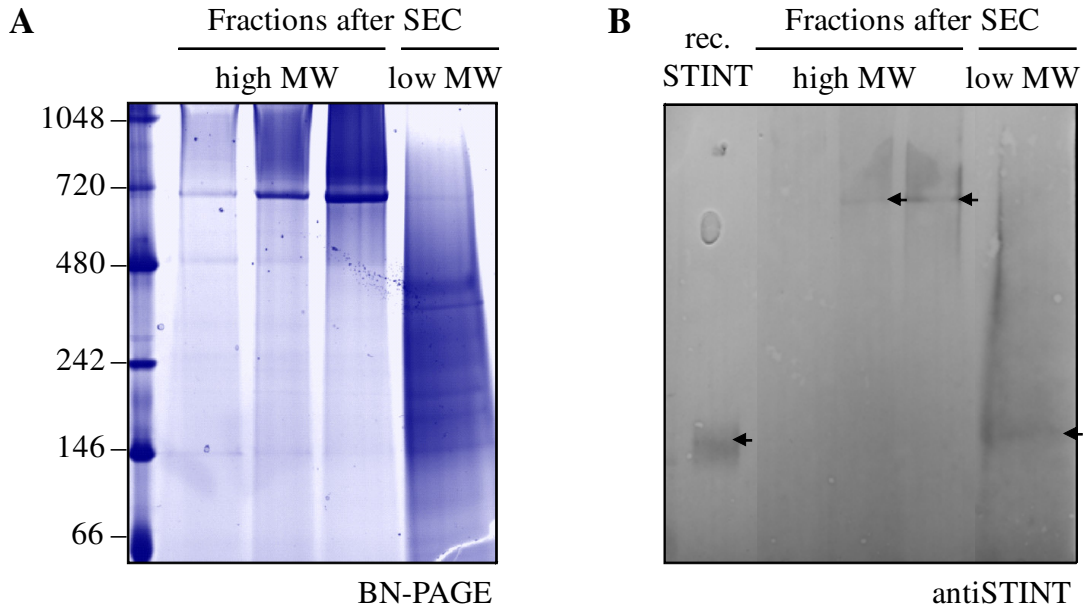


Figure 29: Confirmation of STINT in high and low molecular weight (MW) fractions of size exclusion chromatography (SEC) by BN-PAGE.

A: 25 μ g of high and low MW fractions after SEC from Figure 27 were separated by BN-PAGE, illustrating a main protein band of 720 kDa in high MW fractions and nonpoint protein bands of 146 to 720 kDa in low mw fraction.

B: Immunodetection with antiserum against STINT resulted in detection of STINT at a size of 720 kDa in high mw fraction and 146 kDa in low mw fraction, confirming the presence of STINT as part of a complex and behaviour as a dimer under native conditions.

In order to clarify, if the protein band of that size resembles an aggregation of protein complexes due to column properties, the tobacco cell culture extract was separated using Sephacryl 400 column and a high molecular weight fraction was subsequently subjected to BN-PAGE, resulting in the band of the same size at about 720 kDa (Figure 30A).

Protein lane was excised and incubated with trypsin. Protein identification via LC-ESI-Q-TOF MS/MS was performed on tryptic peptides by searching against the *Viridiplantae* index of Swissprot and Trembl databases. The identification of the 720 kDa complex band resulted in detection of proteasome subunits of different types and species, which were identified with at least two peptides (Figure 30B). This finding indicate that the 720 kDa complex is potentially an accumulation in injection peak as STINT could not be identified within this complex by MS but was detected there by immunoblotting. Therefore, additional biochemical methods were necessary to identify interacting proteins of STIAT/STINT proteins.

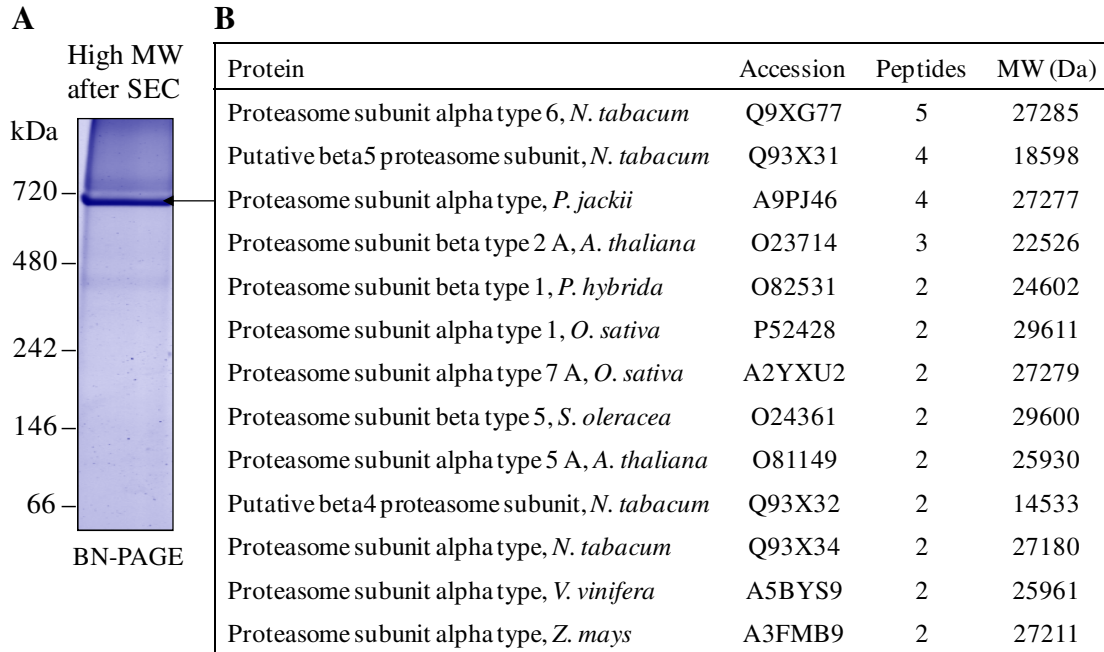


Figure 30: Protein identification of high molecular weight (MW) fraction obtained after size exclusion chromatography.

A: High MW fraction after SEC using Sephacryl 400 column was separated by BN-PAGE, illustrating a main protein band at 720 kDa.

B: Protein identification using LC-ESI-Q-TOF MS. Protein name, accession number, detected peptides, and molecular weight of proteins are given. Protein identification was performed by searching against the *Viridiplantae* index of Swissprot and Trembl databases.

4.4.5. Immunoprecipitation of STIAT interaction partners in Arabidopsis

The interaction partners of the STIAT isoforms were analysed by immunoprecipitation experiments under *in vivo* conditions as shown for the STIAT isoforms in section 4.1.4. Total protein extracts from Arabidopsis leaves grown under control conditions were precipitated by antibody raised against STINT. The eluate fraction was separated by SDS-PAGE, stained by cCBB and resulted in detection of a multitude of 15 protein bands (Figure 31A). The 15 protein bands were excised manually from the cCBB stained gel and incubated with trypsin to verify their identity. Protein identification via MALDI-TOF MS by searching against the *Viridiplantae* index of NCBI database lead to the identification of STIAT, the main putative interaction partners Hsp90 and Hsp70 and additional proteins (Figure 31B).

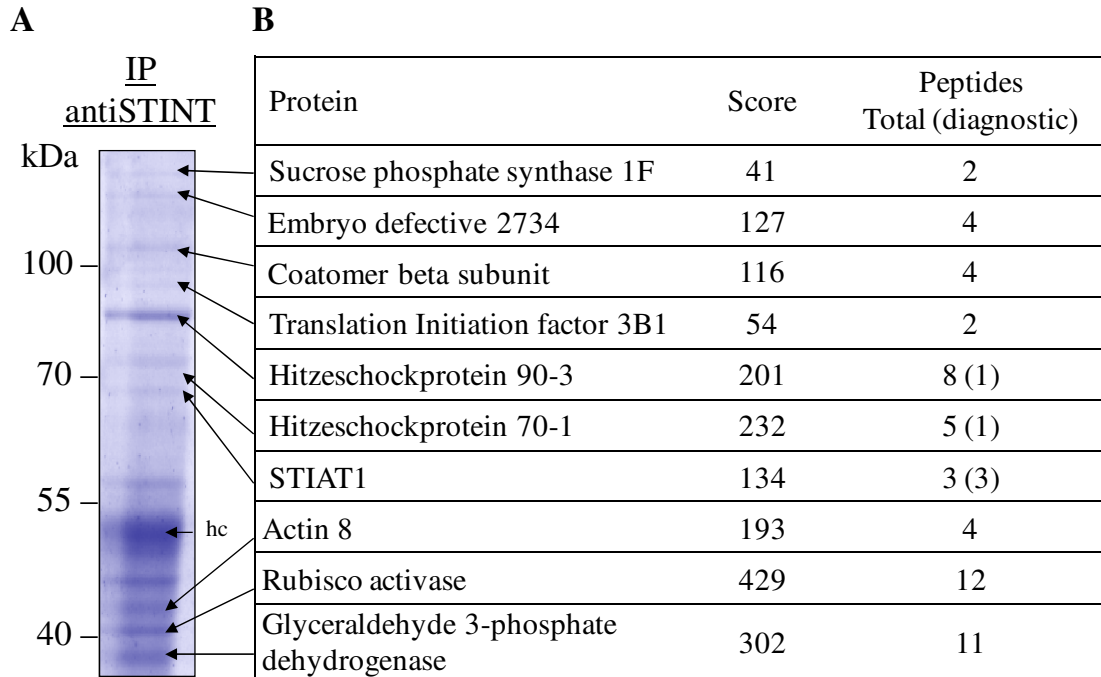


Figure 31: Immunoprecipitation of STIAT isoforms and putative interaction partners from Columbia-0 leaves grown under control conditions using antiSTINT. The results were obtained only once.

A: Separation of precipitated STIAT and interaction partners by SDS-PAGE and visualization by cCBB staining. Hc: heavy chain of the antibody.

B: Protein identification using MALDI-TOF-TOF MS. Protein name, score and number of detected peptides for proteins co-purifying with STIAT are given. Protein identification via MALDI-TOF-TOF MS was performed by searching NCBI database.

The differentiation between the isoforms of the identified protein families was achieved by matching all peptides to the complete protein sequences (Figure 32). Thus, protein bands revealed specific identification of STIAT1, Hsp90-3 and Hsp70-1. All three peptides leading to identification of STIAT1 were diagnostic while at least one specific peptide for the chaperones has been detected. This finding indicated Hsp90 and Hsp70 as interacting partners of STIAT in Arabidopsis, co-precipitating under certain conditions.

Among the remaining proteins identified with very high score were embryo defective and beta-coat protein as well as proteins with lower score such as sucrose phosphatase synthase or translation initiation factor (Figure 31). Since this result was only obtained once, at this point it was not clear whether these proteins were true interaction partners or client proteins of STIAT-Hsp90-Hsp70 complex or contamination.

A	Hsp90-3	NLKLGIHEDSQNRTKIAELLRYHSTKSGDELTSLKDYVTRMK EGQNDIFYITGESK KAVE	474
	Hsp90-4	NLKLGIHEDSQNRTKIAELLRYHSTKSGDELTSLKDYVTRMK EGQNEIFYITGESK KAVE	474
	Hsp90-1	NLKLGIHEDSQNRGKIADLLRYHSTKSGDEMTSFKDYVTRMK EGQKDIFYITGESK KAVE	480
	Hsp90-2	NLKLGIHEDSQNRGKIADLLRYHSTKSGDEMTSFKDYVTRMK EGQKDIFYITGESK KAVE	480
B	Hsp70-1	STITRARFEELNMDLFRKCMPEVVEKCLRDAKMDK STVHDVVLVGGSTR IPKVQQLLQDFF	360
	Hsp70-2	SPITRARFEEMNMDLFRKCMPEVVEKCLRDAKMDKSTVHEIVLVGGSTRIPKVQQLLQDFF	360
	Hsp70_3	APITRARFEELNIDLFRKCMPEVVEKCLRDAKMDKNSIDDVVLVGGSTRIPKVQQLLVDF	360
	Hsp70-3	TTITRARFEELNMDLFRKCMPEVVEKCLRDAKMDKSSVHDVVLVGGSTRIPKVQQLLQDFF	360
C	STIAT1	RASAPNPFDAFQGPMEWSKLTADPSTRGLLKQPDFVNMMEIQ RNP SNLNLYLQDQR V	180
	STIAT2	RA-APNPFDAFQGPMEWTKLTS DPSTRGFLQPDFVNMMEIQK NP SSLNLYLKDQR V	179
	STIAT3	KS---NPFVDAFQGKEMWEKLTADPGTRVYLEQDDFVKT MKEIQRNPNNLNLYMKDKR V	177
	STIAT1	QALGVLLNIQIR-TQQAGDDMEIGEEEMAVPSRKEPEVEK KRKPEPEPEPEP-EFGEEK Q	238
	STIAT2	QSLGVLLNVKFRPPPPQGDEAEVPESDMGQSSNEPEVEK KREPEPEPEPEVTEEEK KE	239
	STIAT3	KALGVLLNVKFG--GSSGEDTEMKEADE----RKEP----- EPMEPEMELTEERQ KE	225
	STIAT1	KRLNEAERAK KELEQQEYYPNI GDEERE KGNDFEKEQKYPDAVRHYTEAIKRNPKDPRA	418
	STIAT2	KRLNDAERAKKEWEQKQYFDPKLGDEEREKGNDFEKEQKYPEAIKHYTEAIKRNPNNDHKA	419
	STIAT3	KKLNDAEKVKKELEQQEYFDPTIAEEEREKGNDFEKEQKYPEAVKHYTEAIKRNPNNDVRA	405

Figure 32: Identification of Hsp90-3, Hsp70-1 and STIAT1 after antiSTINT-IP from Figure 31A MALDI-TOF MS.

The extractions of sequence alignments of isoforms of Hsp90 (A), Hsp70 (B) and STIAT (C) from *Arabidopsis* are shown. The diagnostic tryptic peptides for one isoform per alignment are matched (red).

4.4.6. Heterologous expression of STIAT isoforms and their potential interaction partners in *E. coli*

In contrast to the results of the immunoprecipitation experiments of STIAT isoforms from *Arabidopsis* leaves, *in silico* prediction of STIAT interaction partners revealed several members of Hsp90 and Hsp70 protein families interacting with STIAT isoforms with different affinities. Therefore, STIAT isoform interactions with selected isoforms of Hsp90 and Hsp70 were examined using *in vitro* interaction studies based on the protocol shown for the interaction of STI1 and Hsp70 in yeast (Wegele *et al.* 2003). For that purpose, cloning and production of recombinant STIAT isoforms and selected Hsp90 and Hsp70 proteins in *E. coli* were initiated. The cloning strategy to produce recombinant proteins is depicted in Figure 33. Cloning throughput was achieved by using Gateway-compatible vectors. Where available, entry clones for some candidate proteins were obtained from NASC (Nottingham Arabidopsis Stock Center). Entry clones for the remaining interaction partner were produced and fragments were transferred into expression vector pDEST17.

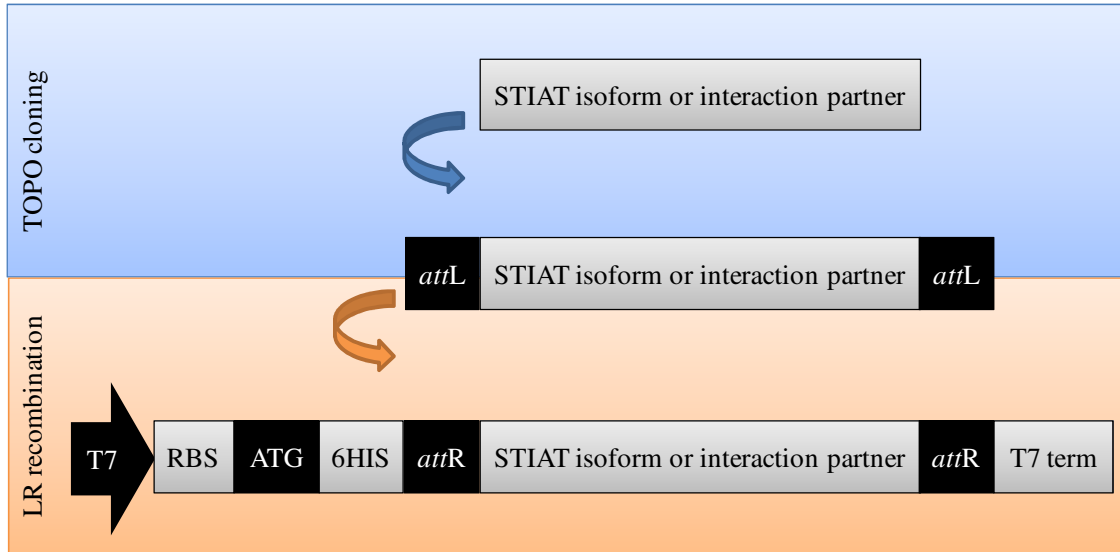


Figure 33: Schematic diagram of the cloning strategy to produce His tagged recombinant proteins. Entry clones were produced by TOPO cloning reaction of ORFs into pENTR/D-TOPO. Subsequently, fragments were assembled into destination vector pDEST17 during a LR reaction to produce the expression clones.

After successful cloning of STIAT isoforms and interaction partners, N-terminally His-tagged proteins were expressed under the control of the T7 promoter and purified from *E. coli*. The overview of proteins produced in *E. coli* is listed in Table 11. In total, nine proteins were selected for production in *E. coli*. Eight of them were successfully cloned into expression vector; one could not be amplified from any template under any condition tested. Five of the remaining eight proteins showed a high expression whereas three proteins, including STIAT3 isoform, revealed only low or no expression.

Table 11: Overview of candidate proteins heterologously expressed in *E. coli*. Protein names, status of cloning and purification are given.

Protein	Cloning	Purification
STIAT1	Successful	Successful
STIAT2	Successful	Successful
STIAT3	Successful	Low expression level
Hsp70-4	Successful	No expression
Hsp70-5	Successful	Successful
Hsp70-14	Successful	Low expression level
Hsp90-1	Successful	Successful
Hsp90-2	Successful	Successful
Hsp90-4	-	-

As an example, purification of STIAT1 is illustrated in Figure 34. Total protein extract from *E. coli* was separated by affinity chromatography using His-trap column and subsequent SDS-PAGE of fractions was performed. Western blot analysis of fractions using antiserum directed against the His-tag validated the elution of recombinant protein in eluat fraction.

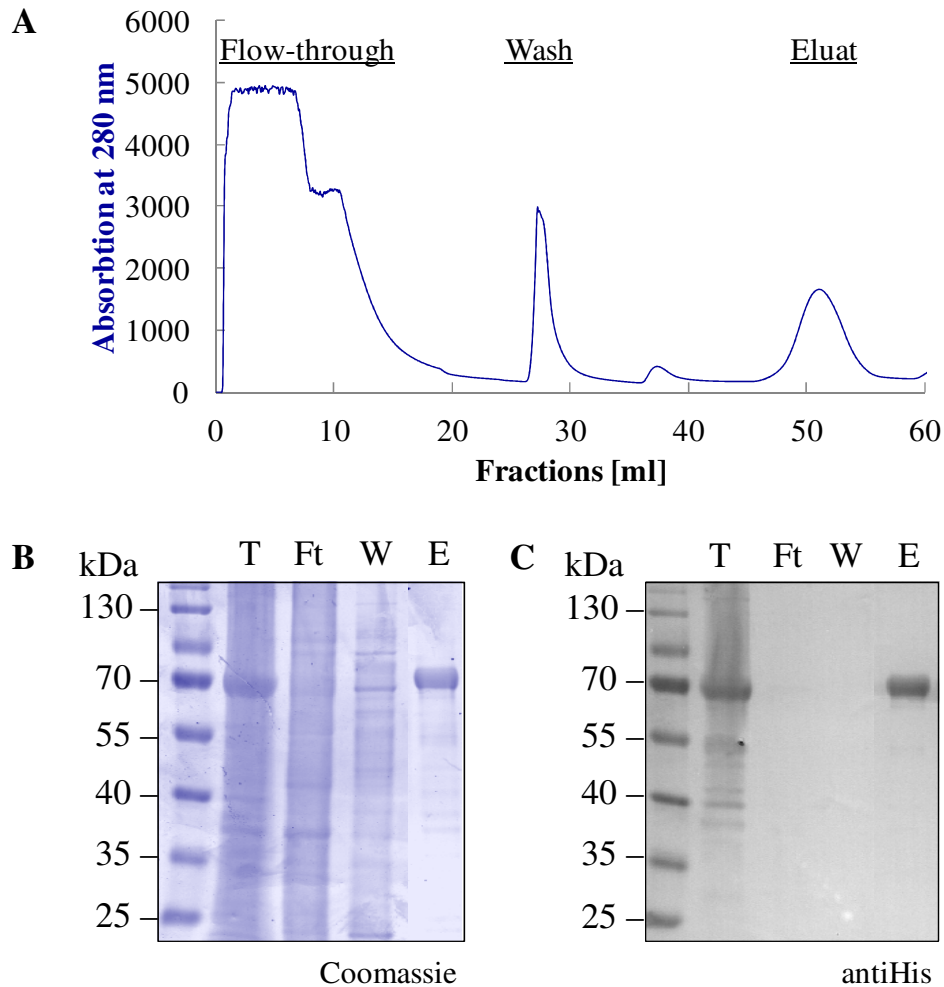


Figure 34: Affinity purification of recombinant STIAT1 isoform from *E. coli*.

A: Separation profile of affinity chromatography using His-trap column. Blue: Absorption at 280 nm.

B: Fractions of each purification step from A were separated by SDS-PAGE and visualised by cCBB staining. T: Total protein, Ft: Flow through, W: Wash, E: Eluat.

C: Western blot analysis of fractions with antibody against the His-tag confirmed the purification of recombinant STIAT1.

4.4.7. *In vitro* interaction studies of STIAT2 with Hsp70-5 revealed plenty of background and unspecific binding of the Hsp

After cloning and production of recombinant proteins, *in vitro* interactions of purified recombinant proteins were studied according to the protocol of Wegele *et al.* (2003) to

validate the interactions. At first, Hsp70-5 was selected for the *in vitro* interaction study to STIAT2 as it belongs to the cytosolic Hsp70 and different affinities to the STIAT isoforms are suggested as shown in Table 10. The recombinant proteins STIAT2 and/or Hsp70-5 were mixed with total protein extracts from Arabidopsis leaves and precipitated by antibodies raised against STINT and Hsp70. All fractions were collected, separated by SDS-PAGE and transferred to PVDF membrane and probed with antiserum directed against the recombinant tobacco protein STINT and Hsp70. The experimental set-up is depicted in Figure 35.

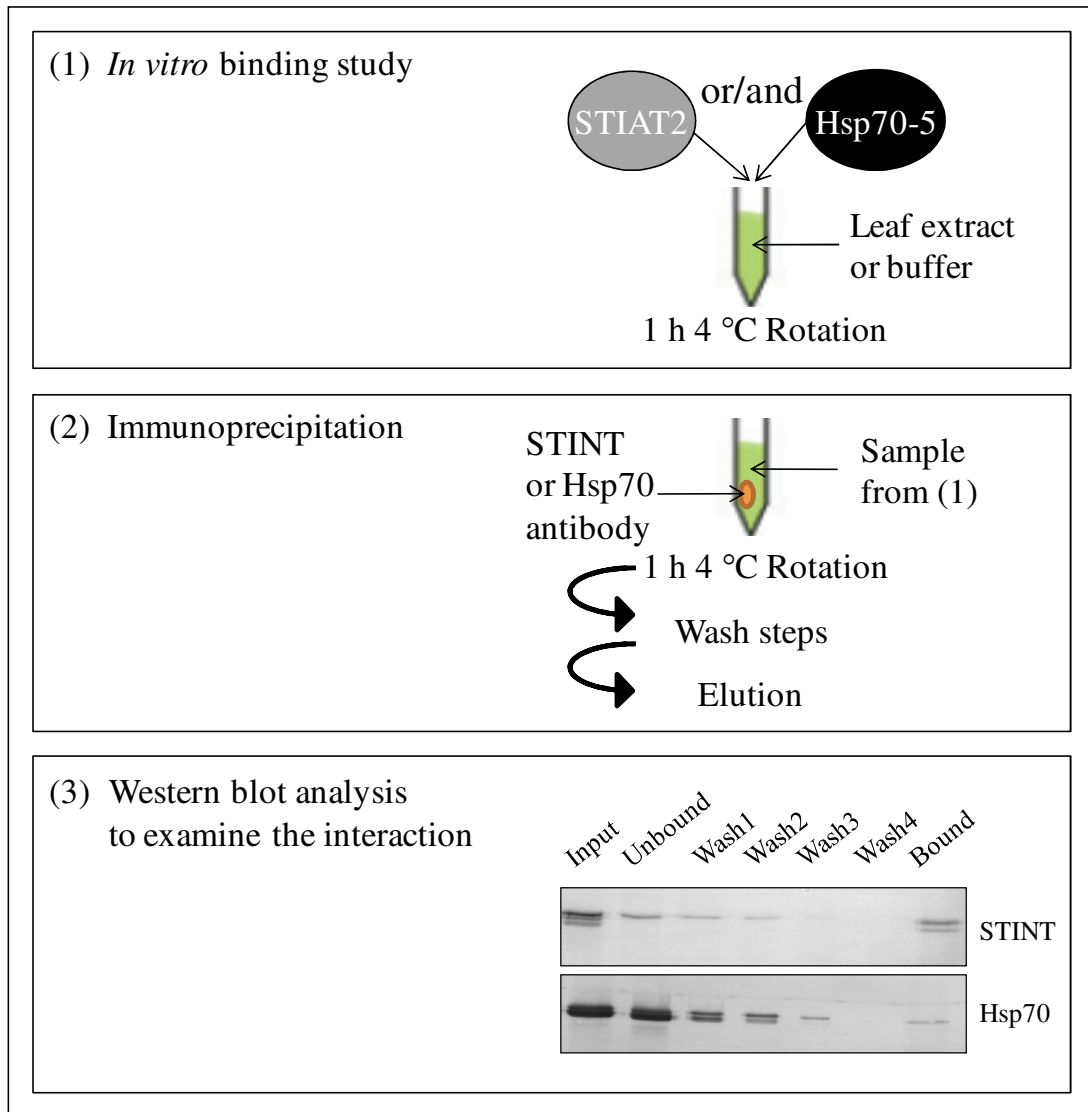


Figure 35: Schematic presentation of the experimental set-up of *in vitro* interaction studies and their subsequent analysis.

Recombinant proteins were mixed with Arabidopsis leaf extract and precipitated using one of the antibodies. All fractions were analysed using Western blot analysis using antiserum against STINT and Hsp70.

The result of the interaction study of STIAT2 with Hsp70-5 spiked in Arabidopsis leaf extract is shown in Figure 36. Immunoblot analysis of STIAT and Hsp70 resulted in co-elution of the STIAT2 with Hsp70-5 when purifying against one of the proteins, but Hsp70 was detected with lower intensity compared to STIAT in both cases (Figure 36, 1-2, lanes bound). In contrast, when only STIAT2 was incubated in leaf extract and purification with the Hsp70 antibody was performed, Hsp70 was detected with higher intensity (Figure 36, 3, lanes bound). This finding indicates the co-elution with the native Hsp70 isoforms from the leaf extract, which was observed for Hsp70 with native STIAT isoforms but with lower intensity (Figure 36, 4, lanes bound).

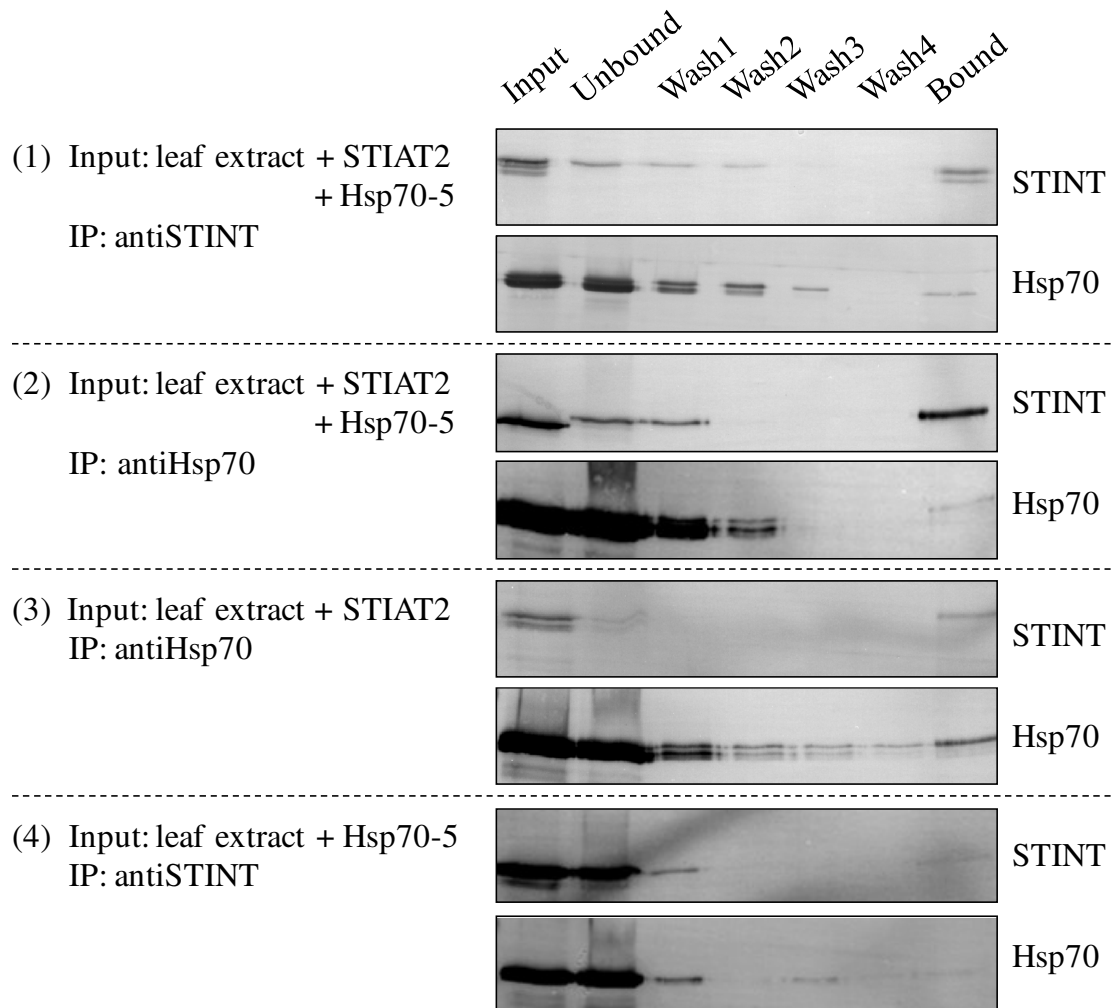


Figure 36: *In vitro* interaction studies of STIAT2 and Hsp70-5 in Columbia-0 leaf extract using antiSTINT and antiHsp70 antibodies for precipitation.

All fractions obtained during precipitation were separated by SDS-PAGE and probed with antiserum against STINT and Hsp70. The precipitations of STIAT2+Hsp70-5 using antibodies against STINT (1) and Hsp70 (2) revealed co-elution of STIAT2 and Hsp70-5. Nearly the same co-elution was observed after purification of the native Hsp70 (3) and native STIAT isoforms (4).

Finally, this experiment could not show clear interaction of STIAT2 and Hsp70-5 due to background signals obtained by co-elution of protein with the native interaction partner from leaf extract. Therefore, the experimental set-up was modified by using buffer instead of leaf extract to exclude the co-elution of proteins with native interacting proteins.

The result of the interaction study of STIAT2 with Hsp70-5 incubated in Hepes buffer is shown in Figure 37. Hsp70-5 was marginal co-eluting with STIAT2 after precipitation with the STINT antibody (Figure 37, 1). To exclude unspecific binding of STIAT2 and Hsp70-5 to the matrix, control precipitation using antiGoat was performed (Figure 37, 2). The precipitation using antiGoat showed the detection of Hsp70-5 in the bound fraction indicating unspecific binding of Hsp70 to the matrix, while unspecific binding of STIAT2 to antiGoat was not detected.

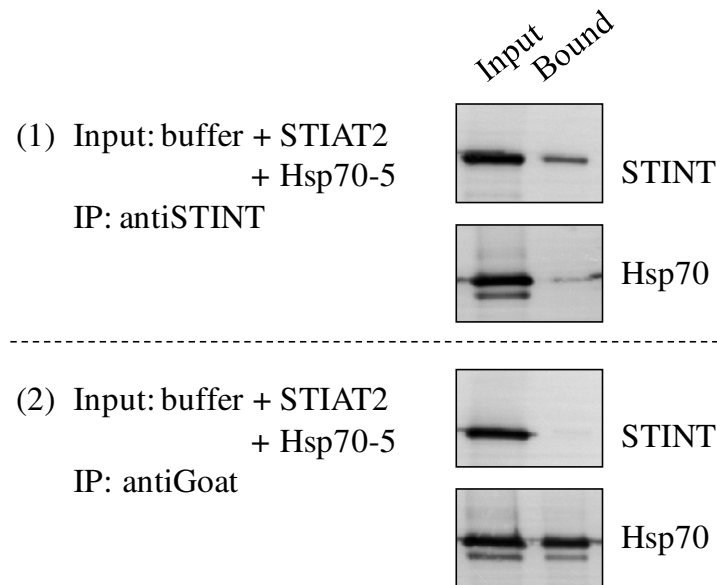


Figure 37: *In vitro* interaction studies of STIAT2 with Hsp70-5 in buffer using antiSTINT or antiGoat antibodies for immunoprecipitation.

The input and bound fraction were separated by SDS-PAGE and probed with antiserum against STINT and Hsp70. Immunodetections revealed a weak co-elution of Hsp70-5 with STIAT2 using STINT antibody (1), but unspecific binding of Hsp70-5 to antiGoat bound matrix (2).

In summary, *in vitro* binding studies of recombinant STIAT2 isoform with its putative interaction partner Hsp70-5 revealed either a high background signals in plant extracts or unspecific binding of the latter protein to the matrix. Therefore, another method for analysing STIAT interaction partners was applied.

4.4.8. Tandem affinity purification of heterologous STINT protein in Arabidopsis revealed Hsp90 and Hsp70 as interacting proteins

Tandem affinity purifications (TAP) were performed on C-terminally and N-terminally TAP-tagged STINT overexpressed under the control of the 35S promoter in Arabidopsis cell culture (Figure 38) by the Functional Proteomics Group at VIB/University Gent, Belgium. Total protein extracts from Arabidopsis cell culture were fractionated using immunoglobulin G (IgG) and calmodulin resins. Eluted proteins were separated by SDS-PAGE and visualized by cCBB staining. Protein lanes were excised and digested with trypsin. Protein identification via MALDI-TOF-TOF MS was performed on tryptic peptides by searching SNAPS database (<http://www.ptools.ua.ac.be>). Background contaminations are an important issue in TAP experiments. In order to assess those, proteins of purifications using wild-type Arabidopsis cell culture and two cultures overexpressing the TAP-tagged proteins β -glucuronidase and green fluorescent protein were excluded from the dataset as shown previously (Van Leene *et al.* 2007).

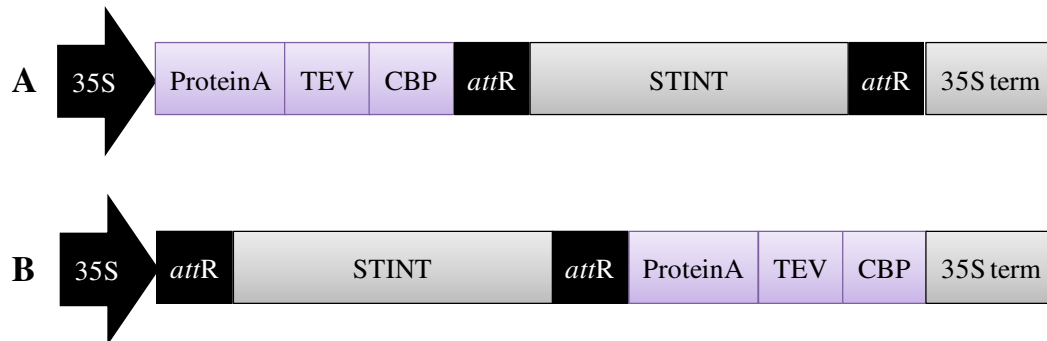


Figure 38: Schematic diagram of STINT TAP expression cassettes used for Arabidopsis cell culture transformation. N-terminal (A) or C-terminal (B) fusions of STINT to the TAP tag, consisting of the three subunits protein A domain, tobacco etch virus (TEV) cleavage site and calmodulin binding protein (CBP), were produced. Expression was controlled by 35S promoter.

The separation and identification of interacting proteins of N-terminally TAP-tagged STINT is shown in Figure 39, resulting in detection of the tagged protein in the most prominent band on the gel. The chaperones Hsp90 and Hsp70 were identified with very high score in multiple isoforms and were present in both experiments and in one purification of C-terminally TAP-tagged STINT (Table A 3). This indicates that Hsp90 and Hsp70 are true interacting proteins of STINT, although chaperones belong to contaminating proteins. In total, four and five accessions for Hsp90 and Hsp70 protein families were identified, respectively, all belonging to cytosolic isoforms.

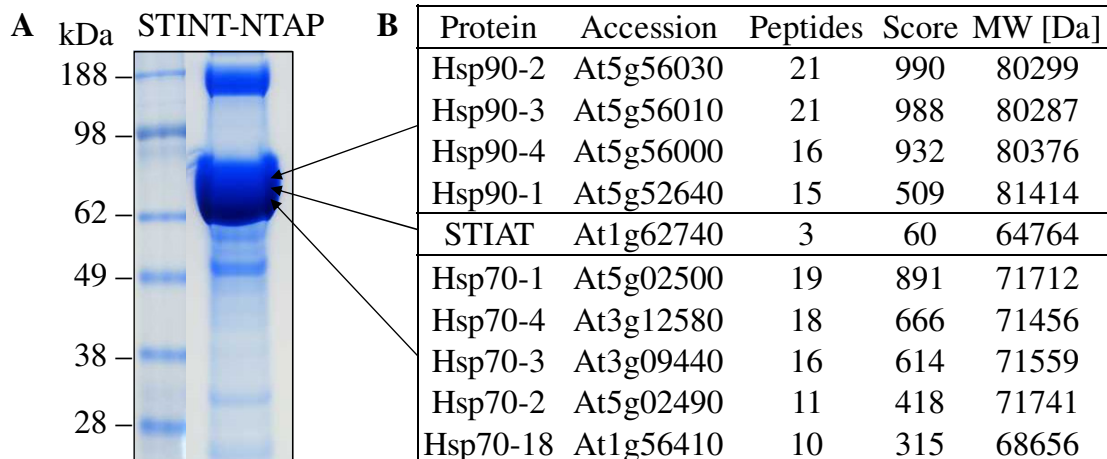


Figure 39: Tandem affinity purification of STINT from Arabidopsis cell culture. The experiments were performed twice to ensure technical reproducibility.

A: Protein complexes isolated by N-terminal TAP-tagged STINT were separated by SDS-PAGE and visualized by cCBB staining.

B: Protein identification using MALDI-TOF-TOF MS. Protein name, accession number, detected peptides, score and molecular weight of proteins co-purifying with the bait protein are given. Protein identification via MALDI-TOF-TOF MS was performed by searching SNAPS database (<http://www.ptools.ua.ac.be>).

4.4.9. Tandem affinity purification of STI1 protein in yeast revealed Hsp90 and Hsp70 as interacting proteins

The tandem affinity purification of STI1 protein with their known interaction partners in yeast was performed as a technical control, in order to identify client proteins by using the TAP method. Therefore, a transgenic STI1 yeast strain, expressing C-terminally TAP-tagged STI1 under its native promoter, was used. Total protein extracts from yeast were fractionated using IgG and Calmodulin resins and fractions were separated by SDS-PAGE and visualized by cCBB staining (Figure 40). The Coomassie stained gel showed four protein bands after first purification step using IgG, but only three protein bands after second purification step using calmodulin in the range of 70 to 90 kDa. This result indicates a lower binding affinity of this band during the second purification step. In order to identify STI1 and all of its interacting proteins, the four proteins after first purification step (IgG bound fraction) were excised manually from the cCBB stained gel, digested with trypsin and subjected to MS analysis. Protein identification by MALDI-TOF MS peptide mass fingerprinting resulted in distinct identification of bait protein STI1 in band #3 (Table 12). Hsp90 and Hsp70 isoforms were detected in remaining bands, but a differentiation of isoforms was only possible when analysis by LC-ESI-Q-TOF MS/MS using the derived *de novo* sequence of tryptic peptides for

homology-based database search was performed. Thus, LC-ESI-Q-TOF MS/MS lead to distinct identification of Hsp90 isoforms in bands #1 and #2 (Table 12), while two of the nine Hsp70 isoforms were identified in band #4, each with three specific peptides.

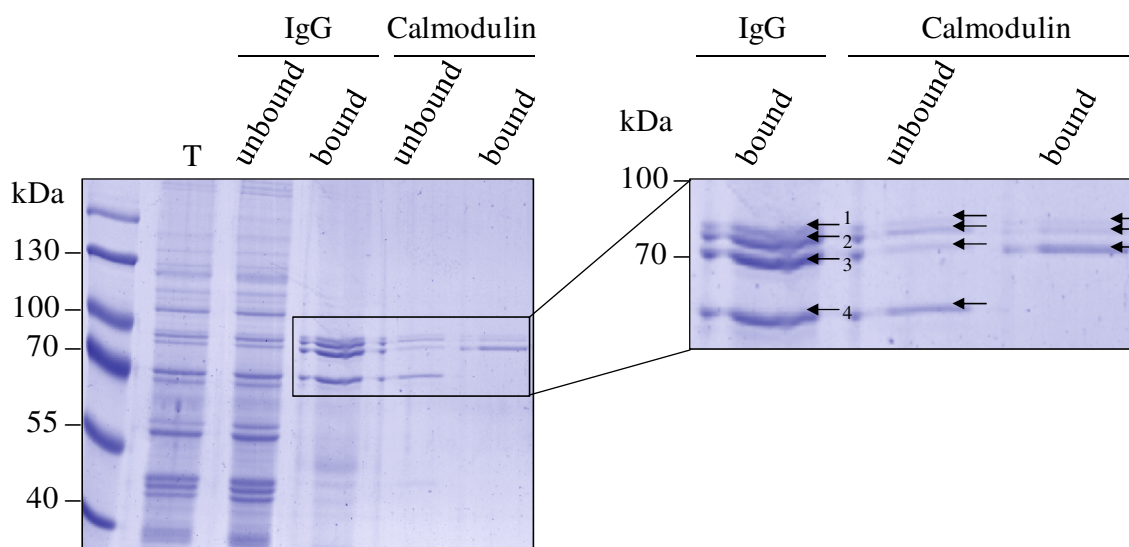


Figure 40: Tandem affinity purification of STI1 from yeast. The experiments were performed twice to ensure technical reproducibility.

10 μ g of total extract (T) and unbound IgG fraction as well as 30 μ l of remaining TAP fractions were separated by SDS-PAGE and visualized by cCBB staining. The indicated area of the Coomassie-stained gel is reproduced with higher magnification on the right side, showing four protein bands after first purification step using IgG compared to three protein bands after second purification step using calmodulin.

Table 12: Identification of TAP purified STI1 interaction partners from yeast by MALDI-TOF MS and LC-ESI-Q-TOF MS/MS. Given are the band as indicated in Figure 40, the protein name and accession number, the detected total and isoform-specific peptides revealed by ESI MS/MS. The isoforms with maximum of diagnostic peptides are shown in bold.

Band	Protein	Accession	Total peptides	Diagnostic peptides
1	Hsp82	P02829	16	3
	Hsc82	P15108	13	0
2	Hsc82	P15108	16	1
	Hsp82	P02829	15	0
3	STI1	P15705	11	11
4	Hsp71	P10591	26	3
	Hsp72	P10592	28	3

Figure 41 shows an example for the distinct identification of the constitutive Hsp90 isoform (Hsc82) in band #2. The identified peptides were analysed for their diagnostic properties by

matching them to the complete protein sequences of the two Hsp90 isoforms (red). One of 16 peptides was found to be diagnostic for Hsc82 (underlined).

HSC82	MAGETFEFQAEITQLMSLIINTVYSNKEIFLR <u>ELISNASDALDKIRY</u> QALSDPK <u>QLETEP</u>	60
HSP82	MASETFEFQAEITQLMSLIINTVYSNKEIFLR <u>ELISNASDALDKIRY</u> KSLSDPK <u>QLETEP</u>	60
...		
HSC82	<u>DLFIR</u> ITPKPEEKVLEIRDSGIGMT <u>KAELINNLGTIAK</u> SGTKAFMEALSAGADVSMIGQF	120
HSP82	<u>DLFIR</u> ITPKPEEQVLEIRDSGIGMT <u>KAELINNLGTIAK</u> SGTKAFMEALSAGADVSMIGQF	120
...		
HSC82	KPKLEEVDEEEEEKKPKTKK <u>VKEEVQEELELNK</u> TKPLWTR <u>NPSDITQEEYNAFYKSI</u> SND	295
HSP82	KPKLEEVDEEEEE-KKPKTKK <u>VKEEVQEEIEELNK</u> TKPLWTR <u>NPSDITQEEYNAFYKSI</u> SND	299
HSC82	<u>WEDPLYVK</u> HFSVEGQLEFRAILFIPKR <u>APFDLFESK</u> KKKNNIKLYVRRVFITDEAEDLIP	355
HSP82	<u>WEDPLYVK</u> HFSVEGQLEFRAILFIPKR <u>APFDLFESK</u> KKKNNIKLYVRRVFITDEAEDLIP	359
HSC82	EWLSFVK <u>GVVDEDLPLNLSREML</u> QQNKIMKVIRKNI <u>VKKLIEAFNEIAEDSEQ</u> FDK	415
HSP82	EWLSFVK <u>GVVDEDLPLNLSREML</u> QQNKIMKVIRKNI <u>VKKLIEAFNEIAEDSEQ</u> FEK	419
HSC82	AFAKNIKLGVEDTQNRAALAKLLRYNSTK <u>SVDELTS</u> LDYVTRMPEHQK <u>NIYYITGESL</u>	475
HSP82	AFSKNIKLGVEDTQNRAALAKLLRYNSTK <u>SVDELTS</u> LDYVTRMPEHQK <u>NIYYITGESL</u>	479
HSC82	<u>KAVEKSPFLDALK</u> AKNFEVLFLTDPIDEYAFQQLKEFEGKTLVDITKDFELEETDEEKAE	535
HSP82	<u>KAVEKSPFLDALK</u> AKNFEVLFLTDPIDEYAFQQLKEFEGKTLVDITKDFELEETDEEKAE	539
HSC82	REKEIKEYEPLTKALKDILGDQVEKVVVSYK <u>LLDAPAAIRTGQFGWSANMER</u> IMKAQALR	595
HSP82	REKEIKEYEPLTKALKEILGDQVEKVVVSYK <u>LLDAPAAIRTGQFGWSANMER</u> IMKAQALR	599
HSC82	<u>DSSMSSYMSSK</u> KTFEISPKSPIIKELKKRVDEGGAQDKTVKDLTNLLFETALLTSGFSLD	655
HSP82	<u>DSSMSSYMSSK</u> KTFEISPKSPIIKELKKRVDEGGAQDKTVKDLTKLLYETALLTSGFSLD	659
HSC82	EPTSFASRINRLISLGLNIDEEETETAPEASTEAPVEEVPADTEMEEVD	705
HSP82	EPTSFASRINRLISLGLNIDEEETETAPEASTAAPVEEVPADTEMEEVD	709

Figure 41: Identification of the second band from Figure 40 as Hsc82 using LC-ESI-Q-TOF MS/MS. The second band was excised from the gel of IgG fraction of TAP of yeast STI1. The sequence alignment of the two yeast Hsp90 isoforms and matching tryptic peptides sequenced by LC-ESI-Q-TOF MS/MS are shown (bold). One diagnostic peptide (red underlined) for Hsc82 was found leading to distinct identification of the Hsp90 isoform.

In summary, MS analysis of tandem affinity purification of STI1 protein in yeast confirmed Hsp90 and Hsp70 isoforms as interaction partner, but provided information on specific isoforms. The identification of client proteins was unsuccessful as shown for STINT. However, stabilization experiments of protein complexes by cross-linking using photo-activateable amino acids supplemented into the media were performed but yeast strains were not growing (not shown).

4.5. Are the STIAT isoforms modified by phosphorylation?

In mammals and yeast, several phosphorylation sites of HOP/STI1 have been described and suggested to modulate the nuclear localisation (Daniel *et al.* 2008) and potentially the interaction with Hsp. Phosphorylation of homologues to HOP/STI1 in plants has not yet been studied by targeted approaches so far. Experimental evidences of phosphorylated peptides in STIAT isoforms were only available from large-scale phosphoproteomic analysis available at the PhosPhAt database (Heazlewood *et al.* 2008). According to this, one phosphopeptide is conserved among all three STIAT isoforms and one phosphopeptide is diagnostic for STIAT1 (Table 13). The phosphorylated peptides of the STIAT isoforms were obtained by using different enrichment techniques of phosphopeptides and various MS analysis methods.

Therefore, this post-translational modification (PTM) was investigated for its appearance in STIAT isoforms.

Table 13: Overview of phosphorylated peptides among the STIAT isoforms obtained by shotgun MS experiments (Heazlewood *et al.* 2008). Phosphorylated peptides, the corresponding isoforms, type of tissue, enrichment technique for phosphorylated peptides, MS instrument and references are given.

Phosphorylated peptide	Isoform	Tissue	Enrichment	Instrument	Reference
GDL(pT)PEELKER	STIAT1 STIAT2 STIAT3	Seedling	Fe-IMAC	Q-TOF	(Li <i>et al.</i> 2009)
GDL(pT)PEELK	STIAT3	Cell culture	TiO ₂	LTQ-Orbitrap	(Nakagami <i>et al.</i> 2010, Sugiyama <i>et al.</i> 2008)
NP(pS)NLNLYLQDQR	STIAT1	Cell culture	TiO ₂	LTQ-Orbitrap	(Nakagami <i>et al.</i> 2010, Sugiyama <i>et al.</i> 2008)

4.5.1. Analysis of 2-D protein pattern of recombinant STIAT1 and STIAT2

First, the detection of possible phosphorylation sites in the STIAT1 and STIAT2 isoform was investigated for its significance within the recombinant proteins. Recombinant STIAT1 and STIAT2 proteins extracted under native conditions were analysed using 2-D gel electrophoresis (Figure 42, Figure 43). The Coomassie stained gels showed separation of recombinant STIAT1 in a chain comprising of 5 spots, whereas 2-D separation of recombinant STIAT2 resulted in a chain of 4 spots. This result indicates a similar 2-D pattern of the two STIAT isoforms.

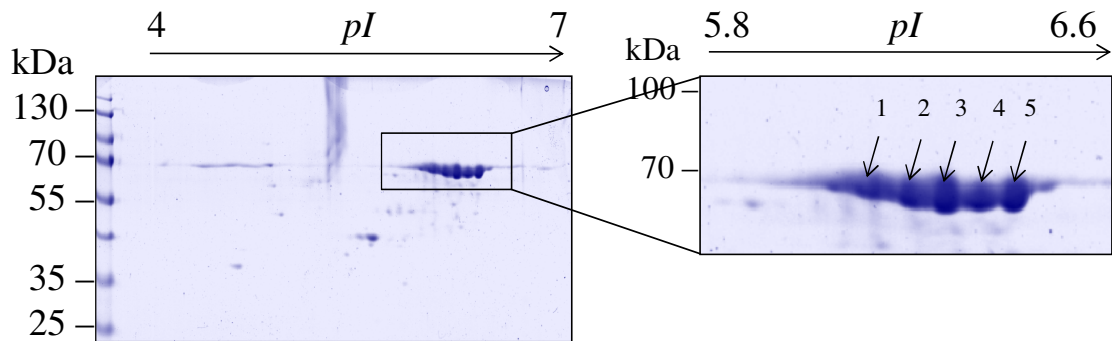


Figure 42: Protein pattern of recombinant STIAT1.

Eight μg of recombinant STIAT1 was separated on 7 cm pH gradients 4-7 and SDS-PAGE and visualized by cCBB staining. The indicated area of the Coomassie-stained gel is reproduced with higher magnification on the right side, showing a chain of five spots for recombinant STIAT1, indicating multiple phosphorylation sites in STIAT1.

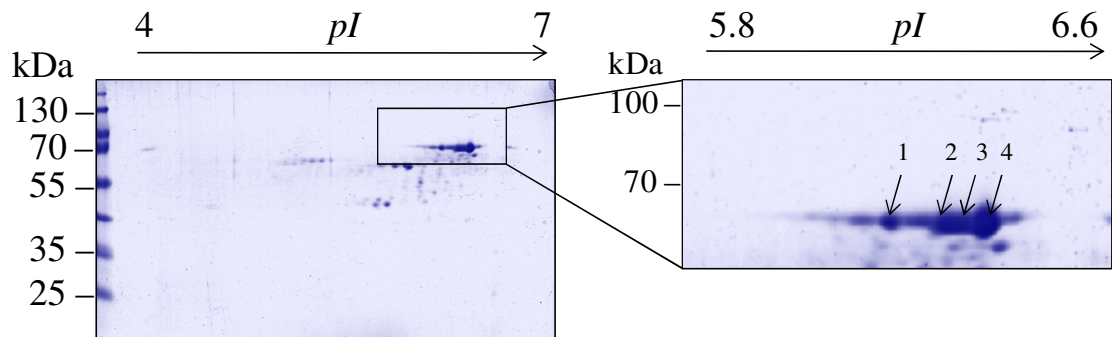
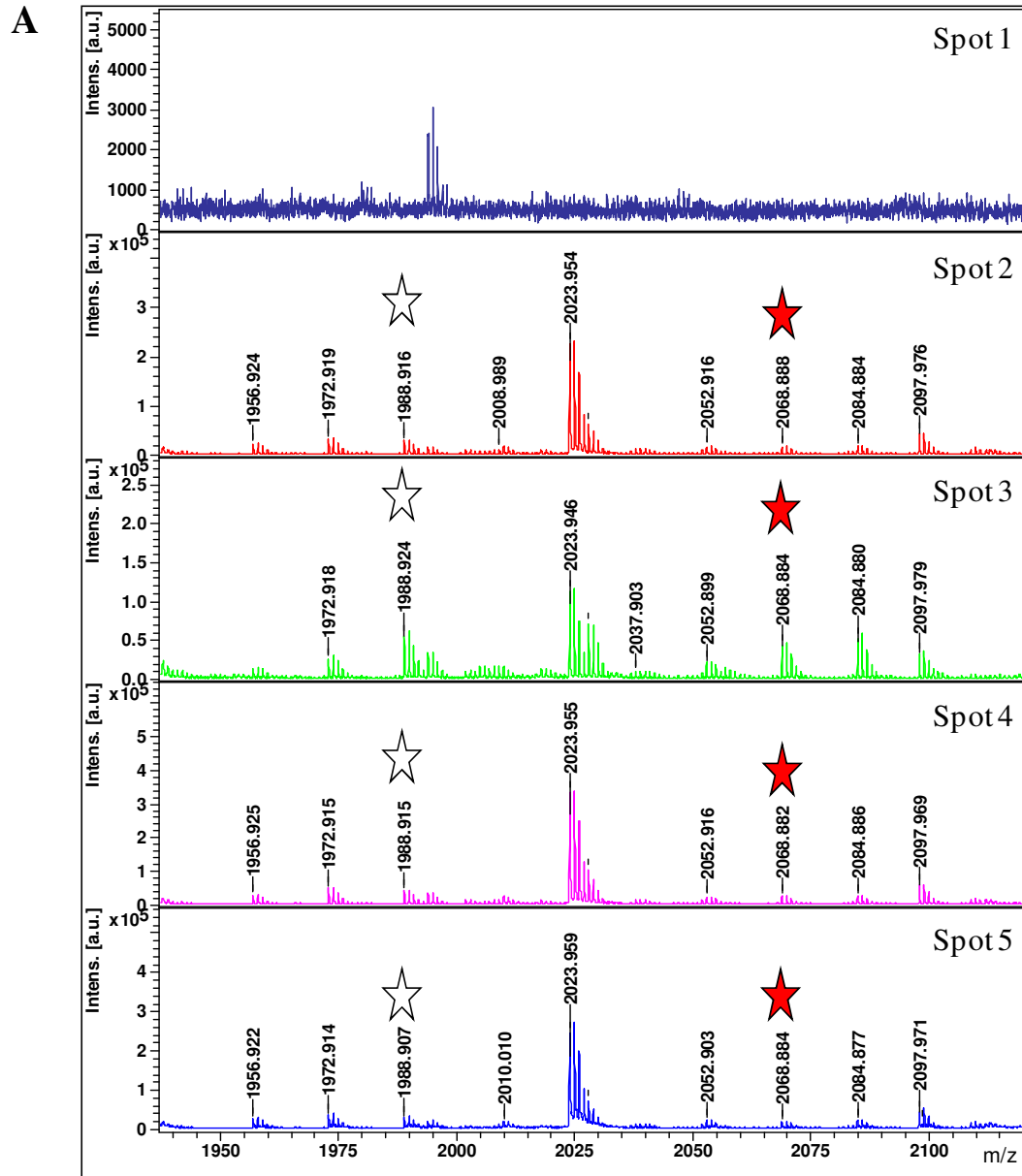


Figure 43: Protein pattern of recombinant STIAT2.

Five μg of recombinant STIAT2 was separated on 7 cm pH gradients 4-7 and SDS-PAGE and visualized by cCBB staining. The indicated area of the Coomassie-stained gel is reproduced with higher magnification on the right side, showing a chain of four spots for recombinant STIAT2, indicating multiple phosphorylation sites in STIAT2.

These five detected spots from Figure 42 were excised manually from the cCBB stained gel and incubated with trypsin. MS analysis by MALDI-TOF MS peptide mass fingerprinting led to identification of a phosphorylated peptide in spots 2-5 (Figure 44). Extractions of MALDI-TOF spectra show the detection of a peptide, which is present in dephosphorylated and phosphorylated state. Matching peptide with its putative phosphorylated amino acid is shown in STIAT1 protein sequence. Thus, the phosphopeptide was identified in four of the five spots. This phosphorylation site seems not to be responsible for *pI* shift suggesting more phosphorylation sites in recombinant STIAT1 protein.



B MADEAKAKGNAAFSSGDFNSAVNHFTDAINLTPTNHVLFSNRSAAHASLNHYDEALSDAK
 KTVELKPDWGGKYSRLGAAHLGLNQFDEAVEAYSKGLEIDPSNEGLKSGLADAKASARS
 RASAPNPFGDAFQGPPEMWSKLTADPSTRGLLKQPDFVNMKEIQRNP SNLNLYLQDQRM
 QALGVLLNIQIRIQAGDDMEIGEEEMAVPSRKEPEVEKRRKPEPEPEPEPEFGEKQKK
 LKAQKEKELGNAAYKKKDFETAIQHYSTAMEIDDEDISYITNRAAVHLEMGYDECIKDC
 DKAVERGRELRSDYKMKVAKALTRKGTALGKMAKVSVDYEPVIQTYQKALTEHRNPETLKR
 LNEAERAKKELEQQEYYDPNIGDEEREKGNDFFKQKYPDAVRHYTEAIKRNPKDPRAYS
 NRAACYTKLGAMPEGLKDAEKCIELDPFLKGYSRKGAVQFFMKEYDNAMETYQKGLEHD
 PNNQELLDGVKRCVQQINKANRGDLTPEELKERQAK **GMQDPEIQNILTDPVMR** QVLSDLQ
 ENPAAAQKHMQNPMIMNKIQKLISSGIVQMK

Figure 44: Identification of the phosphorylated peptides in recombinant STIAT1.

MALDI-TOF spectra of tryptic digestion from the five spots of recombinant STIAT1 from Figure 42 are shown in m/z range of 1950 to 2100. Indicated by colorless and red asterisks are m/z 1988.9 $[M+H]^+$ and m/z 2068.9 $[M+H]^+$ peptide ions representing the dephosphorylated and phosphorylated form of the peptide indicated in red in the sequence of STIAT1 protein sequence. The putative phosphorylated amino acid threonine (T) is underlined.

In contrast to the detection of the phosphorylation sites of STIAT1, the phosphorylated peptides from recombinant STIAT2 isoform should be enriched using enrichment techniques for phosphopeptides. Therefore two enrichment techniques were applied using the standard protein casein.

4.5.2. Method development for enrichment of phosphopeptides from casein using immobilized metal ion affinity chromatography and Phos-tag agarose

Phosphopeptides of casein were enriched either by IMAC according to the protocol of Villen and Gygi (2008) or by Phos-tag agarose (<http://www.phos-tag.com>). Casein was digested in solution with trypsin. All fractions obtained during procedure were subjected to MS analysis by MALDI-TOF MS in order to validate the enrichment technique. Extractions of mass spectra of flow-through and eluate fractions show detection of three and four phosphorylated peptides (Figure 45A), which are all molecular ion variances of the same peptide sequence (Figure 45B). The evaluation of the peak intensity of the high abundant molecular ion m/z 1951.8 $[M+H^+]$ among all fractions resulted in higher abundance in flow-through and wash fractions compared to eluate fraction (Figure 45C). This result indicates a low binding capacity of the phosphopeptide to the matrix during experimental procedure.

Therefore, a second enrichment technique for phosphorylated peptides from casein was used. Casein was digested in solution with trypsin for the enrichment using Phos-tag agarose compared to IMAC. All fractions obtained during Phos-tag agarose enrichment were subjected to MS analysis by MALDI-TOF MS. Extractions of mass spectra before and after enrichment show detection of two phosphorylated peptides specifically detected in the enriched fraction (Figure 46A). The peak intensity of the molecular ion variance m/z 1951.8 $[M+H^+]$ was evaluated in the fractions obtained during enrichment, showing the detection of the phosphopeptide specifically in the eluate fraction with and without desalting (Figure 46B). The phosphopeptide was not detected in flow-through compared to enrichment by IMAC, suggesting a higher binding capacity of the phosphopeptide to the Phos-tag agarose matrix.

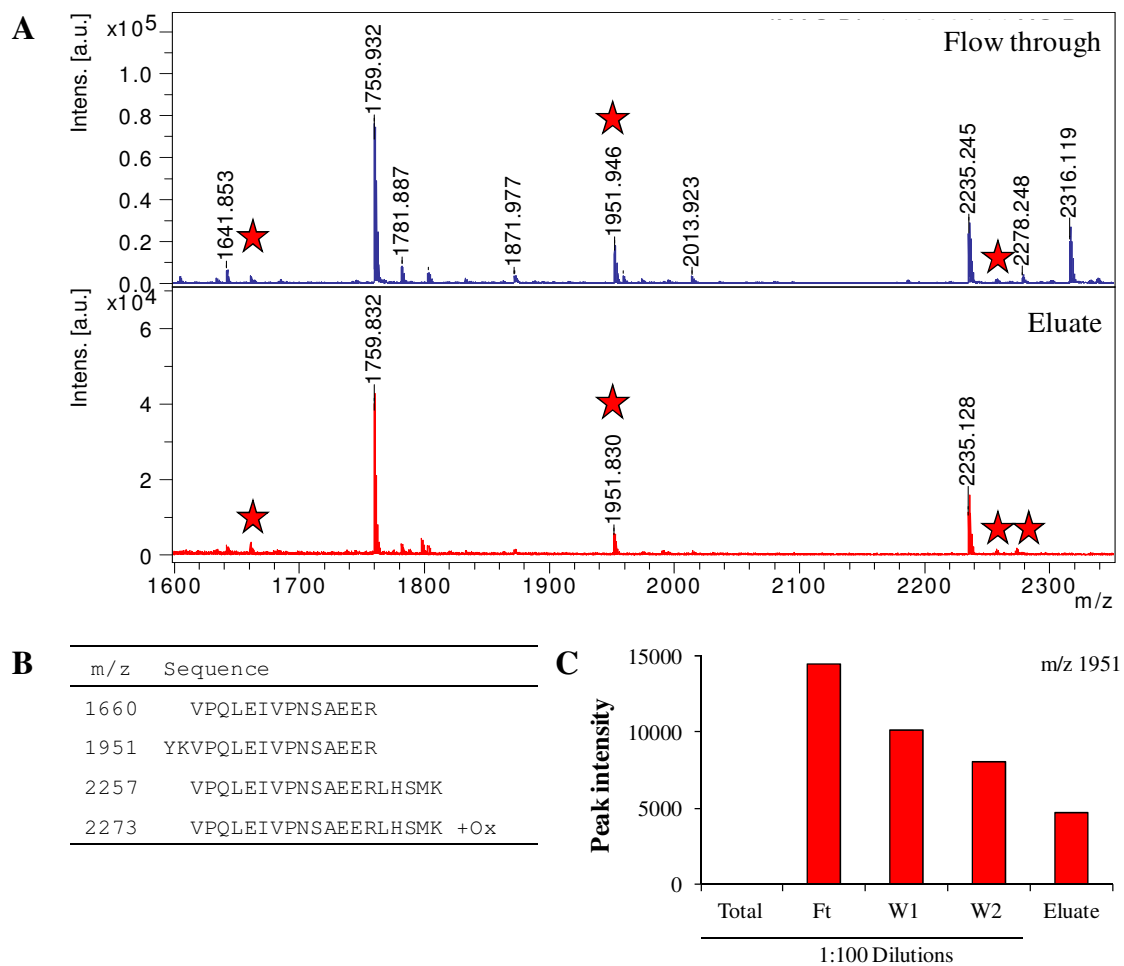


Figure 45: Identification of phosphorylated peptides in casein sing enrichment by IMAC. The experiments were performed twice.

A: MALDI-TOF spectra of IMAC flow-through (upper panel) and after enrichment of phosphopeptides of casein (lower panel) are shown in m/z range of 1600 to 2300. Indicated by red asterisk are m/z 1660.6 [M+H⁺], m/z 1951.8 [M+H⁺], m/z 2257.0 [M+H⁺] and m/z 2273.0 [M+H⁺] peptide ions representing phosphorylated peptides.

B: List of peptide ions from A representing molecular ion variances of the same peptide sequence.

C: Peak intensity of phosphorylated m/z 1951.0 [M+H⁺] peptide ion from A during the enrichment procedure, resulting in depeletion of the phosphorylated peptide during enrichment procedure.

Total: total extract, **Ft:** flow-through, **W1+W2:** wash fractions 1 and 2.

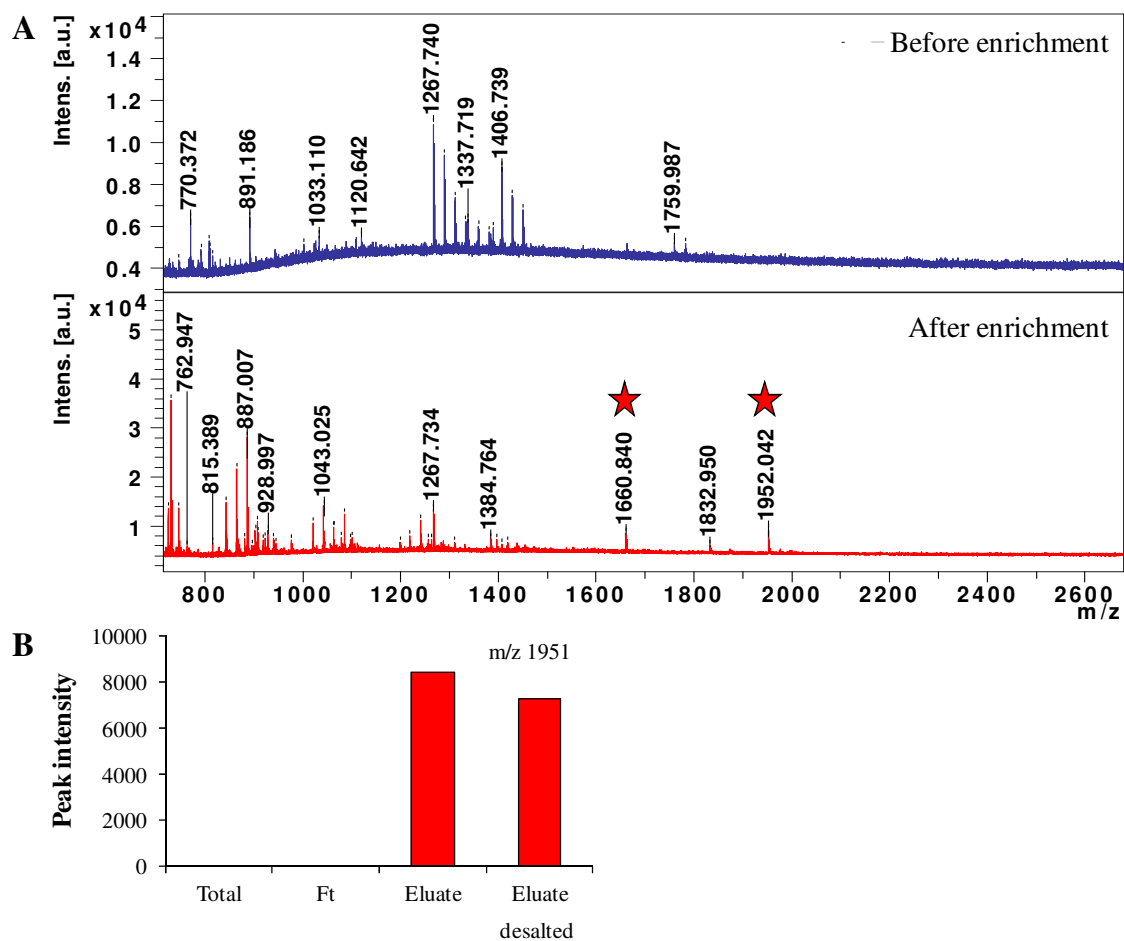


Figure 46: Identification of phosphorylated peptides in casein using Phos-tag agarose enrichment.

A: MALDI-TOF spectra of total trypsin digest of casein (upper panel) and after enrichment of phosphopeptides (lower panel) are shown in m/z range of 800 to 2600. Indicated by red asterisks are m/z 1660.8 $[M+H^+]$ and m/z 1952.0 $[M+H^+]$ peptide ions representing phosphorylated peptides.

B: Peak intensity of phosphorylated m/z 1952.0 $[M+H^+]$ peptide ion from A during the enrichment procedure, resulting in detection of the phosphorylated peptide in the eluate fraction.

Total: total extract, **Ft:** flow through.

4.5.3. Enrichment of phosphopeptides from STIAT2 using Phos-tag agarose

After obtaining specific enrichment of phosphorylated peptide of casein, the enrichment technique was transferred to the recombinant STIAT2. Total peptide mixture and peptides enriched by Phos-tag agarose were subjected to MS analysis by MALDI-TOF. Extractions of mass spectra show detection of the peptide, which is present as dephosphorylated and phosphorylated form in both total and enriched sample (Figure 47A). The peak intensity of the phosphorylated peptide m/z 2176.2 $[M+H^+]$ and the corresponding non-phosphorylated peptide m/z 2016.2 $[M+H^+]$ was evaluated in the samples during enrichment, resulting in the

depletion of the non-phosphorylated peptide m/z 2016.2 $[M+H]^+$ (Figure 47B). The highest intensity of that peptide was detected in the flow through, whereas only a minor intensity of was detected in the eluate fraction. In comparison, the intensity of the phosphorylated peptide m/z 2176.2 $[M+H]^+$ was of higher intensity there. As the phosphorylated peptide was detected with higher intensity in the flow-through compared to the eluate the binding of phosphopeptides from STIAT have to be improved.

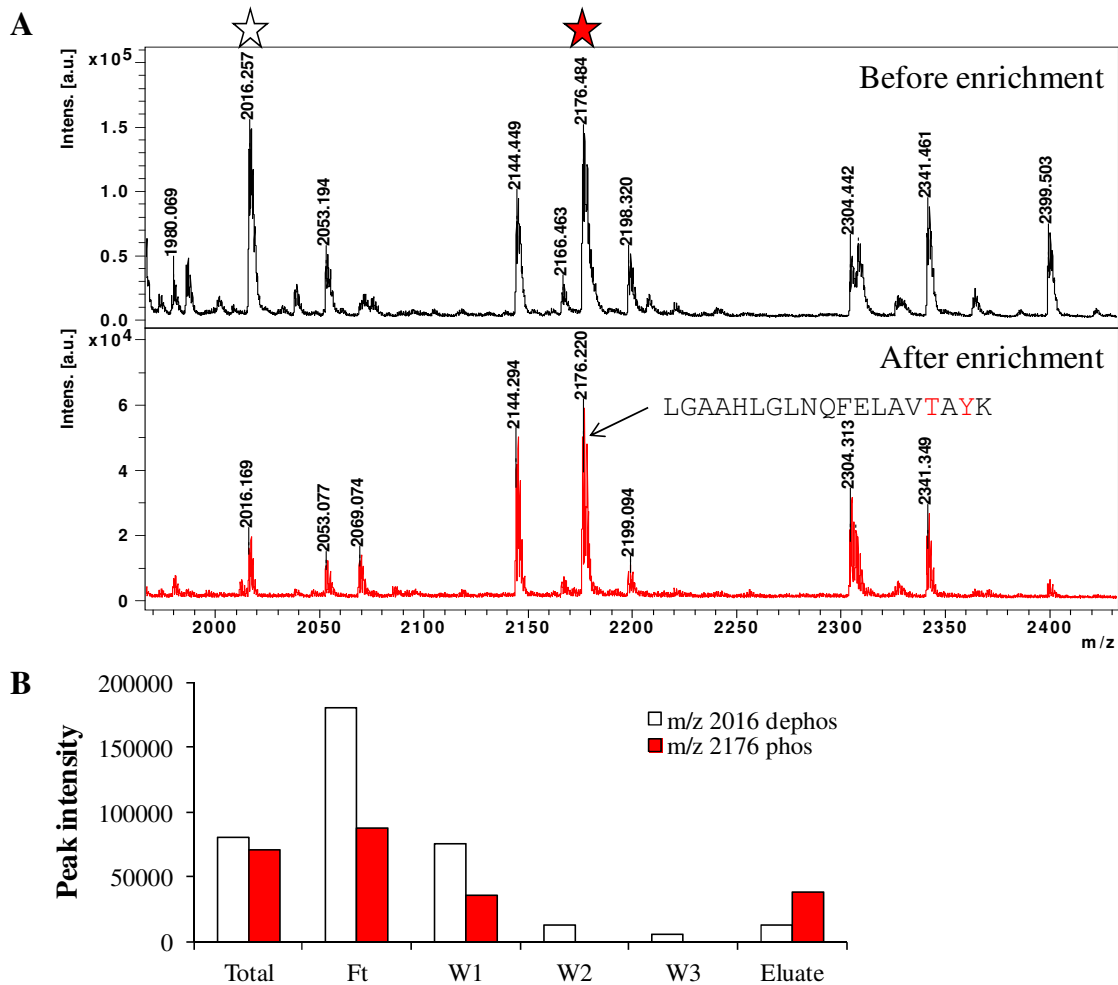


Figure 47: Identification of a phosphorylated peptide in recombinant STIAT2 using Phos-tag agarose enrichment.

A: MALDI-TOF spectra of total trypsin digest of recombinant STIAT2 (upper panel) and after enrichment of phosphopeptides (lower panel) are shown in m/z range of 2000 to 2400. Indicated by colorless and red asterisks are m/z 2016.2 $[M+H]^+$ and m/z 2176.4 $[M+H]^+$ peptide ions representing the dephosphorylated and phosphorylated state of the peptide, respectively.

B: Peak intensities of dephosphorylated m/z 2016.2 $[M+H]^+$ and phosphorylated m/z 2176.4 $[M+H]^+$ peptide ions from A through the enrichment procedure, resulting in depletion of the dephosphorylated peptide.

Total: total extract, Ft: flow through.

4.5.4. Enrichment of STIAT isoforms from Arabidopsis leaf extract using preparative isoelectric focussing

After the finding of possible phosphorylation sites within the recombinant STIAT proteins, the aim was the identification of the possible phosphorylation sites of the STIAT isoforms *in vivo*. As mentioned earlier, the STIAT isoforms had to be enriched from total protein mixtures to confirm their identity using MS analysis leading to requirement of this step in this study. Since IP studies did not lead to the detection of modifications (4.1.4) additional enrichment/fractionation technique for the STIAT isoforms were applied. First, the total protein from Arabidopsis leaves grown under control conditions was separated using preparative IEF in the first dimension and SDS-PAGE in the second dimension (Figure 48).

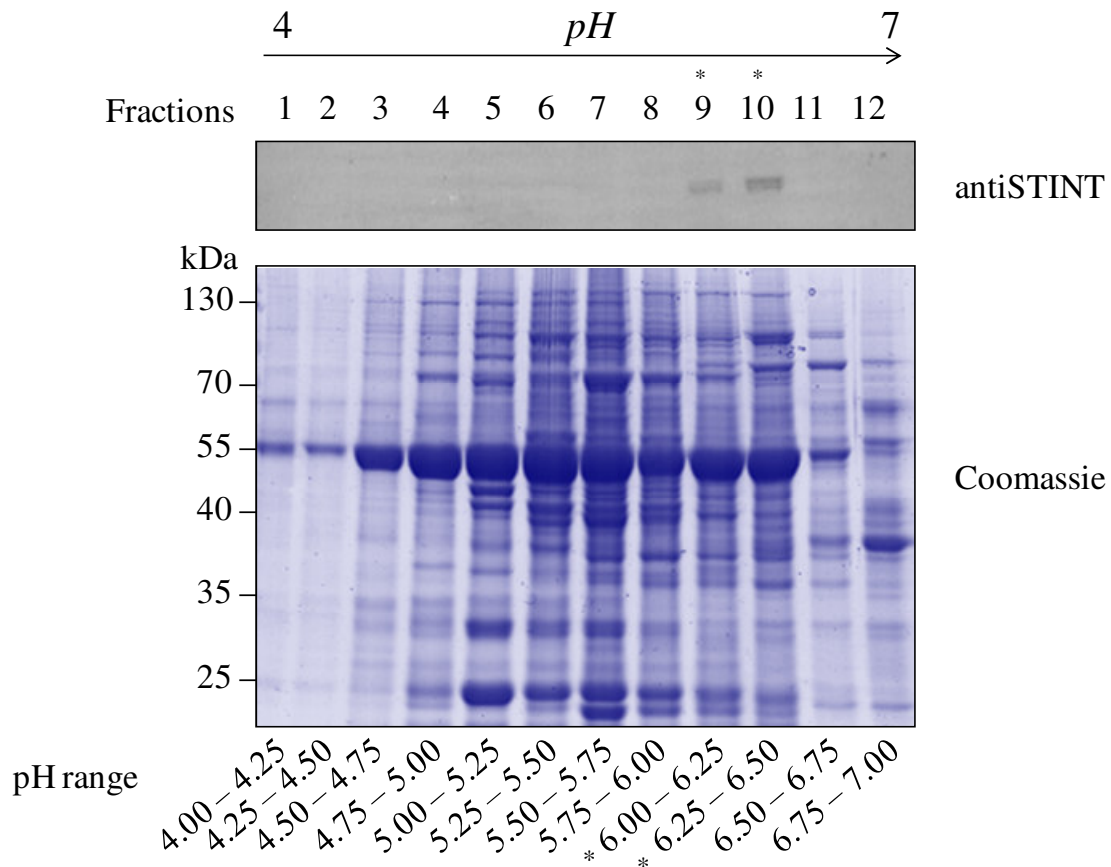


Figure 48: Preparative IEF/SDS-PAGE of STIAT isoforms from Arabidopsis leaves. Experiments were performed twice to ensure technical reproducibility.

One mg of total protein was separated on 12 cm pH gradients 4-7 and soluble proteins were collected in 12 fractions. Fractions were separated by SDS-PAGE and either visualized by cCBB staining or Western blot analysis with antiserum against STINT. The immunodetection revealed the localisation of STIAT isoforms in fractions 9 and 10 (*), representing their *pI* at pH ranges from 6.0 to 6.5.

Western blot analysis of the 12 fractions obtained after preparative IEF using antiserum directed against STINT revealed detection of STIAT1 and STIAT2 in fractions 9 and 10. This result indicates pH ranges of the two STIAT isoforms from 6.0 to 6.5, corresponding to the respective fractions. In order to confirm the identity of the STIAT isoforms and to identify potential phosphorylation sites, the corresponding protein bands from the cCBB stained gel were subjected to MS analysis. The protein bands from the cCBB stained gel were excised manually and incubated with trypsin. LC-ESI-Q-TOF MS/MS resulted in identification of STIAT1 isoform in fraction 10, but only with one peptide and in one replicate (data not shown). Phosphorylation sites were not found within this peptide. This result indicates low enrichment of the STIAT isoforms and the complexity of the fraction, leading to the requirement of another enrichment/fractionation technique for the STIAT isoforms.

4.5.5. Enrichment of STIAT isoforms from Arabidopsis leaf extract using ion exchange chromatography

In order to separate STIAT isoforms from total protein extracts, ion exchange chromatography (IEX) was applied. Total protein extracts of leaves from heat stressed Arabidopsis plants were separated by Resource Q column and subsequent Western blot analysis of fractions using antiserum directed against STINT revealed the elution of the STIAT isoforms in two peaks (Figure 49A). The STIAT isoforms were observed in the first peak of 25-32 ml (early eluting proteins) and within the second peak of 35-50 ml (late eluting proteins). Phosphatase inhibitor treatment of protein extracts prior IEX and subsequent immunoblotting of fractions showed an increase of the STIAT isoforms in the first peak, while alkaline phosphatase treatment resulted in a strong reduction (Figure 49B). This result suggests that both phosphorylated and dephosphorylated forms of STIAT proteins are present in total extracts which can be separated by IEX. The amount of phosphorylated forms during IEX can be increased by using phosphatase inhibitor treatment during protein extraction. Furthermore, the cCBB stained gel shows separation of the high abundant protein RuBisCO from STIAT isoforms, at least partially among the late eluting proteins. This result indicates higher enrichment of the STIAT isoforms compared to preparative IEF (4.5.4) as the complexity of the fraction is reduced.

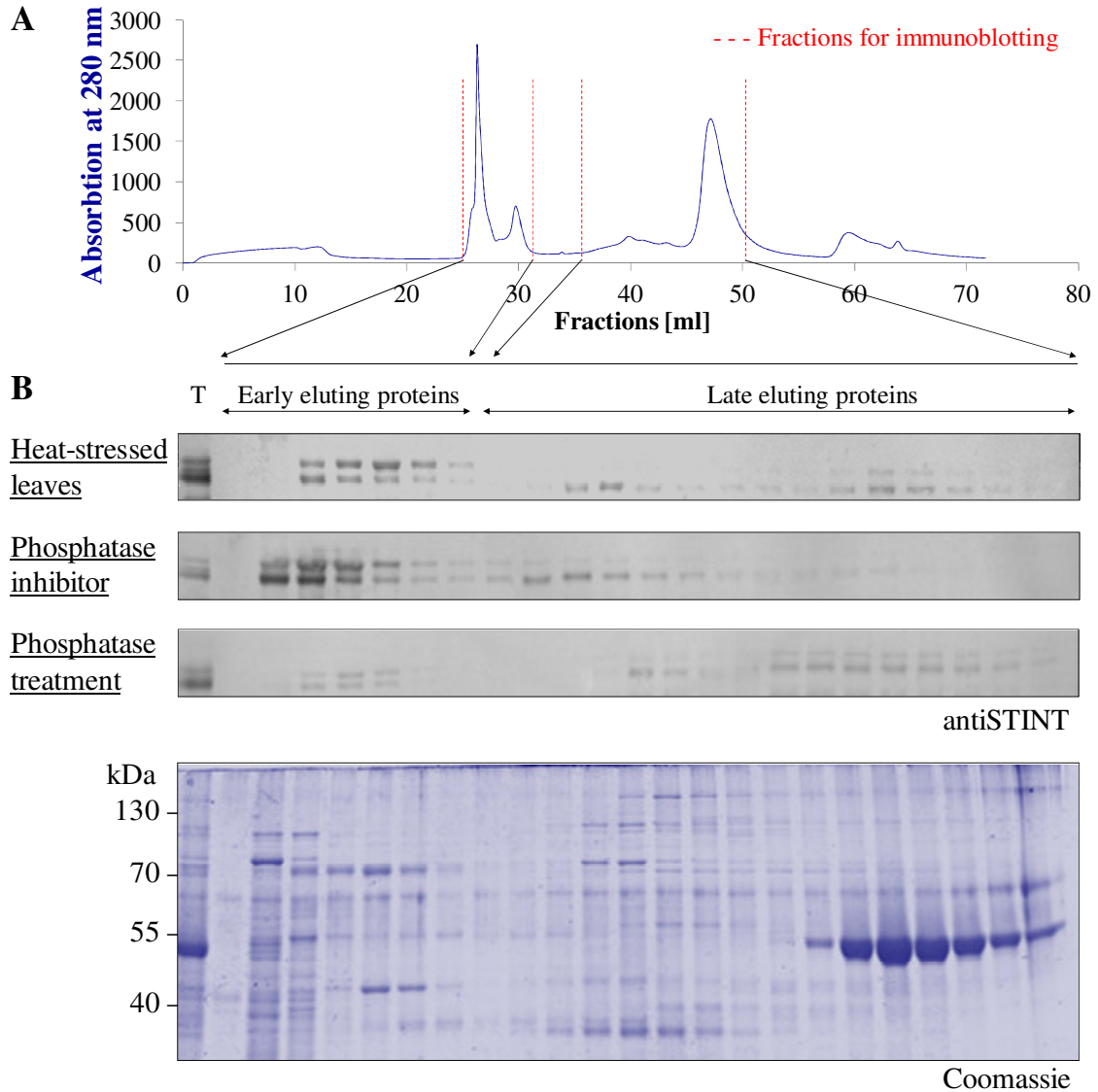


Figure 49: Ion exchange chromatography of STIAT isoforms from heat-stressed Arabidopsis leaves and analysis of phosphorylation patterns. This figure was representative of the results obtained from at least three independently conducted experiments.

A: Separation profile of anion exchange chromatography using Resource Q column. Blue: Absorption at 280 nm. Red: Fractions selected for immunoblotting.

B: Phosphatase treatment of protein extracts prior anion exchange chromatography and subsequent Western blot analysis of fractions with antiserum against STINT illustrated detection of phosphorylated and dephosphorylated STIAT isoforms. The Coomassie stained gel is shown as control. T: total protein extracts.

5. Discussion

5.1. Summary and outline

In this study, Arabidopsis STIAT isoform expression was characterized in T-DNA insertion lines, after abiotic stress application and in different organs (discussed in section 5.2). The phenotypic and biochemical analysis of mutant lines for STIAT1 and STIAT2 isoforms indicated redundant functions of both. The analysis of STIAT isoform expression showed a co-expression of STIAT1 and STIAT2 in leaves under control, cold and heat conditions with higher abundance after stress application. The third isoform STIAT3 was detectable only in leaves after heat treatment. In stem and flower of Arabidopsis all three STIAT isoforms were present under control conditions in different amounts, while they were not detectable in roots. The subcellular localisation of STIAT1 and STIAT2 isoforms under control conditions using fractionation techniques is discussed in section 5.3. STIAT1 and STIAT2 were co-localised in cytosol and nucleus of leaves with lower abundance in the latter compartment. Furthermore, a partial association of these two isoforms to membranes was detected. The subcellular localisation of STIAT3 is still unknown as it was not present under these conditions.

The *in silico* analysis of the putative promoter sequences of STIAT isoforms revealed to possible regulation by diverse abiotic stress factors, phytohormones and light. The multiple, but differential regulation of the STIAT promoters is discussed in section 5.4.

Since STIAT isoforms and its homologous tobacco protein STINT are suggested to be co-chaperones of Hsp90 and Hsp70, the analysis of these interactions was central of this work (discussed in section 5.5). Western blot analysis of STIAT1 and STIAT2, Hsp90 and Hsp70 revealed co-localisation in cytosol and nucleus. TAP purification resulted in cytosolic isoforms of the Hsp's as interacting proteins of tobacco protein STINT in Arabidopsis, but additional components of the protein complex are still unknown. The application of TAP to STI1 in yeast showed the same results, the co-purification of Hsp's with STI1. During the investigations of the STINT complex in tobacco native dimeric state of STINT was obtained.

Last, the modification of STIAT isoforms by phosphorylation is discussed in section 5.6. Recombinant STIAT1 and STIAT2 show a chain of four to five spots on 2-D PAGE. One phosphorylation site in each isoform was identified. For the analysis of STIAT isoform modification *in planta*, enrichment approaches are essential. Ion exchange chromatography separated phosphorylated and dephosphorylated STIAT isoforms. This can be enhanced by the addition of phosphatase inhibitor during protein extraction.

5.2. Characterisation of STIAT isoform expression during plant development

Since the knowledge of the HOP/STI1 family in Arabidopsis was limited to the fact, that Arabidopsis encodes three members, the first and most important question to the STIAT isoform characterization addressed in this study concerned their functional diversity. Therefore T-DNA insertion lines for two STIAT isoforms, STIAT1 (At1g62740) and STIAT2 (At1g12270), were phenotypically characterized during abiotic stress conditions and the protein expression of all three STIAT isoforms was investigated during these conditions. A T-DNA insertion line for STIAT3 (At1g12400) showed a functional protein in all plants analysed. Additionally to the analysis of T-DNA insertion lines, the STIAT protein expression was analysed in different organs of Columbia-0 to determine the functions during development.

5.2.1. STIAT1 and STIAT2 share redundant function

The T-DNA insertion lines for STIAT1 and STIAT2 were characterized during long-term cold and heat stress treatment and revealed normal growth response, indicating functional redundancy of STIAT1 and STIAT2. This assumption is supported by three aspects. First, Western blot analysis using antiserum directed against the homologous protein from tobacco revealed highly similar expression patterns of the two isoforms, which was in accordance with *in silico* transcript data (Hruz *et al.* 2008). Secondly, the expression level of each isoform in the mutants was not much influenced by the loss of the other, when compared to Columbia-0 as control, suggesting that both isoforms are able to compensate and that the remaining isoform is sufficient for complete function. Third, the assumed redundancy of STIAT1 and STIAT2 was detected under both heat and cold stress whereas STIAT3 was exclusively present in leaves after heat application. Therefore, STIAT3 is excluded from presumption of compensating STIAT1 and STIAT2 functions.

To confirm the assumed redundancy of STIAT1 and STIAT2, construction of double knock out line for STIAT1 and STIAT2 is highly appreciated. So far, the production of STIAT1/STIAT2 double knock out line by crossing STIAT1 knock out line with STIAT2 knock out line was not successful, as no developed seeds were obtained within the siliques. Gene silencing of STIAT1 in the STIAT2 mutant background and *vice versa* did not lead to any viable plant. Also, commercially produced double knock out lines are not yet available.

These data indicate the knock down of the two isoforms STIAT1 and STIAT2 causes a lethal effect and suggests that the expression of at least one of the two isoforms is essential for normal plant development. Contrary to this, gene silencing of STINT in tobacco and knock out mutant of STI1 in yeast revealed no lethal effects at control or stress conditions (Chang *et al.* 1997, Hedtmann 2007). Normal developed seeds of tobacco plants containing the RNAi construct for STINT were obtained. The STINT protein is expressed there, but later on it is not detectable in tissues such as leaves, because of degradation by the RNAi construct.

5.2.2. STIAT3 is differentially expressed, indicating specific functions during abiotic stress responses and in developmental processes

The protein expression of STIAT isoforms was investigated in T-DNA insertion lines for STIAT1 and STIAT2 after application of abiotic stresses and in different organs of *Arabidopsis* Columbia-0 plants, indicating specific functions of the STIAT isoforms, which are summarized in Figure 50. Western blot analysis using antiserum directed against the homologous protein from tobacco led to the detection of two isoforms in leaves compared to three isoforms under heat stress conditions, indicating the high homology between HOP/STI1 proteins in *Arabidopsis* and between *Arabidopsis* and tobacco. By the use of immunoprecipitation studies the two isoforms expressed under control conditions were identified as STIAT1 and STIAT2. The third isoform STIAT3 was only identified in leaves under heat stress conditions, implying a specific function of STIAT3 in thermoadaptation of leaves. This finding was in accordance with transcriptional data for *STIAT3* obtained by Genevestigator tool (Hruz *et al.* 2008) which were published recently by Prasad *et al.* (2010). A discrepancy of the STIAT3 protein induction compared to the *STIAT3* transcript abundance was observed. A reason for that could be the different temperatures applied between the studies. In this study, the analysis of the STIAT3 protein was performed at 30 °C, whereas the plants used for transcript studies were subjected to 37 °C. This high temperature was not appropriate for the protein expression study as the plants were subjected to heat stress for 14 d and not only for 30 min.

The identification of an additional STIAT isoform, which is uniquely expressed after certain stress and absent under control conditions, has not yet been described before in mammals or plants. In yeast and human, HOP/STI1 is encoded by a single gene, which is both expressed under control conditions and induced by stress (Honore *et al.* 1992, Nicolet and Craig 1989). In soybean, the same expression profiles are found as shown for yeast and human (Zhang *et*

al. 2011), whereas in rice the two HOP/STI1 isoforms were not yet been studied for their differential expression (Chen *et al.* 2010).

In addition to the specific expression of STIAT3 after heat stress, STIAT1 and STIAT2 were induced at the same time but to minor extent than STIAT3, implying additional functions of STIAT1 and STIAT2 under heat stress. Furthermore, STIAT1 and STIAT2 function under cold stress as they were induced there. A reason for minor induction of STIAT isoforms upon cold stress could reflect the lower severity of this stress parameter in *Arabidopsis* as compared to heat stress. Earlier studies revealed a stunted phenotype in transgenic tobacco plants containing an STINT-RNAi construct after exposure to cold stress whereas no phenotypic differences were observed under heat stress (Hedtmann 2007). This comparison indicates a plant/species-specific regulation of HOP/STI1 homologues in plants, probably regulated through evolutionary environmental adaptation.

STIAT1 and STIAT2 were co-expressed in leaves, stem and flower but lacking signals in roots and therefore a general role during plant development can be assumed. The comparison of transcriptional data for the two isoforms obtained by Genevestigator tool (Hruz *et al.* 2008) did not correlate well as STIAT2 was more abundant than STIAT1 on protein level which was reversed on transcriptional level and the isoforms were not detected in roots during immunoblottings. A reason for the latter result could be found in the age of the plants and culture conditions. Plant roots for microarray analysis were grown under sterile conditions and harvested at seedlings stage. In this thesis, the plants were eight weeks old and grown on soil. Nevertheless, the expression of STIAT1 and STIAT2 isoforms under control conditions was in accordance with earlier studies showing the expression of other plant HOP transcripts, *e.g.* soybean leaves (Zhang *et al.* 2003).

Contrary to this, STIAT3 was expressed in stem and flower but not in leaves under control conditions indicating specific function of STIAT3 in stem and flower development. This expression was also contrary to transcriptional data (Hruz *et al.* 2008) where *STIAT3* was not expressed in the respective tissues. Prasad *et al.* (2010) showed a higher abundance of *STIAT3* transcript in petal and carpel compared to *STIAT1* and *STIAT2*.

In summary, STIAT3 is involved in specific cellular responses such as flowering while the other two isoforms play roles in general developmental processes.

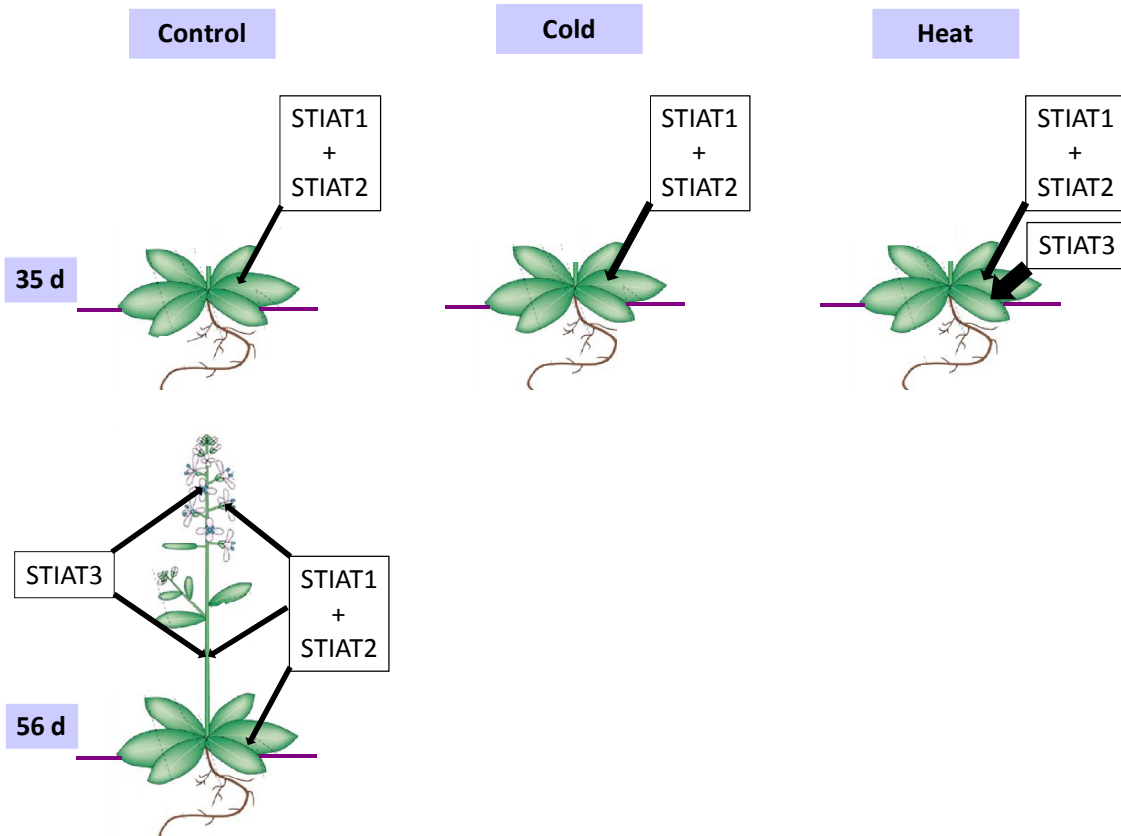


Figure 50: STIAT isoform expression during plant development and in heat stress response. The isoforms were analysed in different tissues of one developmental stage and in the same tissue during different abiotic stresses. Arrow strength indicates the expression intensities.

5.3. Intracellular distribution of STIAT isoforms

5.3.1. STIAT1 and STIAT2 are localised in cytosol and nucleus

Further insights into the molecular functions of STIAT isoforms were obtained by the subcellular localisation of these proteins. The subcellular localisation of STIAT1 was visualised by fusion of STIAT1 to GFP and revealed a nuclear and cytosolic localisation (Hedtmann 2005). To validate these findings, a subcellular fractionation of leaf nuclei from *Arabidopsis* grown under control conditions was initiated to detect STIAT isoforms by immunoblotting. Analysis of STIAT isoforms using antiserum directed against the recombinant tobacco protein STINT revealed detection of STIAT1 and STIAT2 in cytosol and nucleus, whereas the STIAT3 isoform was not present under these conditions. The signal intensity of Western blot signal from STIAT isoforms was more dominant in cytosol compared to the nuclei, indicating a more prominent role of the proteins in cytosol compared to nucleus under control conditions.

The detection of STIAT1 in both compartments confirmed its localisation using GFP fusion protein. The STIAT2 isoform was detected in these compartments for the first time and results are in accordance with *in silico* prediction tools (Emanuelsson *et al.* 2000, Horton *et al.* 2007).

Further experimental evidences for the detection of STIAT1 and STIAT2 were provided by Ito *et al.* (2011) as the two isoforms were detected among the cytosolic proteome of an Arabidopsis cell culture by LC-MS.

From these data, it can be assumed that the proposed nuclear localisation signal (NLS) of these two isoforms is functional *in vivo*. The subcellular localisation of STIAT3 is still not known. The NLS of STIAT3 is similar to the other ones of STIAT1 and STIAT2, indicating a nuclear localisation of that isoform (Figure 51). This hypothesis needs to be verified by analysing the presence of STIAT3 in nuclei of Arabidopsis leaves grown under heat stress conditions.

```

STIAT1 232 EFGEEK-----QKKLKAQKEKELGNAAYKKKDFETAIQHYSTAMEIDDEDISY 279
STIAT2 233 EEKEKK-----ERKEKAKKEKELGNAAYKKKDFETAIQHYSTAIEIDDEDISY 280
STIAT3 215 ELTEEERQK-----KRKEKALKEKEGENVAYKKKDFGRAVEHYTKAMELDDEDISY 266
STINT 233 EVGEEEEKEI-----KRKAKAQKEKEAGNAAYKKKDFETAIQHYSKAIELDDEDISF 284
scSTI1 239 APQKEESKESEPMEVDEDDSKIEADKEKAEGNKFYKARQFDEAIEHYNKAWELH-KDITY 297
hsHOP 213 PMEEDLP-----ENKKQALKEKELGNDAYKKKDFDTALKHYDKAKELDPTNMTY 261

```

Figure 51: Annotation of NLS in alignment of HOP/STI1 of Arabidopsis, tobacco, yeast and human.

STIAT: *A. thaliana*, STINT: *N. tabacum*, scSTI1: *S. cerevisiae*, hsHOP: *H. sapiens*. NLS is shown in bold.

5.3.2. STIAT1 and STIAT2 are partially associated to membranes

In addition to the nuclear and cytosolic localisation of HOP (Lassle *et al.* 1997, Longshaw *et al.* 2004), the presence of HOP in Golgi apparatus (Honore *et al.* 1992) and its integration into the plasma membrane as part of a PrPC complex was proposed, although HOP lacks a signal peptide for membrane transport (Zanata *et al.* 2002).

Therefore, the detection of STIAT isoforms in endomembrane and plasma membranes from Arabidopsis leaves grown under control conditions was investigated. The Western blot analysis of STIAT isoforms using antiserum directed against the recombinant tobacco protein STINT revealed detection of STIAT1 and STIAT2 in the endomembrane and plasma membrane, whereas the STIAT3 isoform was not present under control conditions. The signal intensity of Western blot signal from STIAT isoforms was more dominant in cytosol as compared to the membrane fractions, confirming the more dominant role of the proteins in cytosol, but indicating possible attachment to both membrane types.

A detection of STIAT1 and STIAT2 in endomembranes and plasma membranes was shown for the first time. From these data, an association can only be assumed. The possible attachment of STIAT1 to plasma membrane is supported by the transmembrane domain predicted by DAS (Cserzo *et al.* 1997) and by SUB-cellular location database for Arabidopsis proteins (SUBA) (Heazlewood *et al.* 2008). This *in silico* database contains experimental evidences for the detection of STIAT1 in plasma membranes. Benschop *et al.* (2007) detected STIAT1 among 1186 Arabidopsis proteins from their plasma membranes enriched fraction by LC-MS during large-scale proteomics approach.

The findings for STIAT2 were in contrast to *in silico* data, where only a transmembrane segment was detected and no plasma membrane localisation was predicted. Interestingly, the *in silico* prediction of the rice HOP/STI1 using the tools described in section 3.6.1 revealed a localisation in cytosol or mitochondria, but not in membrane structures. Chen *et al.* (2010) showed the localisation of HOP/STI1 in endomembranes and plasma membranes of rice and provided further evidence for the localisation in the endoplasmatic reticulum by YFP fusion of rice HOP/STI1 and co-localisation with an ER marker. Evidences of a localisation of homologous HOP/STI1 in plasma membranes of roots of a salt-tolerant barley cultivar using a LC-MS-based approach are also provided (Witzel, Matros and Mock, unpublished data). Due to these findings a potential association of STIAT2 to plasma membranes has to be validated. This can be done by analysing fusion of STIAT2 to a fluorescent protein.

The subcellular localisation of STIAT3 is not yet known but a similar transmembrane domain was detected in STIAT3 as for STIAT1, suggesting an association to membranes. This hypothesis has to be validated by analysing the presence of STIAT3 in Arabidopsis plasma membranes grown under heat stress conditions.

The results of studying the subcellular distribution of STIAT isoforms are summarized in Table 14. The presence of STIAT1 in cytosol and nucleus was shown by GFP fusion and immunoblottings of cytosolic and nuclear fractions. During the latter study, an evidence for co-localisation of STIAT2 with STIAT1 was provided, but needs further confirmation. Besides the cytosolic and nuclear localisation of these two isoforms, an association of them to membranes is possible. Experimental evidence for STIAT3 localisation has not been obtained so far as the isoform is not present under control conditions. The predicted subcellular localization of STIAT3 to nucleus, mitochondria and plastids (Claros and Vincens 1996, Small *et al.* 2004) has to be validated by enriching the compartments from heat stressed Arabidopsis plant material. Up to date, STIAT isoforms were not described in the proteomes

of nuclei (Calikowski *et al.* 2003), chloroplasts (Kleffmann *et al.* 2004) or mitochondria (Klodmann *et al.* 2011, Millar *et al.* 2001).

Table 14: Summary of STIAT protein localisation.

Localisation	STIAT1	STIAT2	STIAT3
Cytosol	(Hedtman 2005) (Conde <i>et al.</i> 2011) this study	(Conde <i>et al.</i> 2011) this study	no evidence
Nucleus	(Hedtman 2005) this study	this study	predicted
Plasma membrane	(Benschop <i>et al.</i> 2007) this study	this study	no evidence
Endomembranes	this study	this study	no evidence
Mitochondria	no evidence	no evidence	contrary predictions
Chloroplast	no evidence	no evidence	no evidence

5.4. *In silico* analysis of regulatory elements of STIAT isoforms

The activation of genes by transcription factors is an important part in re-establishing the cellular homeostasis and to protect or repair damaged proteins and membranes within the complex stress response network. Nothing is known about transcriptional regulation of HOP/STI1 in plants or even in yeast and mammals, and therefore, the first step to obtain information on *STIAT* isoform regulation was the analysis of their promoter sequences for cis-acting regulatory DNA elements. The DNA-binding domains of 4-20 nucleotides recognized by one or more transcription factors can be detected by *in silico* programs (Davuluri *et al.* 2003, Higo *et al.* 1999, O'Connor *et al.* 2005).

Numerous potential cis-elements were found among the three 3 kb *STIAT* promoters showing a regulation by abiotic factors, phytohormones and light, indicating a multiple regulation of them and supporting the role in stress defence. Conserved DNA-binding domains were detected among the three *STIAT* promoter sequences indicating the same transcriptional regulation. They all contained the DRE (drought responsive element) which is known to be involved in drought and cold responses (Kasuga *et al.* 1999). Additionally the cis-elements DPBF (Dc3 promoter-binding factor), GAREAT, MYB1AT, MYBATRD22 and MYCATERD22 were detected and those are regulated by abscisic acid and its antagonist gibberellic acid (Abe *et al.* 2003, Abe *et al.* 1997, Kim *et al.* 1997, Ogawa *et al.* 2003, Simpson

et al. 2003). Furthermore, STIAT promoters showed conservation of the cis-elements GATABOX, SORLIP1, SV40CORE and TBOX which are described to be controlled by light (Chan *et al.* 2001, Green *et al.* 1987, Hudson *et al.* 2003, Teakle *et al.* 2002).

Interestingly, specific cis-elements for one or two isoforms were found among the promoter sequences. ARF (auxin response factor) and ATB2/AtbZIP were only present in promoters of *STIAT1* and *STIAT2* and are known to be induced either by auxin and brassinosteroids or by hypoosmolarity (Sato *et al.* 2002, Ulmasov *et al.* 1999). This finding suggests on the one hand a transcriptional regulation of the two isoforms apart from *STIAT3* and on the other a putative co-regulation of the two isoforms under certain conditions which confirms the observation on translational level. In contrast, HSE (heat shock element) was detected only in the *STIAT3* promoter which is described to be regulated by heat transcription factors (Hubel *et al.* 1995). This result supports the specific regulation of *STIAT3* apart from *STIAT1* and *STIAT2* and correlates well with the observed protein expression patterns of *STIAT3* being induced after heat stress.

The promoters of *STIAT1* and *STIAT2* contained specific DNA-binding domains assuming individual regulation under certain conditions. The cis-elements E2F and E2FAT were originally identified as regulators of cell cycle-related genes and were detected in the *STIAT1* promoter (Chaboute *et al.* 2000). Recent results indicate, that stress defence genes including heat shock proteins are regulated by E2F (Ramirez-Parra *et al.* 2003).

The *STIAT2* promoter contained several specific DNA-binding domains involved in different pathways. The GBOX is found in numerous diverse plant genes suggesting a general induction by diverse stimulatory pathways (Menkens *et al.* 1995). This DNA-binding domain points to the role of *STIAT2* as the isoform with most important function. The UPRMOTIFII is a cis-element which plays a role in gene activation related to unfolded protein response and was detected in the promoter of Hsp90 (Martinez and Chrispeels 2003). The mechanism follows a cellular stress response rising from the endoplasmatic reticulum. Folding of newly synthesized proteins and refolding of misfolded proteins are monitored by chaperone network within this process. Probably, *STIAT2* has a function in that process by interacting with the molecular chaperone families, driving the association of *STIAT2* to endomembranes.

Finally, specific DNA-binding domains for *STIAT2* induction related to abiotic stresses were detected. Besides the cis-element CBF2, which is involved in water stress responses (Pla *et al.* 1993), *STIAT2* promoter contained LTRE (low temperature responsive element) and RAV1 which are induced by low temperature or cold stress (Kagaya *et al.* 1999, Nordin *et al.* 1993).

The latter cis-element RAV1 consists of a bipartite motif, RAV1A and B, being variable spaced and oriented (Kagaya *et al.* 1999). It is recognized by its correspondent cold responsive transcription factor RAV1 [Related to *ABI3 (ABSCISIC ACID-INSENSITIVE3)/VP1(VIVIPAROUS1)*] by binding of the AP2 (APETALA2) and B3-like DNA-binding domains to the RAV1A and B motifs. Both binding motifs were exclusively found in the *STIAT2* promoter, whereas RAV1B motif was absent in the *STIAT1* and *STIAT3* promoters indicating a sole regulation of *STIAT2* by that transcription factor.

The regulation of the *STIAT* promoters by a variety of abiotic stresses was shown. A conserved regulation of all three isoforms under drought stress can be assumed as the corresponding cis-element was found in all promoters. Specific regulation of *STIAT3* under heat stress is supposed, whereas *STIAT2* is mainly induced by water and cold stress.

The possible function of *STIAT* isoform during drought and water stress or the influence of phytohormones needs to be validated by analysing Arabidopsis plants under respective stress conditions using immunoblottings on protein level or RT-PCR on transcript level. The fusion of each *STIAT* promoter sequence to a reporter protein, *e.g.* GUS, is highly appreciated to detect specific responses of each isoform. The fusion of each *STIAT* promoter sequence to a reporter protein, *e.g.* GUS, is highly would be more beneficial, in order to detect specific responses of each isoform.

5.5. Isolation and characterisation of STINT/ STIAT interaction partners

As outlined before, the expression and induction of stress-related proteins including chaperones is known to be important within the stress response network. The interaction between all components is of particular interest in investigating their function.

The complex formation of the chaperones Hsp90 and Hsp70 with HOP/STI1 in yeast and mammals is one of the best studied interaction (Chen *et al.* 1996, Smith *et al.* 1993), whereas the knowledge in plants is rather limited. The first interaction of HOP/STI1 plant homologues with Hsp90 was shown using *in vitro* studies (Zhang *et al.* 2003). The HOP/STI1 interaction with Hsp90 in rice innate immunity using *in vitro* studies was proposed very recently (Chen *et al.* 2010), indicating the difficult task to study interaction of HOP/STI1 with chaperones *in planta*.

Nevertheless, to obtain insights into the function of HOP/STI1 in Arabidopsis and tobacco, the identification of interacting proteins was of great interest. In this study, diverse

biochemical approaches were applied to study the protein-protein interactions of STIAT/STINT. The application of these methods is discussed, since synthetic genetic approaches like yeast two hybrid and bimolecular fluorescence complementation were either lacking interaction partner for STINT (personal communication HP Mock) or producing false positive interacting proteins for STIAT isoforms (Endreß 2010).

5.5.1. Co-expression of putative STIAT interaction partners in Arabidopsis

Since it is known that putative interaction partners are often co-expressed or co-localised within their system, co-expression analysis of the homologous STIAT isoforms with specific isoforms of Hsp90 and Hsp70 by immunoblottings was performed.

In particular, this co-expression analysis of STIAT isoforms with Hsp90-1 and Hsp70-1 to Hsp70-5 was investigated in cytosol and nuclear fractions of leaves grown under control conditions. The Western blot signals for Hsp90-1 and the Hsp70 isoforms revealed detection of them in cytosol and nuclei with a more dominant signal in cytosol. This result is consistent with the subcellular localisation of the STIAT isoforms in these compartments and with the description for the abundant chaperone families. (Krishna and Gloor 2001, Lin *et al.* 2001).

5.5.2. STINT participates in protein complexes and is present as a native dimer

Experimental evidences for the the participation of the homologous tobacco protein STINT in protein complexes were obtained by size exclusion chromatography. This fractionation technique revealed the involvement in protein complexes, occurring in sizes up to 440 kDa. Additionally, these studies indicated the presence of STINT protein as a dimer under native conditions, which was validated by separation using BN-PAGE. These findings are in accordance with the molecular state of human HOP, described as dimeric (Prodromou *et al.* 1999) or monomeric (Yi *et al.* 2010). However, when analysing the complex fraction from two different size exclusion chromatography columns containing STINT using BN-PAGE, the size of the complex was about 720 kDa. The proteins in this complex were identified as proteasome subunits. STINT or chaperones were not among the proteins identified by MS, although a signal for STINT in the protein complex was obtained by immunoblotting. This result indicated the requirement of other methods to isolate STINT/STIAT protein complexes, *e.g.* based on affinities.

5.5.3. Identification of STIAT interaction partners in Arabidopsis

First experimental indications for Hsp90 and Hsp70 being interaction partners of STIAT isoforms were gathered in immunoprecipitation and *in vitro* binding studies. The analysis of interacting protein by immunoprecipitation was selected as this method reflects the closest physiological conditions in the tissue. The method is very fast as the purified antibody of the recombinant tobacco protein was available and no other cloning steps were necessary.

STIAT isoforms were precipitated from total leaf extracts under control and heat stress conditions using a purified STINT antibody resulting in the specific enrichment of the STIAT isoforms. Immunoprecipitation validated their expression as discussed in section 5.2 and yielded in co-purification of putative interaction partners in only one experiment. STIAT1 was detected among the identified proteins together with Hsp90-3, Hsp70-1 and some more proteins, probably client proteins. Whereas the co-elution of Hsp seemed reliable, the co-elutions of the additional proteins remain questionable. Nevertheless, an interesting candidate among these identified proteins was a coatamer beta subunit, which belongs to the cytosolic COPI (coat protein I) complex composed of seven proteins (Waters *et al.* 1991). The COPI complex is part of the vesicular protein transport system functioning in retrograde transport from the Golgi to endoplasmic reticulum (Kreis *et al.* 1995). Besides its cytosolic localization evidences for the binding of a COPI subcomplex to membranes are known (Lowe and Kreis 1995). Interestingly, the interaction of STIAT1 to the coatamer beta prime subunit was predicted using the *in silico* database Arabidopsis interaction viewer, which was built from orthologous interactions in yeast, nematode worm, fruit fly and human (Geisler-Lee *et al.* 2007). This specific interaction was obtained by affinity capture-MS in yeast as STI1, Hsp90, Hsp70 and further coatamer subunits were identified with SEC27 (coatamer beta prime subunit) (Ho *et al.* 2002). Since the general function of Hsp90 in protein trafficking is known, specific roles of Hsp90 were described for the endoplasmic reticulum to Golgi protein trafficking in yeast by COPII complex (Chen and Balch 2006) and more recently in intracellular vesicle transport in human (Lotz *et al.* 2008). Therefore, a possible function of Hsp90 in the third vesicle transport pathway via COPI is assumed, whereas HOP/STI1 have a function by indirect or direct binding to COPI. In order to verify the possible interaction of STIAT to COPI, the Arabidopsis COPI complex has to be isolated according to Waters *et al.* (1991)

A second interesting candidate among the putative client proteins is GAPDH (Glyceraldehyde 3-phosphate dehydrogenase), which has a general function in plant metabolism. Tisdale and

Artalejo (2007) provided evidences of the involvement of GAPDH in the COPI vesicle transport by influencing the formation of COPI vesicles via Rab2 (Ras-related in brain) binding.

Besides the putative function of Hsp90-STIAT-Hsp70 complex in vesicle transport, the identification of RuBisCO activase leads to the assumption of possible contamination during purification procedure or a putative role in that complex. A possible stabilisation of RuBisCO activase at higher temperatures (Salvucci *et al.* 2001) or the degradation of the aggregated enzyme can be assumed.

However, the co-purification of chaperones with STIAT and especially the client proteins by immunoprecipitation is very difficult due to the transient nature of interactions. Presumably, the Hsp90-STIAT-Hsp70 complexes are best studied by using cross-linked plant material or antibodies against the chaperones.

Recombinant proteins of STIAT and Hsp70 were investigated in *in vitro* binding studies since the requirement of large amounts in comparisons to the physiological concentrations *in planta*. The interaction of STIAT2 with Hsp70-5 was studied as it was predicted with high level in *in silico* database Arabidopsis interaction viewer. First, the interaction study was performed by purification of the recombinant proteins supplemented to an Arabidopsis leaf extract using one of the antibodies against one of the proteins. The STIAT isoform was co-eluting with the Hsp70 isoform and *vice versa*. Quantitative statements of these interactions were not possible as the endogenous proteins from the Arabidopsis leaf extract competed for the interaction of the recombinant proteins. The attempts to purify the proteins without the Arabidopsis leaf extracts were not successful as the Hsp70 isoform was binding to the control antibody although it was co-eluting with the STIAT isoform. In yeast the interactions of the recombinant STI1 and Hsp70 were shown (Wegele *et al.* 2003), but authors used a different matrix for antibody coupling. A reason for the weak co-elution of Hsp70-5 and STIAT isoform could be found in the incorrect annotated interaction from the orthologous system in yeast as the Arabidopsis Hsp70-4 and Hsp70-5 isoforms show the same homology to the Hsp70 (SSA proteins) in yeast. Therefore, the interaction of Hsp70-4 with STIAT isoforms could be investigated.

In future the usage of a different matrix instead of magnetic beads, a tag-specific antibody or even a protein fusion tag is suggested to study the interaction of recombinant STIAT isoforms with their binding partners. To obtain quantitative data of protein-protein interactions the

interaction of STIAT isoforms should be analysed by surface plasmon resonance spectroscopy.

5.5.4. Heterologous STINT interacts with cytosolic Hsp90 and Hsp70 members in Arabidopsis

Tandem affinity purification of heterologous STINT in Arabidopsis was performed to isolate the STINT complex partner in Arabidopsis cell culture. TAP is an innovative method to purify protein complexes, which was first demonstrated in yeast by Rigaut *et al.* (1999) and later adapted to plants by Rohila *et al.* (2004). This technique has the advantages of higher specificity compared to one step purification procedures and resembles more the physiological conditions as the fusion protein is expressed under almost physiological conditions. For example in yeast, TAP fusion tag was introduced by homologous recombination to the endogenous gene.

In the study present here, TAP of STINT was followed according to Van Leene *et al.* (2007), containing the classical TAP tag of two IgG-binding domains from *Staphylococcus aureus* Protein A, the TEV protease cleavage site and the calmodulin-binding peptide. The tagged STINT protein was overexpressed under the control of 35S promoter in the presence of the endogenous protein, which was necessary for competing of the tagged STINT with the endogenous STIAT isoforms for the interaction partners in the Arabidopsis cell culture with high ploidy level. This is common for TAP in higher eukaryotes, since the level of tagged protein is an important issue for protein complex isolation.

TAP of STINT resulted in the detection of chaperones Hsp90 and Hsp70 as interaction partners, identified with very high score in multiple isoforms and present in two experiments of N-terminally TAP-tagged STINT and in one of C-terminal TAP fusion of STINT. These findings indicate that Hsp90 and Hsp70 are real interacting proteins of STINT in Arabidopsis, although chaperones are found often as contaminating proteins because of their high abundance (Van Leene *et al.* 2007). These background contaminations are an important issue in TAP experiments and were assessed by control purifications using wild-type Arabidopsis cell culture and two cultures overexpressing the TAP-tagged proteins β -glucuronidase and GFP. Usually, proteins identified in these control purifications are excluded from the dataset derived from the tagged protein purifications. However, the chaperones Hsp90 and Hsp70 with their very high score were not excluded from identification lists of STINT-TAP experiments (personal communication J. v. Leene & G. De Jaeger).

The chaperones Hsp90 and Hsp70 were identified in multiple isoforms all having the same subcellular localisation. The Hsp90 isoforms are described to the cytosolic and nuclear compartments (Krishna and Gloor 2001). The Hsp70 isoforms are only cytosolic (Lin *et al.* 2001), but a nuclear localisation of Hsp70-1 has been shown (Sung and Guy 2003). This finding is in good accordance with the subcellular localisation of STIAT1 and STIAT2 in these compartments as interacting proteins should be co-expressed for a possible interaction. The detection of the Hsp in multiple isoforms leads to the assumption that many diverse Hsp90-STINT-Hsp70 complexes can be formed *in planta* indicating a more diverse interaction network compared to yeast and human.

No further interacting proteins of STINT could be identified besides Hsp chaperones using this method, indicating that interactions are transient or lost during purification.

In conclusion, the TAP of STINT showed for the first time the interaction of a plant HOP to both Hsp90 and Hsp70 *in planta* using a biochemical approach. Earlier studies provided evidences only for the interaction of HOP/STI1 with the chaperones by *in vitro* approach in presence of wheat germ lyaste (Fellerer *et al.* 2011, Krishna and Kanelakis 2003, Zhang *et al.* 2003) or with Hsp90 using yeast-2-hybrid method and heterologous expression in yeast (Chen *et al.* 2010).

Thus, the interaction of HOP/STI1, Hsp90 and Hsp70 represents a general complex in eukaryotes including plants. However, as long as the client proteins of the STINT-chaperone complex are not identified, specificity and function of plant complex remain unknown. Recently, known chloroplast preproteins being client proteins of Hsp90 during their synthesis were tested in wheat germ lysate and revealed in the identification of HOP as part of the complex (Fellerer *et al.* 2011). Following the targeted *in vitro* approach, the client proteins of STINT-chaperone complex could be purified by TAP using alternative tags (reviewed by Li 2011) like the His-biotin tag which is more useful for transient interaction and compatible with *in vivo* cross-linking (Tagwerker *et al.* 2006) but not yet used *in planta*.

5.5.5. Comparison of the interaction partners of STINT in Arabidopsis and STI1 in yeast

The possible isolation of client proteins of the Hsp90-HOP/STI1-Hsp70 complex by the TAP technique was verified by TAP of yeast STI1. Therefore, STI1 protein contained the identical TAP-tag as used for STINT. For the first time, the STI1 interaction partner were purified

under physiological conditions in yeast using this technique and resulted in the detection of the two major interaction partners Hsp90 and Hsp70 as obtained for TAP of STINT. All earlier studies showing the interaction of STI1 to Hsp90 and Hsp70 in yeast were obtained indirectly by co-immunoprecipitation with high abundant Hsp90 (Chang and Lindquist 1994) or under non-physiological conditions by overexpression of His-tagged STI1 with subsequent purification using His antibody (Flom *et al.* 2007, Reidy and Masison 2010). Only one study showed the co-immunoprecipitation of Hsp90 and Hsp70 with STI1 under physiological conditions (Chang *et al.* 1997). The co-purification of client proteins like Ydj1/Hsp40 and Cpr6, a prolyl isomerase highly abundant in Hsp90 complexes, was not successful when using the STI1 antibody for immunoprecipitation of Hsp90-STI1-Hsp70 complex in yeast (Chang *et al.* 1997). TAP performed here provided evidence for STI1 interaction partners by MS analysis for the first time and confirmed the immunoprecipitation studies by Chang *et al.* (1997).

MS analysis resulted in detection of the two Hsp90 isoforms, the heat-shock inducible isoform Hsp82 and the constitutive isoform Hsc82, and Hsp70-1 and Hsp70-2 as interaction partners of STI1. Although the Hsp90 isoforms share 97 % identity, their distinct identification was possible due to the electrophoretic separation, which was reached by using 7.5 % SDS gels and increased running time of electrophoresis. All of the identified Hsp are known to be localised in the cytosol (Werner-Washburne *et al.* 1987) (www.yeastgenome.org), corresponding to the findings in Arabidopsis. The interaction of STI1 to both Hsp90 and Hsp70 was detected only after first purification step using IgG and not after second purification using calmodulin. This result indicates a stronger interaction of STI1 to Hsp90 compared to Hsp70 and confirmed the immunoprecipitation results by Chang *et al.* (1997), a study lacking the differentiation between the Hsp90 isoforms. Evidences for the low affinity binding of STI1 to Hsp70-1 were provided studying the purified proteins in surface plasmon resonance spectroscopy (Wegele *et al.* 2003).

The client proteins of Hsp90-STI1-Hsp70 complex under physiological conditions could not be purified using the TAP method as shown for TAP of STINT indicating the transient interaction. This is supported by a very recent study by Reidy & Masison (2010), where even the interaction of His-tagged versions of STI1 and Hsp70 by immunoprecipitation against one of the proteins failed. Here, STI1-Hsp70 interactions in the yeast strains were not efficient enough to overcome the purification conditions (Reidy & Masison 2010). In future, stabilization of protein complexes by cross-linking should be considered.

5.6. Are the STIAT isoforms modified by phosphorylation?

Several phosphorylation sites of HOP/STI1 have been described in mammals and yeast, which influence the cellular localisation (Daniel *et al.* 2008) and potentially the interaction with Hsp. The phosphorylation of HOP/STI1 homologues has not yet been studied by targeted approaches *in planta*. One conserved phosphopeptide in all three STIAT isoforms and one diagnostic phosphopeptide for STIAT1 were detected in the PhosPhAt database (Heazlewood *et al.* 2008). The data were obtained from large-scale phosphoproteomics experiments (Li *et al.* 2009, Nakagami *et al.* 2010, Sugiyama *et al.* 2008). Based on those findings, this post-translational modification was investigated for its appearance in STIAT isoforms by two targeted approaches: the enrichment of phosphopeptides from a recombinant STIAT isoform and the enrichment of phosphorylated isoforms from Arabidopsis leaf extracts.

5.6.1. Phosphorylated peptides in recombinant STIAT1 and STIAT2

At first, the recombinant proteins STIAT1 and STIAT2 were analysed for their protein patterns on 2-D PAGE. The separation of both recombinant STIAT1 and STIAT2 resulted in chains of multiple spots with similar molecular weight but different isoelectric point, indicating multiple phosphorylations of the recombinant proteins. This finding was in agreement with *in vivo* phosphorylation of murine STI1 and human HOP having the same patterns of multiple spots in Western blot analysis (Daniel *et al.* 2008, Lassle *et al.* 1997).

MS analysis of the protein spots of STIAT1 was attempted and led to the detection of one and the same phosphopeptide in more than one spot suggesting other phosphopeptides responsible for the *pI* shift than the detected ones.

The enrichment of phosphopeptides within recombinant STIAT isoforms was initiated as further phosphopeptides besides the already detected ones were assumed to be present. Phosphopeptide enrichment was first established for the standard protein casein by comparing two different enrichment techniques, IMAC and Phos-tag agarose. Phosphopeptide enrichment by IMAC according to Villen and Gygi (2008) led to an insufficient enrichment of the phosphopeptides of the standard protein casein although the authors could characterize 5,500 and 13,000 phosphorylation events from mouse liver and *Drosophila* embryos. The phosphopeptide detected in this study was either lost by a lack of phosphopeptide binding to the matrix and by the washing steps during purification procedure, indicating the high demand of studying phosphopeptide analysis using targeted approaches.

The phosphopeptide enrichment of casein using Phos-tag agarose (Kinoshita *et al.* 2005) was more promising compared to IMAC, as the phosphopeptide detected was observed specifically in the eluted fraction. Therefore the phosphopeptide enrichment using Phos-tag agarose was transferred to STIAT2, resulting in the detection of a phosphorylated peptide which were already present in the total digest. This result suggests that the enrichment illustrates more a depletion of dephosphorylated peptides and has to be optimised for the STIAT isoforms.

5.6.2. Ion exchange chromatography separates phosphorylated STIAT isoforms

After the detection of possible phosphorylation sites within the recombinant STIAT proteins, the aim was the identification of the possible phosphorylation sites of the STIAT isoforms *in planta*. Therefore the STIAT isoforms need to be enriched from total protein mixtures since they are low abundant. Enrichment by immunoprecipitation did not lead to the detection of modifications and additional fractionation techniques for the STIAT isoforms were applied such as preparative IEF and ionexchange chromatography. Preparative IEF of proteins from Arabidopsis leaves revealed enrichment of the STIAT isoforms in specific fractions, but resulted in weak identification of the isoforms there due to sample complexity. The high abundant RuBisCO was present in the fractions containing STIAT isoforms and in most of the fractions, probably due to the wide range of *pI* or its abundance.

In contrast, ion exchange chromatography of STIAT isoforms resulted in the separation of the STIAT isoforms from RuBisCO. Furthermore and more meaningful, the analysis of phosphorylation patterns resulted in separation of phosphorylated and dephosphorylated isoforms indicating that a subpopulation of STIAT isoforms is modified by phosphorylation *in vivo*. This finding is in agreement with *in vivo* phosphorylation of murine STI1 and HOP (Daniel *et al.* 2008, Lassle *et al.* 1997) but was shown for the first time for a plant HOP. Out of these data it can be assumed, that phosphorylation of HOP/STI1 proteins is a general modification process across all kingdoms.

Downstream analysis of a fraction containing the phosphorylated STIAT isoforms using MS analysis revealed the detection of phosphorylated proteins among 300-400 proteins but failed to detect the STIAT isoforms. This finding leads to the assumption that the fraction obtained after IEX was still complex and the STIAT isoforms were low abundant.

Although the detection of the specific phosphorylation sites *in planta*, especially in Arabidopsis, has not yet been shown, the phosphorylated subpopulation of STIAT isoforms can be stabilized by phosphatase inhibitor treatment before IEX. Additional purification steps of the phosphorylated subpopulation of STIAT isoforms before MS analysis are recommended in order to reduce the complexity of the sample. Immunoprecipitation of the phosphorylated STIAT isoforms would be a key tool to link both methods (Figure 52) and to identify the phosphorylation sites *in vivo*.

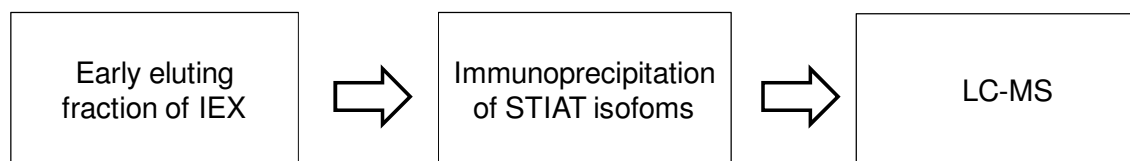


Figure 52: Strategy to investigate the STIAT phosphorylation sites *in planta*.

IEX separates STIAT isoforms according to their phosphorylation state. The early eluting fraction of IEX containing the phosphorylated subpopulation of STIAT isoforms is purified by immunoprecipitation as the IEX fraction is too complex for direct analysis by LC-MS. The phosphorylation sites are identified by LC-MS.

5.7. Summary: What are the possible functions of STIAT isoforms?

Molecular chaperones, such as Hsp70 and Hsp90, interact with a wide range of co-chaperones that regulate their activity or aid in the folding of specific substrate proteins (Buchner *et al.* 1998, Hartl 1996). The Hsp70/Hsp90 organising protein is a co-chaperone which reversibly couples Hsp70 and Hsp90 (Chen and Smith 1998). Plant heterologs of HOP/STI1 were described in numerous studies (Chen *et al.* 2010, Krishna and Gloor 2001, Krishna and Kanelakis 2003, Torres *et al.* 1995, Zhang *et al.* 2003) varying in the number of *HOP* genes per plant species. All three different STIAT isoforms in Arabidopsis were analysed to different extents using functional proteomics in order to clarify their expression and possible functions.

STIAT isoform expression is regulated during plant development and to some extent by stress defence mechanisms for STIAT1 and STIAT2, while STIAT3 has a specific function in thermoadaptation of leaves (Figure 50).

In addition to the characterisation of the STIAT isoform expression, the STIAT isoforms were analyzed for their intracellular distribution, interaction partners and their regulation by the post translational modification by phosphorylation, summarized in a current model (Figure

53). STIAT1 is the best characterized isoform as its subcellular localisation in cytosol and nucleus has been validated. It was shown that this isoform is interacting with Hsp90 and Hsp70 using TAP of the homologous protein STINT. A function in vesicle transport from ER to Golgi is supposed which is in agreement with its possible association to endomembranes. STIAT2 is co-localised with STIAT1 in numerous studies and the same functions can be assumed. The role of STIAT3 is less characterized, but is specifically expressed after heat assuming a function in thermoadaptation. All three STIAT isoforms are modified by phosphorylation, as phosphorylated and dephosphorylated subpopulations of them can be fractionated by ion exchange chromatography.

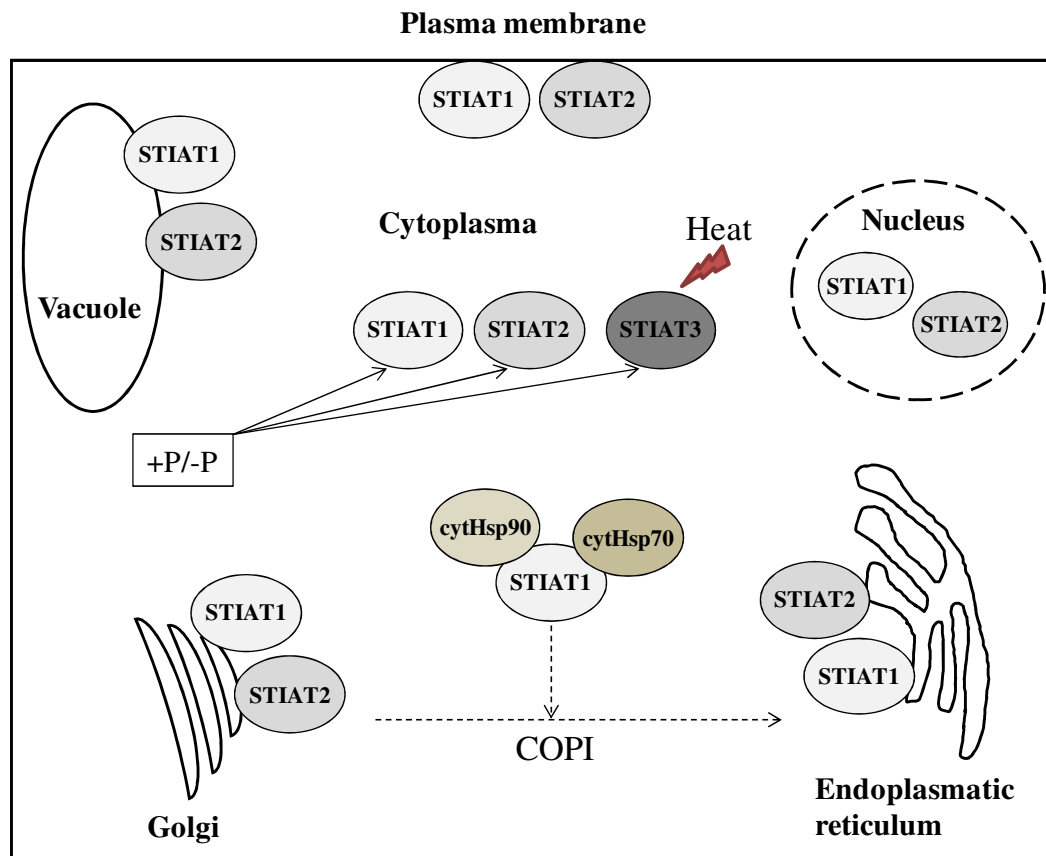


Figure 53: Current model of the intracellular distribution, the interaction partners and the modification of the STIAT isoforms by phosphorylation in Arabidopsis.

STIAT1 and STIAT2 are present in cytosol and nucleus and associate to membranes, *e.g.* endomembranes from vacuole, Golgi and endoplasmic reticulum and plasma membrane. No experimental evidence has been gathered for STIAT3 so far, since this isoform is present under non-control conditions like heat.

STIAT1 has been shown to be interacting with cytosolic isoforms of Hsp90 and Hsp70 by TAP of homologous STINT protein. In this regard, a function in vesicle transport from Golgi to ER is hypothesized which needs further confirmation.

STIAT isoforms are modified by phosphorylation, as phosphorylated and dephosphorylated subpopulations can be fractionated by ion exchange chromatography. Phosphorylation sites are still only partly known.

6. References

- Abbas-Terki, T., Briand, P.A., Donze, O. and Picard, D.** (2002) The Hsp90 co-chaperones Cdc37 and Sti1 interact physically and genetically. *Biol Chem*, **383**, 1335-1342.
- Abbas-Terki, T., Donze, O., Briand, P.A. and Picard, D.** (2001) Hsp104 interacts with Hsp90 co-chaperones in respiring yeast. *Mol Cell Biol*, **21**, 7569-7575.
- Abe, H., Urao, T., Ito, T., Seki, M., Shinozaki, K. and Yamaguchi-Shinozaki, K.** (2003) Arabidopsis AtMYC2 (bHLH) and AtMYB2 (MYB) function as transcriptional activators in abscisic acid signaling. *Plant Cell*, **15**, 63-78.
- Abe, H., Yamaguchi-Shinozaki, K., Urao, T., Iwasaki, T., Hosokawa, D. and Shinozaki, K.** (1997) Role of Arabidopsis MYC and MYB homologs in drought- and abscisic acid-regulated gene expression. *Plant Cell*, **9**, 1859-1868.
- Alonso, J.M., Stepanova, A.N., Leisse, T.J., Kim, C.J., Chen, H., Shinn, P., Stevenson, D.K., Zimmerman, J., Barajas, P., Cheuk, R., Gadriab, C., Heller, C., Jeske, A., Koesema, E., Meyers, C.C., Parker, H., Prednis, L., Ansari, Y., Choy, N., Deen, H., Geralt, M., Hazari, N., Hom, E., Karnes, M., Mulholland, C., Ndubaku, R., Schmidt, I., Guzman, P., Aguilar-Henonin, L., Schmid, M., Weigel, D., Carter, D.E., Marchand, T., Risseuw, E., Brogden, D., Zeko, A., Crosby, W.L., Berry, C.C. and Ecker, J.R.** (2003) Genome-wide insertional mutagenesis of *Arabidopsis thaliana*. *Science*, **301**, 653-657.
- Amme, S., Rutten, T., Melzer, M., Sonsmann, G., Vissers, J.P.C., Schlesier, B. and Mock, H.P.** (2005) A proteome approach defines protective functions of tobacco leaf trichomes. *Proteomics*, **5**, 2508-2518.
- Bäumlein, H., Nagy, I., Villarreal, R., Inze, D. and Wobus, U.** (1992) Cis-analysis of a seed protein gene promoter - The conservative ry repeat CATGCATG within the legumin box is essential for tissue-specific expression of a legumin gene. *Plant J*, **2**, 233-239.
- Benschop, J.J., Mohammed, S., O'Flaherty, M., Heck, A.J.R., Slijper, M. and Menke, F.L.H.** (2007) Quantitative phosphoproteomics of early elicitor signaling in Arabidopsis. *Mol Cell Proteomics*, **6**, 1198-1214.
- Blatch, G.L. and Lässle, M.** (1999) The tetratricopeptide repeat: a structural motif mediating protein-protein interactions. *BioEssays*, **21**, 932-939.
- Boston, R.S., Viitanen, P.V. and Vierling, E.** (1996) Molecular chaperones and protein folding in plants. *Plant Mol Biol*, **32**, 191-222.
- Bradford, M.** (1976) A rapid and sensitive method for the quantitation of microgram quantities of protein utilizing the principle of protein-dye binding. *Anal Biochem*, **7**, 248-254.
- Buchner, J.** (1999) Hsp90 & Co. - A holding for folding. *Trends Biochem Sci*, **24**, 136-141.
- Buchner, J., Bose, S., Mayr, C. and Jakob, U.** (1998) Purification and characterization of prokaryotic and eukaryotic Hsp90. In *Molecular Chaperones*. San Diego: Academic Press Inc, pp. 409-418.
- Bullock, W.O., Fernandez, J.M. and Short, J.M.** (1987) XL1-Blue - A high efficiency plasmid transforming recA Escherichia coli strain with beta-galactosidase selection. *Biotechniques*, **5**, 376-&.
- Calikowski, T.T., Meulia, T. and Meier, I.** (2003) A proteomic study of the Arabidopsis nuclear matrix. *Journal of Cellular Biochemistry*, **90**, 361-378.
-

- Carrigan, P.E., Nelson, G.M., Roberts, P.J., Stoffer, J.N., Riggs, D.L. and Smith, D.F.** (2004) Multiple domains of the co-chaperone Hop are important for Hsp70 binding. *J Biol Chem*, **279**, 16185-16193.
- Cazalé, A.-C., Clément, M., Chiarenza, S., Roncato, M.-A., Pochon, N., Creff, A., Marin, E., Leonhardt, N. and Noël, L.D.** (2009) Altered expression of cytosolic/nuclear Hsc70-1 molecular chaperone affects development and abiotic stress tolerance in *Arabidopsis thaliana*. *J Exp Bot*, **60**, 2653-2664.
- Chaboute, M.E., Clement, B., Sekine, M., Philipps, G. and Chaubet-Gigot, N.** (2000) Cell cycle regulation of the tobacco ribonucleotide reductase small subunit gene is mediated by E2F-like elements. *Plant Cell*, **12**, 1987-1999.
- Chakravarthy, S., Tuori, R.P., D'Ascenzo, M.D., Fobert, P.R., Després, C. and Martin, G.B.** (2003) The tomato transcription factor Pti4 regulates defense-related gene expression via GCC box and non-GCC box cis elements. *Plant Cell*, **15**, 3033-3050.
- Chan, C.S., Guo, L. and Shih, M.C.** (2001) Promoter analysis of the nuclear gene encoding the chloroplast glyceraldehyde-3-phosphate dehydrogenase B subunit of *Arabidopsis thaliana*. *Plant Mol Biol*, **46**, 131-141.
- Chang, H.C. and Lindquist, S.** (1994) Conservation of Hsp90 macromolecular complexes in *Saccharomyces cerevisiae*. *J Biol Chem*, **269**, 24983-24988.
- Chang, H.C.J., Nathan, D.F. and Lindquist, S.** (1997) *In vivo* analysis of the Hsp90 cochaperone Sti1 (p60). *Mol Cell Biol*, **17**, 318-325.
- Chaubet, N., Flenet, M., Clement, B., Brignon, P. and Gigot, C.** (1996) Identification of cis-elements regulating the expression of an *Arabidopsis* histone H4 gene. *Plant J*, **10**, 425-435.
- Chen, C.Y. and Balch, W.E.** (2006) The Hsp90 chaperone complex regulates GDI-dependent rab recycling. *Mol Biol Cell*, **17**, 3494-3507.
- Chen, L., Hamada, S., Fujiwara, M., Zhu, T., Thao, N.P., Wong, H.L., Krishna, P., Ueda, T., Kaku, H., Shibuya, N., Kawasaki, T. and Shimamoto, K.** (2010) The Hop/Sti1-Hsp90 chaperone complex facilitates the maturation and transport of a PAMP receptor in rice innate immunity. *Cell Host Microbe*, **7**, 185-196.
- Chen, S., Prapapanich, V., Rimerman, R.A., Honoré, B. and Smith, D.F.** (1996) Interactions of p60, a mediator of progesterone receptor assembly, with heat shock proteins Hsp90 and Hsp70. *Mol Endocrinol*, **10**, 682-693.
- Chen, S. and Smith, D.F.** (1998) Hop as an adaptor in the heat shock protein 70 (Hsp70) and Hsp90 chaperone machinery. *J Biol Chem*, **273**, 35194-35200.
- Claros, M.G. and Vincens, P.** (1996) Computational method to predict mitochondrially imported proteins and their targeting sequences. *Eur J Biochem*, **241**, 779-786.
- Conde, A., Chaves, M.M. and Geros, H.** (2011) Membrane transport, sensing and signaling in plant adaptation to environmental stress. *Plant Cell Physiol*, **52**, 1583-1602.
- Cserzo, M., Wallin, E., Simon, I., vonHeijne, G. and Elofsson, A.** (1997) Prediction of transmembrane alpha-helices in prokaryotic membrane proteins: the dense alignment surface method. *Protein Eng*, **10**, 673-676.
- Daniel, S., Bradley, G., Longshaw, V.M., Soti, C., Csermely, P. and Blatch, G.L.** (2008) Nuclear translocation of the phosphoprotein Hop (Hsp70/Hsp90 organizing protein) occurs under heat shock, and its proposed nuclear localization signal is involved in Hsp90 binding. *BBA-Mol Cell Res*, **1783**, 1003-1014.
- Davuluri, R., Sun, H., Palaniswamy, S., Matthews, N., Molina, C., Kurtz, M. and Grotewold, E.** (2003) AGRIS: *Arabidopsis* gene regulatory information server, an

- information resource of Arabidopsis cis-regulatory elements and transcription factors. *BMC Bioinformatics*, **4**, 25.
- Demand, J., Luders, J. and Hohfeld, J.** (1998) The carboxy-terminal domain of Hsc70 provides binding sites for a distinct set of chaperone cofactors. *Mol Cell Biol*, **18**, 2023-2028.
- Dittmar, K.D., Hutchison, K.A., OwensGrillo, J.K. and Pratt, W.B.** (1996) Reconstitution of the steroid receptor center dot Hsp90 heterocomplex assembly system of rabbit reticulocyte lysate. *J Biol Chem*, **271**, 12833-12839.
- Emanuelsson, O., Nielsen, H., Brunak, S. and von Heijne, G.** (2000) Predicting subcellular localization of proteins based on their N-terminal amino acid sequence. *J Mol Biol*, **300**, 1005-1016.
- Endreß, S.** (2010) Untersuchungen zur Interaktion des Co-Chaperons STIAT mit ausgewählten Vertretern der Hsp70 und Hsp90 Proteinfamilien: Eberhard Karls Universität Tübingen, pp. 61.
- Eulgem, T., Rushton, P.J., Robatzek, S. and Somssich, I.E.** (2000) The WRKY superfamily of plant transcription factors. *Trends Plant Sci*, **5**, 199-206.
- Fellerer, C., Schweiger, R., Schöngruber, K., Soll, J. and Schwenkert, S.** (2011) Cytosolic Hsp90 co-chaperones Hop and FKBP interact with freshly synthesized chloroplast preproteins of Arabidopsis. *Mol Plant*, **4**, 1133-1145.
- Flom, G., Behal, R.H., Rosen, L., Cole, D.G. and Johnson, J.L.** (2007) Definition of the minimal fragments of Stl1 required for dimerization, interaction with Hsp70 and Hsp90 and in vivo functions. *Biochem J*, **404**, 159-167.
- Fowler, S. and Thomashow, M.F.** (2002) Arabidopsis transcriptome profiling indicates that multiple regulatory pathways are activated during cold acclimation in addition to the CBF cold response pathway. *Plant Cell*, **14**, 1675-1690.
- Frydman, J.** (2001) Folding of newly translated proteins *in vivo*: The role of molecular chaperones. *Annu Rev Biochem*, **70**, 603-647.
- Gandhi, T.K.B., Zhong, J., Mathivanan, S., Karthick, L., Chandrika, K.N., Mohan, S.S., Sharma, S., Pinkert, S., Nagaraju, S., Periaswamy, B., Mishra, G., Nandakumar, K., Shen, B.Y., Deshpande, N., Nayak, R., Sarker, M., Boeke, J.D., Parmigiani, G., Schultz, J., Bader, J.S. and Pandey, A.** (2006) Analysis of the human protein interactome and comparison with yeast, worm and fly interaction datasets. *Nature Genet*, **38**, 285-293.
- Geisler-Lee, J., O'Toole, N., Ammar, R., Provart, N.J., Millar, A.H. and Geisler, M.** (2007) A predicted interactome for Arabidopsis. *Plant Physiol*, **145**, 317-329.
- Giot, L., Bader, J.S., Brouwer, C., Chaudhuri, A., Kuang, B., Li, Y., Hao, Y.L., Ooi, C.E., Godwin, B., Vitols, E., Vijayadamar, G., Pochart, P., Machineni, H., Welsh, M., Kong, Y., Zerhusen, B., Malcolm, R., Varrone, Z., Collis, A., Minto, M., Burgess, S., McDaniel, L., Stimpson, E., Spriggs, F., Williams, J., Neurath, K., Ioime, N., Agee, M., Voss, E., Furtak, K., Renzulli, R., Aanensen, N., Carrola, S., Bickelhaupt, E., Lazovatsky, Y., DaSilva, A., Zhong, J., Stanyon, C.A., Finley, R.L., White, K.P., Braverman, M., Jarvie, T., Gold, S., Leach, M., Knight, J., Shimkets, R.A., McKenna, M.P., Chant, J. and Rothberg, J.M.** (2003) A protein interaction map of *Drosophila melanogaster*. *Science*, **302**, 1727-1736.
- Giuliano, G., Pichersky, E., Malik, V.S., Timko, M.P., Scolnik, P.A. and Cashmore, A.R.** (1988) An evolutionarily conserved protein-binding sequence upstream of a plant light-regulated gene. *P Natl Acad Sci USA*, **85**, 7089-7093.

-
- Glover, J.R. and Lindquist, S.** (1998) Hsp104, Hsp70, and Hsp40: A novel chaperone system that rescues previously aggregated proteins. *Cell*, **94**, 73-82.
- Green, P.J., Kay, S.A. and Chua, N.H.** (1987) Sequence-specific interactions of a pea nuclear factor with light-responsive elements upstream of the RbcS-3A gene. *Embo J*, **6**, 2543-2549.
- Green, P.J., Yong, M.H., Cuozzo, M., Kanomurakami, Y., Silverstein, P. and Chua, N.H.** (1988) Binding-site requirements for a pea nuclear-protein factor GT1 correlate with sequences required for light-dependent transcriptional activation of the RbcS-3A gene. *Embo J*, **7**, 4035-4044.
- Haralampidis, K., Milioni, D., Rigas, S. and Hatzopoulos, P.** (2002) Combinatorial interaction of cis-elements specifies the expression of the Arabidopsis AtHsp90-1 gene. *Plant Physiol*, **129**, 1138-1149.
- Hartl, F.U.** (1996) Molecular chaperones in cellular protein folding. *Nature*, **381**, 571-580.
- Heazlewood, J.L., Durek, P., Hummel, J., Selbig, J., Weckwerth, W., Walther, D. and Schulze, W.X.** (2008) PhosPhAt: a database of phosphorylation sites in *Arabidopsis thaliana* and a plant-specific phosphorylation site predictor. *Nucleic Acids Res*, **36**, D1015-D1021.
- Hedtmann, C.** (2005) Isolation und Charakterisierung von Trichom-spezifischen Promotoren aus *Nicotiana tabacum* SNN: Leibniz-Universität Hannover, pp. 43.
- Hedtmann, C.** (2007) Charakterisierung von einem Stress-induzierten Protein aus *Nicotiana tabacum* mit Homologie zum Genprodukt von At1g62740: Leibniz Universität Hannover, pp. 71.
- Hernandez, M.P., Sullivan, W.P. and Toft, D.O.** (2002) The assembly and intermolecular properties of the Hsp70-Hop-Hsp90 molecular chaperone complex. *J Biol Chem*, **277**, 38294-38304.
- Higo, K., Ugawa, Y., Iwamoto, M. and Korenaga, T.** (1999) Plant cis-acting regulatory DNA elements (PLACE) database: 1999. *Nucleic Acids Res*, **27**, 297-300.
- Hirokawa, T., Boon-Chieng, S. and Mitaku, S.** (1998) SOSUI: classification and secondary structure prediction system for membrane proteins. *Bioinformatics*, **14**, 378-379.
- Ho, Y., Gruhler, A., Heilbut, A., Bader, G.D., Moore, L., Adams, S.-L., Millar, A., Taylor, P., Bennett, K., Boutilier, K., Yang, L., Wolting, C., Donaldson, I., Schandorff, S., Shewnarane, J., Vo, M., Taggart, J., Goudreault, M., Muskat, B., Alfarano, C., Dewar, D., Lin, Z., Michalickova, K., Willems, A.R., Sassi, H., Nielsen, P.A., Rasmussen, K.J., Andersen, J.R., Johansen, L.E., Hansen, L.H., Jespersen, H., Podtelejnikov, A., Nielsen, E., Crawford, J., Poulsen, V., Sorensen, B.D., Matthiesen, J., Hendrickson, R.C., Gleeson, F., Pawson, T., Moran, M.F., Durocher, D., Mann, M., Hogue, C.W.V., Figgeys, D. and Tyers, M.** (2002) Systematic identification of protein complexes in *Saccharomyces cerevisiae* by mass spectrometry. *Nature*, **415**, 180-183.
- Honore, B., Leffers, H., Madsen, P., Rasmussen, H.H., Vandekerckhove, J. and Celis, J.E.** (1992) Molecular cloning and expression of a transformation-sensitive human protein containing the TPR motif and sharing identity to the stress-inducible yeast protein Sti1. *J Biol Chem*, **267**, 8485-8491.
- Horton, P., Park, K.J., Obayashi, T., Fujita, N., Harada, H., Adams-Collier, C.J. and Nakai, K.** (2007) WoLF PSORT: Protein localization predictor. *Nucleic Acids Res*, **35**, W585-W587.
-

- Hruz, T., Laule, O., Szabo, G., Wessendorp, F., Bleuler, S., Oertle, L., Widmayer, P., Gruissem, W. and Zimmermann, P.** (2008) Genevestigator V3: A reference expression database for the meta-analysis of transcriptomes. *Adv Bioinformatics*, **2008**.
- Huang, B.R. and Xu, C.P.** (2008) Identification and characterization of proteins associated with plant tolerance to heat stress. *J Integr Plant Biol*, **50**, 1230-1237.
- Hubel, A., Lee, J.H., Wu, C. and Schoffl, F.** (1995) Arabidopsis heat shock factor is constitutively active in Drosophila and human cells. *Mol Gen Genetics*, **248**, 136-141.
- Hudson, M.E., Lisch, D.R. and Quail, P.H.** (2003) The Fhy3 and Far1 genes encode transposase-related proteins involved in regulation of gene expression by the phytochrome A-signaling pathway. *Plant J*, **34**, 453-471.
- Johnson, B.D., Schumacher, R.J., Ross, E.D. and Toft, D.O.** (1998) Hop modulates Hsp70/Hsp90 interactions in protein folding. *J Biol Chem*, **273**, 3679-3686.
- Jungkunz, I., Link, K., Vogel, F., Voll, L.M., Sonnewald, S. and Sonnewald, U.** (2011) AtHsp70-15-deficient Arabidopsis plants are characterized by reduced growth, a constitutive cytosolic protein response and enhanced resistance to TuMV. *Plant J*, **66**, 983-995.
- Kagaya, Y., Ohmiya, K. and Hattori, T.** (1999) RAV1, a novel DNA-binding protein, binds to bipartite recognition sequence through two distinct DNA-binding domains uniquely found in higher plants. *Nucleic Acids Res*, **27**, 470-478.
- Kang, D.H., Gho, Y.S., Suh, M.K. and Kang, C.H.** (2002) Highly sensitive and fast protein detection with coomassie brilliant blue in sodium dodecyl sulfate-polyacrylamide gel electrophoresis. *B Kor Chem Soc*, **23**, 1511-1512.
- Kasuga, M., Liu, Q., Miura, S., Yamaguchi-Shinozaki, K. and Shinozaki, K.** (1999) Improving plant drought, salt, and freezing tolerance by gene transfer of a single stress-inducible transcription factor. *Nat Biotechnol*, **17**, 287-291.
- Kim, S.Y., Chung, H.J. and Thomas, T.L.** (1997) Isolation of a novel class of bZIP transcription factors that interact with ABA-responsive and embryo-specification elements in the Dc3 promoter using a modified yeast one-hybrid system. *Plant J*, **11**, 1237-1251.
- Kinoshita, E., Yamada, A., Takeda, H., Kinoshita-Kikuta, E. and Koike, T.** (2005) Novel immobilized zinc(II) affinity chromatography for phosphopeptides and phosphorylated proteins. *J Sep Sci*, **28**, 155-162.
- Kleffmann, T., Russenberger, D., von Zychlinski, A., Christopher, W., Sjolander, K., Gruissem, W. and Baginsky, S.** (2004) The Arabidopsis thaliana chloroplast proteome reveals pathway abundance and novel protein functions. *Current Biology*, **14**, 354-362.
- Klodmann, J., Senkler, M., Rode, C. and Braun, H.P.** (2011) Defining the protein complex proteome of plant mitochondria. *Plant Physiol*, **157**, 587-598.
- Knight, H. and Knight, M.R.** (2001) Abiotic stress signalling pathways: Specificity and cross-talk. *Trends Plant Sci*, **6**, 262-267.
- Kotak, S., Larkindale, J., Lee, U., von Koskull-Döring, P., Vierling, E. and Scharf, K.-D.** (2007) Complexity of the heat stress response in plants. *Curr Opin Biol*, **10**, 310-316.
- Kreis, T.E., Lowe, M. and Pepperkok, R.** (1995) COPs regulating membrane traffic. *Annu Rev Cell Dev Bi*, **11**, 677-706.
- Krishna, P. and Gloor, G.** (2001) The Hsp90 family of proteins in *Arabidopsis thaliana*. *Cell Stress Chaperon*, **6**, 238-246.

- Krishna, P. and Kanelakis, K.C.** (2003) The 70-kDa protein bound to hsp90 in wheat germ lysate is a plant homologue of animal Hop. *Physiol Plant*, **119**, 456-462.
- Laemmli, U.K.** (1970) Cleavage of structural proteins during assembly of head of bacteriophage T4. *Nature*, **227**, 680-&.
- Lassle, M., Blatch, G.L., Kundra, V., Takatori, T. and Zetter, B.R.** (1997) Stress-inducible, murine protein mSTII - Characterization of binding domains for heat shock proteins and in vitro phosphorylation by different kinases. *J Biol Chem*, **272**, 1876-1884.
- Latijnhouwers, M., Xu, X.-M. and Møller, S.** (2010) Arabidopsis stromal 70-kDa heat shock proteins are essential for chloroplast development. *Planta*, **232**, 567-578.
- Lee, S., Lee, D.W., Lee, Y., Mayer, U., Stierhof, Y.-D., Lee, S., Jürgens, G. and Hwang, I.** (2009) Heat shock protein cognate 70-4 and an E3 ubiquitin ligase, CHIP, mediate plastid-destined precursor degradation through the ubiquitin-26S proteasome system in Arabidopsis. *Plant Cell*, **21**, 3984-4001.
- Li, H., Wong, W.S., Zhu, L., Guo, H.W., Ecker, J. and Li, N.** (2009) Phosphoproteomic analysis of ethylene-regulated protein phosphorylation in etiolated seedlings of Arabidopsis mutant ein2 using two-dimensional separations coupled with a hybrid quadrupole time-of-flight mass spectrometer. *Proteomics*, **9**, 1646-1661.
- Li, S.M., Armstrong, C.M., Bertin, N., Ge, H., Milstein, S., Boxem, M., Vidalain, P.O., Han, J.D.J., Chesneau, A., Hao, T., Goldberg, D.S., Li, N., Martinez, M., Rual, J.F., Lamesch, P., Xu, L., Tewari, M., Wong, S.L., Zhang, L.V., Berriz, G.F., Jacotot, L., Vaglio, P., Reboul, J., Hirozane-Kishikawa, T., Li, Q.R., Gabel, H.W., Elewa, A., Baumgartner, B., Rose, D.J., Yu, H.Y., Bosak, S., Sequerra, R., Fraser, A., Mango, S.E., Saxton, W.M., Strome, S., van den Heuvel, S., Piano, F., Vandenhaute, J., Sardet, C., Gerstein, M., Doucette-Stamm, L., Gunsalus, K.C., Harper, J.W., Cusick, M.E., Roth, F.P., Hill, D.E. and Vidal, M.** (2004) A map of the interactome network of the metazoan *C. elegans*. *Science*, **303**, 540-543.
- Li, Y.F.** (2011) The tandem affinity purification technology: An overview. *Biotechnol Lett*, **33**, 1487-1499.
- Lin, B.L., Wang, J.S., Liu, H.C., Chen, R.W., Meyer, Y., Barakat, A. and Delseny, M.** (2001) Genomic analysis of the Hsp70 superfamily in *Arabidopsis thaliana*. *Cell Stress Chaperon*, **6**, 201-208.
- Linsmeier, E.M. and Skoog, F.** (1965) Organic growth factor requirements of tobacco tissue cultures. *Physiol Plant*, **18**, 100-127.
- Lohmann, J.U., Hong, R.L., Hobe, M., Busch, M.A., Parcy, F., Simon, R. and Weigel, D.** (2001) A Molecular Link between Stem Cell Regulation and Floral Patterning in Arabidopsis. *Cell*, **105**, 793-803.
- Longshaw, V.M., Chapple, J.P., Balda, M.S., Cheetham, M.E. and Blatch, G.L.** (2004) Nuclear translocation of the Hsp70/Hsp90 organizing protein mSTII is regulated by cell cycle kinases. *J Cell Sci*, **117**, 701-710.
- Lotz, G.P., Brychzy, A., Heinz, S. and Obermann, W.M.J.** (2008) A novel HSP90 chaperone complex regulates intracellular vesicle transport. *J Cell Sci*, **121**, 717-723.
- Lowe, M. and Kreis, T.E.** (1995) *In vitro* assembly and disassembly of coatomer. *J Biol Chem*, **270**, 31364-31371.
- Maliga, P., Szbrenzo, A. and Marton, L.** (1973) Streptomycin-resistant plants from callus culture of haploid tobacco. *Nature-New Biol*, **244**, 29-30.

- Martinez, I.M. and Chrispeels, M.J.** (2003) Genomic analysis of the unfolded protein response in *Arabidopsis* shows its connection to important cellular processes. *Plant Cell*, **15**, 561-576.
- Meiri, D. and Breiman, A.** (2009) *Arabidopsis* Rof1 (FKBP62) modulates thermotolerance by interacting with HSP90-1 and affecting the accumulation of HsfA2-regulated sHsps. *Plant J*, **59**, 387-399.
- Menkens, A.E., Schindler, U. and Cashmore, A.R.** (1995) The G-box - A ubiquitous regulatory DNA element in plants bound by the GBF family of BZIP proteins. *Trends Biochem Sci*, **20**, 506-510.
- Millar, A.H., Sweetlove, L.J., Giege, P. and Leaver, C.J.** (2001) Analysis of the *Arabidopsis* mitochondrial proteome. *Plant Physiol*, **127**, 1711-1727.
- Murashige, T. and Skoog, F.** (1962) A revised medium for rapid growth and bio assays with tobacco tissue cultures. *Physiol Plant*, **15**, 473-497.
- Nakagami, H., Sugiyama, N., Mochida, K., Daudi, A., Yoshida, Y., Toyoda, T., Tomita, M., Ishihama, Y. and Shirasu, K.** (2010) Large-scale comparative phosphoproteomics identifies conserved phosphorylation sites in plants. *Plant Physiol*, **153**, 1161-1174.
- Nicolet, C.M. and Craig, E.A.** (1989) Isolation and characterization of *Sti1*, a stress-inducible gene from *Saccharomyces cerevisiae*. *Mol Cell Biol*, **9**, 3638-3646.
- Noël, L.D., Cagna, G., Stuttmann, J., Wirthmüller, L., Betsuyaku, S., Witte, C.-P., Bhat, R., Pochon, N., Colby, T. and Parker, J.E.** (2007) Interaction between SGT1 and cytosolic/nuclear Hsc70 chaperones regulates *Arabidopsis* immune responses. *Plant Cell*, **19**, 4061-4076.
- Nordin, K., Vahala, T. and Palva, E.T.** (1993) Differential expression of 2 related, low-temperature-induced genes in *Arabidopsis thaliana* (L) Heynh. *Plant Mol Biol*, **21**, 641-653.
- O'Connor, T.R., Dyreson, C. and Wyrick, J.J.** (2005) Athena: a resource for rapid visualization and systematic analysis of *Arabidopsis* promoter sequences. *Bioinformatics*, **21**, 4411-4413.
- Odunuga, O.O., Longshaw, V.M. and Blatch, G.L.** (2004) Hop: more than an Hsp70/Hsp90 adaptor protein. *Bioessays*, **26**, 1058-1068.
- Ogawa, M., Hanada, A., Yamauchi, Y., Kuwalhara, A., Kamiya, Y. and Yamaguchi, S.** (2003) Gibberellin biosynthesis and response during *Arabidopsis* seed germination. *Plant Cell*, **15**, 1591-1604.
- Ohgishi, M., Oka, A., Morelli, G., Ruberti, I. and Aoyama, T.** (2001) Negative autoregulation of the *Arabidopsis* homeobox gene *ATHB-2*. *Plant J*, **25**, 389-398.
- Pedersen, B.P., Buch-Pedersen, M.J., Preben Morth, J., Palmgren, M.G. and Nissen, P.** (2007) Crystal structure of the plasma membrane proton pump. *Nature*, **450**, 1111-1114.
- Pla, M., Vilardell, J., Gultinan, M.J., Marcotte, W.R., Niogret, M.F., Quatrano, R.S. and Pages, M.** (1993) The cis-regulatory element CCACGTGG is involved in ABA and water-stress responses of the maize gene *Rab28*. *Plant Mol Biol*, **21**, 259-266.
- Prasad, B.D., Goel, S. and Krishna, P.** (2010) *In silico* identification of carboxylate clamp type tetratricopeptide repeat proteins in *Arabidopsis* and rice as putative co-chaperones of Hsp90/Hsp70. *Plos One*, **5**, e12761.
- Prodromou, C., Siligardi, G., O'Brien, R., Woolfson, D.N., Regan, L., Panaretou, B., Ladbury, J.E., Piper, P.W. and Pearl, L.H.** (1999) Regulation of Hsp90 ATPase
-

- activity by tetratricopeptide repeat (TPR)-domain co-chaperones. *Embo J*, **18**, 754-762.
- Ramirez-Parra, E., Frundt, C. and Gutierrez, C.** (2003) A genome-wide identification of E2F-regulated genes in Arabidopsis. *Plant J*, **33**, 801-811.
- Reidy, M. and Masison, D.C.** (2010) Sti1 regulation of Hsp70 and Hsp90 is critical for curing of *Saccharomyces cerevisiae* PSI(+) prions by Hsp104. *Mol Cell Biol*, **30**, 3542-3552.
- Richter, K. and Buchner, J.** (2001) Hsp90: Chaperoning signal transduction. *J Cell Physiol*, **188**, 281-290.
- Rigaut, G., Shevchenko, A., Rutz, B., Wilm, M., Mann, M. and Séraphin, B.** (1999) A generic protein purification method for protein complex characterization and proteome exploration. *Nat Biotechnol*, **17**, 1030-1032.
- Rohila, J.S., Chen, M., Cerny, R. and Fromm, M.E.** (2004) Improved tandem affinity purification tag and methods for isolation of protein heterocomplexes from plants. *Plant J*, **38**, 172-181.
- Rosso, M.G., Li, Y., Strizhov, N., Reiss, B., Dekker, K. and Weisshaar, B.** (2003) An *Arabidopsis thaliana* T-DNA mutagenized population (GABI-Kat) for flanking sequence tag-based reverse genetics. *Plant Mol Biol*, **53**, 247-259.
- Rual, J.F., Venkatesan, K., Hao, T., Hirozane-Kishikawa, T., Dricot, A., Li, N., Berriz, G.F., Gibbons, F.D., Dreze, M., Ayivi-Guedehoussou, N., Klitgord, N., Simon, C., Boxem, M., Milstein, S., Rosenberg, J., Goldberg, D.S., Zhang, L.V., Wong, S.L., Franklin, G., Li, S.M., Albala, J.S., Lim, J.H., Fraughton, C., Llamas, E., Cevik, S., Bex, C., Lamesch, P., Sikorski, R.S., Vandenhaute, J., Zoghbi, H.Y., Smolyar, A., Bosak, S., Sequerra, R., Doucette-Stamm, L., Cusick, M.E., Hill, D.E., Roth, F.P. and Vidal, M.** (2005) Towards a proteome-scale map of the human protein-protein interaction network. *Nature*, **437**, 1173-1178.
- Salvucci, M.E., Osteryoung, K.W., Crafts-Brandner, S.J. and Vierling, E.** (2001) Exceptional sensitivity of rubisco activase to thermal denaturation *in vitro* and *in vivo*. *Plant Physiol*, **127**, 1053-1064.
- Santoni, V.** (2007) Plant plasma membrane protein extraction and solubilization for proteomic analysis. *Methods Mol Biol*, **355**, 93-109.
- Satoh, R., Nakashima, K., Seki, M., Shinozaki, K. and Yamaguchi-Shinozaki, K.** (2002) ACTCAT, a novel cis-acting element for proline- and hypoosmolarity-responsive expression of the ProDH gene encoding proline dehydrogenase in Arabidopsis. *Plant Physiol*, **130**, 709-719.
- Scheufler, C., Brinker, A., Bourenkov, G., Pegoraro, S., Moroder, L., Bartunik, H., Hartl, F.U. and Moarefi, I.** (2000) Structure of TPR domain-peptide complexes: Critical elements in the assembly of the Hsp70/Hsp90 multichaperone machine. *Cell*, **101**, 199-210.
- Schindler, J., Lewandrowski, U., Sickmann, A. and Friauf, E.** (2008) Aqueous polymer two-phase systems for the proteomic analysis of plasma membranes from minute brain samples. *J Proteome Res*, **7**, 432-442.
- Schlesier, B. and Mock, H.-P.** (2006) Protein isolation and second-dimension electrophoretic separation, pp. 381-391.
- Shen, Q.H., Saijo, Y., Mauch, S., Biskup, C., Bieri, S., Keller, B., Seki, H., Ulker, B., Somssich, I.E. and Schulze-Lefert, P.** (2007) Nuclear activity of MLA immune

- receptors links isolate-specific and basal disease-resistance responses. *Science*, **315**, 1098-1103.
- Shirsat, A., Wilford, N., Croy, R. and Boulter, D.** (1989) Sequences responsible for the tissue specific promoter activity of a pea legumin gene in tobacco. *Mol Gen Genetics*, **215**, 326-331.
- Simpson, S.D., Nakashima, K., Narusaka, Y., Seki, M., Shinozaki, K. and Yamaguchi-Shinozaki, K.** (2003) Two different novel cis-acting elements of *erd1*, a *clpA* homologous Arabidopsis gene function in induction by dehydration stress and dark-induced senescence. *Plant J*, **33**, 259-270.
- Small, I., Peeters, N., Legeai, F. and Lurin, C.** (2004) Predotar: A tool for rapidly screening proteomes for N-terminal targeting sequences. *Proteomics*, **4**, 1581-1590.
- Smith, D.F., Sullivan, W.P., Marion, T.N., Zaitso, K., Madden, B., McCormick, D.J. and Toft, D.O.** (1993) Identification of a 60-kilodalton stress-related protein, p60, which interacts with Hsp90 and Hsp70. *Mol Cell Biol*, **13**, 869-876.
- Song, H., Fan, P. and Li, Y.** (2009a) Overexpression of organellar and cytosolic AtHsp90 in *Arabidopsis thaliana* impairs plant tolerance to oxidative stress. *Plant Mol Biol Rep*, **27**, 342-349.
- Song, H.M., Fan, P.X., Shi, W.L., Zhao, R.M. and Li, Y.X.** (2010) Expression of five AtHsp90 genes in *Saccharomyces cerevisiae* reveals functional differences of AtHsp90s under abiotic stresses. *J Plant Physiol*, **167**, 1172-1178.
- Song, H.M., Zhao, R.M., Fan, P.X., Wang, X.C., Chen, X.Y. and Li, Y.X.** (2009b) Overexpression of AtHsp90.2, AtHsp90.5 and AtHsp90.7 in *Arabidopsis thaliana* enhances plant sensitivity to salt and drought stresses. *Planta*, **229**, 955-964.
- Song, Y. and Masison, D.C.** (2005) Independent regulation of Hsp70 and Hsp90 chaperones by Hsp70/Hsp90-organizing protein Sti1 (Hop1). *J Biol Chem*, **280**, 34178-34185.
- Su, P.-H. and Li, H.-M.** (2008) Arabidopsis stromal 70-kD heat shock proteins are essential for plant development and important for thermotolerance of germinating seeds. *Plant Physiol*, **146**, 1231-1241.
- Sugiyama, N., Nakagami, H., Mochida, K., Daudi, A., Tomita, M., Shirasu, K. and Ishihama, Y.** (2008) Large-scale phosphorylation mapping reveals the extent of tyrosine phosphorylation in Arabidopsis. *Mol Syst Biol*, **4**.
- Sung, D.Y. and Guy, C.L.** (2003) Physiological and molecular assessment of altered expression of Hsc70-1 in Arabidopsis. Evidence for pleiotropic consequences. *Plant Physiol*, **132**, 979-987.
- Tagwerker, C., Flick, K., Cui, M., Guerrero, C., Dou, Y.M., Auer, B., Baldi, P., Huang, L. and Kaiser, P.** (2006) A tandem affinity tag for two-step purification under fully denaturing conditions - Application in ubiquitin profiling and protein complex identification combined with in vivo cross-linking. *Mol Cell Proteomics*, **5**, 737-748.
- Takahashi, A., Casais, C., Ichimura, K. and Shirasu, K.** (2003) Hsp90 interacts with RAR1 and SGT1 and is essential for RPS2-mediated disease resistance in Arabidopsis. *P Natl Acad Sci USA*, **100**, 11777-11782.
- Tamagnone, L., Merida, A., Parr, A., Mackay, S., Culianez-Macia, F.A., Roberts, K. and Martin, C.** (1998) The AmMYB308 and AmMYB330 transcription factors from *antirrhinum* regulate phenylpropanoid and lignin biosynthesis in transgenic tobacco. *Plant Cell*, **10**, 135-154.
- Tang, W.N. and Perry, S.E.** (2003) Binding site selection for the plant MADS domain protein AGL15 - An *in vitro* and *in vivo* study. *J Biol Chem*, **278**, 28154-28159.

-
- Teakle, G.R., Manfield, I.W., Graham, J.F. and Gilmartin, P.M.** (2002) Arabidopsis thaliana GATA factors: Organisation, expression and DNA-binding characteristics. *Plant Mol Biol*, **50**, 43-57.
- Tisdale, E.J. and Artalejo, C.R.** (2007) A GAPDH mutant defective in Src-dependent tyrosine phosphorylation impedes Rab2-mediated events. *Traffic*, **8**, 733-741.
- Torres, J.H., Chatellard, P. and Stutz, E.** (1995) Isolation and characterization of gmsti, a stress-inducible gene from soybean (*Glycine max*) coding for a protein belonging to the TPR (tetratricopeptide repeats) family. *Plant Mol Biol*, **27**, 1221-1226.
- Tusnady, G.E. and Simon, I.** (2001) The HMMTOP transmembrane topology prediction server. *Bioinformatics*, **17**, 849-850.
- Ulmasov, T., Hagen, G. and Guilfoyle, T.J.** (1999) Dimerization and DNA binding of auxin response factors. *Plant J*, **19**, 309-319.
- Van Leene, J., Stals, H., Eeckhout, D., Persiau, G., De Slijke, E.V., Van Isterdael, G., De Clercq, A., Bonnet, E., Laukens, K., Remmerie, N., Henderickx, K., De Vijlder, T., Abdelkrim, A., Pharazyn, A., Van Onckelen, H., Inze, D., Witters, E. and De Jaeger, G.** (2007) A tandem affinity purification-based technology platform to study the cell cycle interactome in *Arabidopsis thaliana*. *Mol Cell Proteomics*, **6**, 1226-1238.
- Vierling, E.** (1991) The roles of heat-shock proteins in plants. *Annu Rev Plant Phys*, **42**, 579-620.
- Vierling, E. and Kimpel, J.A.** (1992) Plant responses to environmental stress. *Curr Opin Biotech*, **3**, 164-170.
- Vij, S. and Tyagi, A.K.** (2007) Emerging trends in the functional genomics of the abiotic stress response in crop plants. *Plant Biotechnol J*, **5**, 361-380.
- Villen, J. and Gygi, S.P.** (2008) The SCX/IMAC enrichment approach for global phosphorylation analysis by mass spectrometry. *Nat Protoc*, **3**, 1630-1638.
- Wagner, G.J.** (1991) Secreting glandular trichomes - More than just hairs. *Plant Physiology*, **96**, 675-679.
- Wang, E., Gan, S. and Wagner, G.J.** (2002) Isolation and characterization of the CYP71D16 trichome-specific promoter from *Nicotiana tabacum* L. *J Exp Bot*, **53**, 1891-1897.
- Wang, W., Vinocur, B., Shoseyov, O. and Altman, A.** (2004) Role of plant heat-shock proteins and molecular chaperones in the abiotic stress response. *Trends Plant Sci*, **9**, 244-252.
- Wang, W.X., Vinocur, B. and Altman, A.** (2003) Plant responses to drought, salinity and extreme temperatures: towards genetic engineering for stress tolerance. *Planta*, **218**, 1-14.
- Wang, W.X., Vinocur, B., Shoseyov, O. and Altman, A.** (2001) Biotechnology of plant osmotic stress tolerance: Physiological and molecular considerations. *Acta Hort*, **560**, 285-292.
- Wang, Z.Y., Kenigsbuch, D., Sun, L., Harel, E., Ong, M.S. and Tobin, E.M.** (1997) A Myb-related transcription factor is involved in the phytochrome regulation of an Arabidopsis Lhcb gene. *Plant Cell*, **9**, 491-507.
- Waters, M.G., Serafini, T. and Rothman, J.E.** (1991) 'Coatomer': a cytosolic protein complex containing subunits of non-clathrin-coated Golgi transport vesicles. *Nature*, **349**, 248-251.
-

- Wegele, H., Haslbeck, M., Reinstein, J. and Buchner, J.** (2003) Sti1 is a novel activator of the Ssa proteins. *J Biol Chem*, **278**, 25970-25976.
- Werner-Washburne, M., Stone, D.E. and Craig, E.A.** (1987) Complex interactions among members of an essential subfamily of Hsp70 genes in *Saccharomyces cerevisiae*. *Mol. Cell. Biol.*, **7**, 2568-2577.
- Wessel, D. and Flügge, U.I.** (1984) A method for the quantitative recovery of protein in dilute solution in the presence of detergents and lipids. *Anal Biochem*, **138**, 141-143.
- Witzel, K., Surabhi, G.K., Jyothsnakumari, G., Sudhakar, C., Matros, A. and Mock, H.P.** (2007) Quantitative proteome analysis of barley seeds using ruthenium(II)-tris-(bathophenanthroline-disulphonate) staining. *J Proteome Res*, **6**, 1325-1333.
- Xu, X., Song, H., Zhou, Z., Shi, N., Ying, Q. and Wang, H.** (2010) Functional characterization of AtHsp90.3 in *Saccharomyces cerevisiae* and *Arabidopsis thaliana* under heat stress. *Biotechnol Lett*, **32**, 979-987.
- Yamasaki, K., Kigawa, T., Inoue, M., Tateno, M., Yamasaki, T., Yabuki, T., Aoki, M., Seki, E., Matsuda, T., Tomo, Y., Hayami, N., Terada, T., Shirouzu, M., Osanai, T., Tanaka, A., Seki, M., Shinozaki, K. and Yokoyama, S.** (2004) Solution structure of the B3 DNA binding domain of the Arabidopsis cold-responsive transcription factor RAV1. *Plant Cell*, **16**, 3448-3459.
- Yi, F., Doudevski, I. and Regan, L.** (2010) Hop is a monomer: Investigation of the oligomeric state of the co-chaperone Hop. *Protein Sci*, **19**, 19-25.
- Young, J.C., Moarefi, I. and Hartl, F.U.** (2001) Hsp90: A specialized but essential protein-folding tool. *J Cell Biol*, **154**, 267-273.
- Young, J.C., Obermann, W.M.J. and Hartl, F.U.** (1998) Specific binding of tetratricopeptide repeat proteins to the C-terminal 12-kDa domain of Hsp90. *J Biol Chem*, **273**, 18007-18010.
- Zanata, S.M., Lopes, M.H., Mercadante, A.F., Hajj, G.N.M., Chiarini, L.B., Nomizo, R., Freitas, A.R.O., Cabral, A.L.B., Lee, K.S., Juliano, M.A., de Oliveira, E., Jachieri, S.G., Burlingame, A., Huang, L., Linden, R., Brentani, R.R. and Martins, V.R.** (2002) Stress-inducible protein 1 is a cell surface ligand for cellular prion that triggers neuroprotection. *Embo J*, **21**, 3307-3316.
- Zhang, K.Q., Dittmar, J., Ross, M. and Bergh, C.** (2011) Assessment of sea level rise impacts on human population and real property in the Florida Keys. *Climatic Change*, **107**, 129-146.
- Zhang, Z.M., Quick, M.K., Kanelakis, K.C., Gijzen, M. and Krishna, P.** (2003) Characterization of a plant homolog of Hop, a co-chaperone of Hsp90. *Plant Physiol*, **131**, 525-535.
- Zhu, X.T., Zhao, X., Burkholder, W.F., Gragerov, A., Ogata, C.M., Gottesman, M.E. and Hendrickson, W.A.** (1996) Structural analysis of substrate binding by the molecular chaperone DnaK. *Science*, **272**, 1606-1614.
- Zimmermann, P., Hirsch-Hoffmann, M., Hennig, L. and Gruissem, W.** (2004) Genevestigator. Arabidopsis microarray database and analysis toolbox. *Plant Physiol*, **136**, 2621-2632.
-

7. Abbreviations

ABA	abscisic acid
ABC	ammonium bicarbonate
ABI3	abscisic acid-insensitive3
ACN	acetonitril
ANOVA	analysis of variance
au	arbitrary units
BCIP	5-bromo-4-chloro-3-indolyl phosphate
bp	base pair
BN-PAGE	blue native polyacrylamide gel electrophoresis
BSA	bovine serum albumin
CaMV 35S	<i>Cauliflower mosaic virus</i> 35S promoter
CBP	calmodulin binding protein
cCBB	colloidal Coomassie Brilliant Blue
CHAPS	3-[(3-Cholamidopropyl)dimethylammonio]-1-propanesulfonat
CP	client protein
CV	confidence interaction value
Da	Dalton
DNA	desoxyribonucleid acid
DP	aspartate-proline
DTE/ DTT	dithioerythritol/ dithiothreitol
EDTA	Ethylenediaminetetraacetic acid
ESI	electrospray ionisation
FA	formic acid
Ft	flow through
Fw	fresh weight
GFP	green fluorescent protein
GUS	β -glucuronidase
HAcO	acetic acid
HCCA	α -cyano-4-hydroxycinnamic-acid
Hepes	4-(2-hydroxyethyl)-1-piperazineethanesulfonic acid
HOP	Hsp70/Hsp90 organising protein
Hsp	heat shock protein
IEF	isoelectric focussing
IEX	ion exchange chromatography
IgG	Immunoglobulin G
IMAC	Immobilized metal ion affinity chromatography
IP	immunoprecipitation
IPG	immobilised pH gradient
LC	liquid chromatography
M	mol

MALDI	matrix-assisted laser desorption ionisation
MDAR	monodehydroascorbate reductase
MOPS	3-(N-morpholino)propanesulfonic acid
MS	mass spectrometry
M _w	Molecular weight
<i>m/z</i>	mass-to-charge
NBT	nitroblue tetrazolium chloride
NLS	nuclear localisation signal
PBS(T)	phosphate buffered saline (supplemented with Tween-20)
PCR	polymerase chain reaction
<i>pI</i>	isoelectric point
PM	plasma membrane
PTM	post-translational modification
PVDF	polyvinylidene fluoride
Q-TOF	quadrupole time-of-flight
RAV	Related to ABI3/VP1
RNAi	RNA interference
RT	room temperature
SEC	size exclusion chromatography
SDS-PAGE	sodium dodecyl polyacrylamide gel electrophoresis
STI1	stress-inducible protein in <i>Saccharomyces cerevisiae</i>
STIAT	stress-inducible protein in <i>Arabidopsis thaliana</i> , name of the protein
<i>STIAT</i>	name of the gene, mRNA, or cDNA
<i>stiat</i>	mutant allele
STINT	stress-inducible protein in <i>Nicotiana tabacum</i>
TAP	tandem affinity purification
TCA	trichloroacetic acid
TEV	tobacco etch virus
TFA	trifluoroacetic acid
TOF	time-of-flight
TPR	tetratricopeptide repeat
Vol	volume
VP1	viviparous 1
v/v	volume-to-volume ratio
w/w	weight-to-weight ratio
w/v	weight-to-volume ratio
x g	gravitation force

8. Acknowledgements

This page I want to use for thanking all colleagues and friends contributing to this work.

My particular thanks go to my PhD supervisor PD Dr Hans-Peter Mock for giving me the opportunity to continue my work in his group, his continuous guidance, permanent support, advice and discussion.

For reviewing my thesis I'm very grateful to Prof Dr Klaus Humbeck at the Martin-Luther-University in Halle and Prof Dr Hans-Jörg Jacobsen at the Leibniz University Hanover.

For internal and external cooperation concerning the TAP experiments I would like to thank Prof Gotthard Kunze from the Yeast genetics group (IPK) and Dr Geert de Jaeger at the VIB/University of Gent, Belgium.

I am very grateful to all current and former members of the Applied Biochemistry Group at the IPK for their support and cooperation. My special thanks go to Petra Linow for excellent technical assistance and the pleasant daily routine in the lab. I would like to thank Drs Andrea Matros and Katja Witzel for valuable advice with handling the MS instrumentation, helpful STIAT/STINT-discussions and the nice atmosphere in and between the offices. I thank both Steffen. Steffen Amme, who found STINT, and my diploma student Steffen Endress, who supported the interaction studies of STIAT isoforms by fighting with the BIFC method. All co-workers evolved in STIAT/STINT experiments are gratefully acknowledged, mainly Barbara Kettig, Annegret Wolf and all trainees.

Furthermore I'm grateful to Enk Geyer and his co-workers in the greenhouse, Heike Ernst for taking pictures, the graphic office team and Knut Hoffmann for solving computer problems.

Financial support of the work from IPK, the Federal State of Saxonia-Anhalt and COST organisation (FA0603-03178) is gratefully acknowledged.

I would like to thank all my friends for their continuous support and distraction from work, especially Katja, Yude, Stephanie, Steffi, Rico, Kathleen, Manu, Hanna, Anne and Nicole.

Finally, my special thanks go to my parents Karin and Jürgen, my sister Kathrin and her husband Falk for their patience and constant support.

9. Curriculum vitae

Name: Christiane Hedtmann
 Date of Birth: January 28th, 1983
 Place of Birth: Osterburg, Germany
 Nationality: German
 Marital Status: Unmarried

SCIENTIFIC CAREER

11/2007 –	PhD student	Leibniz Institute of Plant Genetics and Crop Plant Research Gatersleben, Dept. Physiology and Cell Biology, Applied Biochemistry Group
08/2007 – 10/2007	Graduate Research Assistant	Leibniz Institute of Plant Genetics and Crop Plant Research Gatersleben, Dept. Molecular Cell Biology, Applied Biochemistry Group
02/2004 – 04/2004	Undergraduate Research Assistant	IPF Pharmaceuticals GmbH Hanover, Department Analytical Peptide Chemistry

EDUCATION

08/2006 – 07/2007	Master thesis ‘Characterization of a Stress-induced Protein from <i>N. tabacum</i> with Homology to the Gene Product of At1g62740 at the Leibniz Institute of Plant Genetics and Crop Plant Research Gatersleben, Department Molecular Cell Biology, Applied Biochemistry Group
03/2005 – 08/2005	Bachelor thesis ‘Isolation and Characterization of the Promoter of a Trichome-specific Protein from <i>N. tabacum</i> ’ at the Leibniz Institute of Plant Genetics and Crop Plant Research Gatersleben, Department Molecular Cell Biology, Applied Biochemistry Group
2002 - 2007	Study of Plant Biotechnology, Leibniz University Hanover, Germany, Natural Sciences Faculty

2002 Final secondary-school examinations, Markgraf-Albrecht-Gymnasium, Osterburg

HONORS

04/2009 – 03/2011 Post Graduate Grant Martin-Luther-University Halle-Wittenberg
Germany, Natural Sciences Faculty I

2005 Poster Prize Proteomlux Conference, Luxembourg

PUBLICATIONS

John, H., Huynh, KD., Hedtmann, C., Walden, M., Schulz, A., Anspach, FB. and Forssmann, WG. (2005) In vitro degradation of the antimicrobial human peptide HEM- γ 130-146 in plasma analyzed by a validated quantitative LC-MS/MS procedure. *Analytical Biochemistry*, 341, 173-186.

ORAL PRESENTATIONS

C. Hedtmann, A. Matros and H.-P. Mock. Functional characterization of stress-inducible proteins with homology to the human protein HOP (Hsp70/Hsp90-organizing protein) in Arabidopsis - Final COST Meeting FA0603, Dijon, 25-27.05.2011

Elucidation of plant co-chaperone interaction partners by proteomics approaches. – Proteomlux Conference, Luxemburg, 18.-20.10.2010

A chaperone works not alone, but who is the counterpart? – IPK Student Conference, Gatersleben, 15.-18.06.2010

POSTER PRESENTATIONS

C. Hedtmann, A. Matros and H.-P. Mock. Investigation of Arabidopsis HOP/STI1 co-chaperone function and their regulation during stress response. - Institut's Day IPK, Gatersleben, 04.-06.10.2011

C. Hedtmann, A. Matros and H.-P. Mock. Elucidating the molecular functions of stress-inducible proteins with homology to the human protein HOP (Hsp70/Hsp90-organizing protein) in tobacco and Arabidopsis. – Botanikertagung, Berlin, 18.-23.09.2011

C. Hedtmann, S. Endress, A. Matros, G. de Jaeger and H.-P. Mock. Biochemical analysis of plant co-chaperone function and their potential interaction partners. - Institut's Day IPK, Gatersleben, 04.-06.10.2010

C. Hedtmann, A. Matros, G. Kunze, G. de Jaeger and H.-P. Mock. MS analysis to elucidate interaction partners of plant co-chaperones with homology to the human protein HOP (heat shock organizing protein). – DGMS (German Association for Mass Spectrometry), 43th Annual Meeting, Halle. 07.-10.03.2010

C. Hedtmann, A. Matros, G. Kunze, G. de Jaeger and H.-P. Mock. Biochemical characterization of proteins with homology to the co-chaperone HOP and their interaction partners in tobacco, Arabidopsis and yeast. - Institut's Day IPK, Gatersleben, 12.-13.10.2009

C. Hedtmann, A. Matros and H.-P. Mock. Functional characterization of the stress-induced protein STINT. – Plant Science Student Conference, IPK, Gatersleben, 15.-18.06.2008

S. Amme, C. Hedtmann, A. Matros and H.-P. Mock. Stress response networks in tobacco trichomes. – Proteomlux Conference, Luxembourg, 11.-14.10.2005

10. Affirmation

Hereby, I declare that all the work presented in this dissertation is my own, carried out solely with the help of the literature and aids cited.

Hiermit erkläre ich, dass ich mich mit der vorliegenden wissenschaftlichen Arbeit erstmals um die Erlangung des Doktorgrades bewerbe.

Ich erkläre, dass ich die Arbeit selbständig und ohne fremde Hilfe verfasst, nur die von mir angegebenen Quellen und Hilfsmittel benutzt und die den benutzten Werken wörtlich oder inhaltlich entnommenen Stellen als solche kenntlich gemacht habe.

Gatersleben, Januar 2012

Christiane Hedtmann

11. Appendix

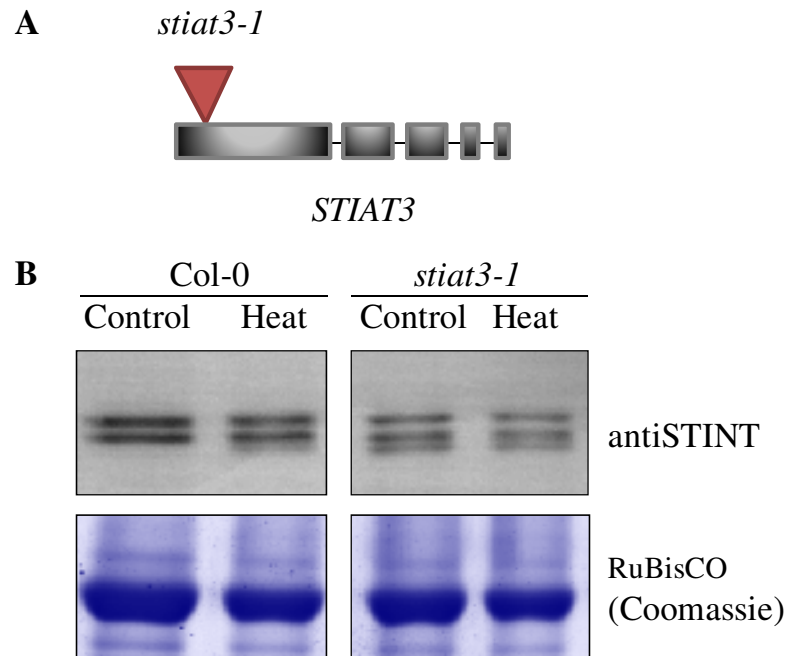


Figure A 1: Analysis of T-DNA insertion lines of *STIAT3* in Columbia-0 ecotype.

A: Relative positions of T-DNA insertions in *STIAT3* gene, indicated by red triangle.

B: Immunodetection of *STIAT* isoforms in T-DNA insertion line *stiat3-1* and Col-0 under control conditions and heat stress treatment. Five μ g of total leaf protein extracts were separated on SDS-PAGE and probed with antiserum against STINT. Knock-out line for *STIAT3* presence of all three *STIAT* isoforms even under control conditions, indicating no functional T-DNA insertion for *STIAT3*. The cCBB staining of ribulose-1,5-bisphosphate carboxylase-oxygenase (RuBisCO) was used as loading control.

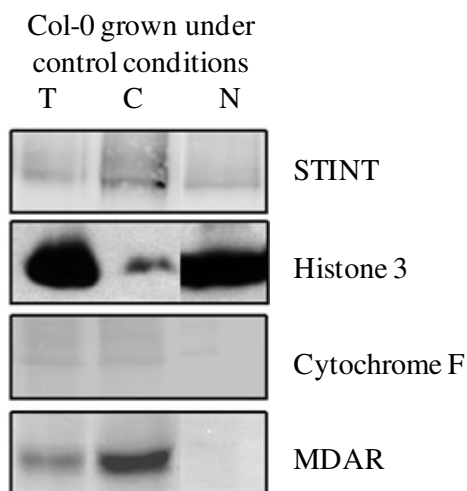


Figure A 2: Distribution of STINT in nuclei separated fractions of tobacco leaves.

Equal amounts of total (T), cytosolic (C) and nuclear (N) extracts were separated on SDS-PAGE and transferred to PVDF membrane. Immunological detection with antiserum against STINT and marker for nuclei (Histone3), cytosol (monodehydroascorbate reductase MDAR) and chloroplasts (cytochrome F) revealed a predominantly cytoplasmatic localisation of STINT compared to its amount in the nucleus.

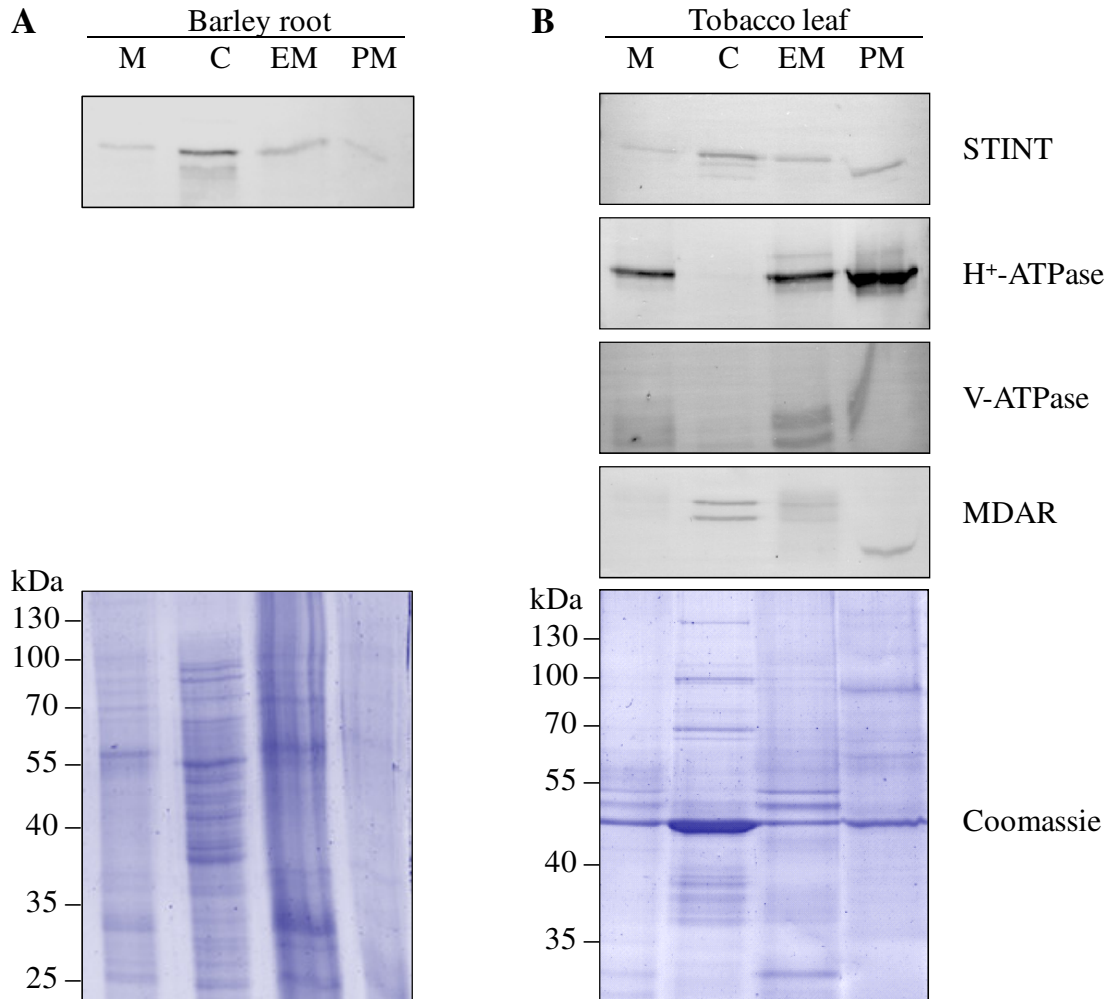


Figure A 3: Subcellular distribution of HOP/STII in membrane fractions of barley root (A) and tobacco leaf (B).

Five μg of protein of microsomal (M), cytosolic (C), endomembrane (EM) and plasma membrane (PM) fractions were separated by SDS-PAGE and visualized by cCBB staining. The specific band patterns indicate the fractionation using aqueous two-phase partitioning. The quality of membrane preparations was assessed using immunoblotting with antibodies against the subcellular marker proteins H⁺-ATPase, MDAR and V-ATPase. Western blot analysis with antiserum against STII revealed a predominantly cytoplasmatic localisation of STII but also its association to membranes.

Table A 1: *In silico* prediction of STIAT isoform localisation using TargetP (Emanuelsson *et al.* 2000).

Ranking of likelihood scores revealed another localisation than in chloroplasts, mitochondria or endoplasmatic reticulum.

Isoform	chloTP	mitoTP	SecrPathw	other
STIAT1	0.394	0.127	0.099	0.544
STIAT2	0.201	0.143	0.108	0.631
STIAT3	0.193	0.125	0.078	0.722

Table A 2: *In silico* prediction of STIAT isoform targeting to mitochondria using Mitoprot (Claros and Vincens 1996) and Predotar (Small *et al.* 2004).

Ranking of likelihood scores revealed a very low probability of export to mitochondria using both online tools. Cleavage site of mitochondrial targeting was not detectable using Mitoprot.

Isoform	Probability of export to mitochondria		Mitoprot Cleavage site
	Predotar	Mitoprot	
STIAT1	0.01	0.0090	not predictable
STIAT2	0.01	0.0285	not predictable
STIAT3	0.01	0.0184	not predictable

Table A 3: Protein identification of TAP tagged STINT complexes from Arabidopsis cell culture using MALDI-TOF-TOF MS.

The experiments were performed twice to ensure technical reproducibility. Protein name, accession number, detected peptides, score and molecular weight of proteins co-purifying with the bait protein are given. Protein identification via MALDI-TOF-TOF MS was performed by searching SNAPS database (<http://www.ptools.ua.ac.be>).

Protein	Accession	C-TAP1		C-TAP2		N-TAP-1		N-TAP-2	
		Peptides	Score	Peptides	Score	Peptides	Score	Peptides	Score
Hsp90-1	At5g52640	7	233	6	215	17	458	15	509
Hsp90-2	At5g56030	17	567	7	214	19	909	21	990
Hsp90-3	At5g56010	17	566	7	213	19	908	21	988
Hsp90-4	At5g56000	15	545	6	208	16	870	16	932
STIAT1	At1g62740	3	70	6	48	2	57	3	60
Hsp70-1	At5g02500	-	-	3	111	10	208	19	891
Hsp70-2	At5g02490	-	-	7	83	4	155	11	418
Hsp70-3	At3g09440	-	-	3	111	10	139	16	614
Hsp70-4	At3g12580	-	-	8	87	6	166	18	666
Hsp70-18	At1g56410	-	-	7	83	5	159	10	315